DEVELOPMENT OF DESIGN METHODOLOGY AND SOFTWARE FOR MICROIRRIGATION SUBUNITS

Thesis

Submitted to the

G. B. Pant University of Agriculture and Technology

PANTNAGAR-263145. Uttaranchal, INDIA

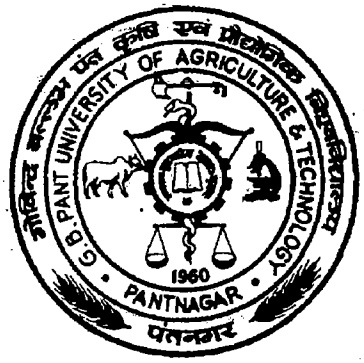

By

Sudhir Kumar Jain

IN PARTIAL FULFILMENT OF THE REQUIREMENTS

FOR THE DEGREE OF

Doctor of Philosophy

(IRRIGATION AND DRAINAGE ENGINEERING)

JUNE, 2001

Dr. K. K. Singh
Professor and Head

Department of Irrigation and Drainage Engineering,
G. B. Pant University of Agriculture and Technology, Pantnagar

CERTIFICATE

This is to certify that the thesis entitled **Development of Design Methodology and Software for Microirrigation Subunits**, submitted in partial fulfillment of requirements for the degree of **Doctor of Philosophy** with major in **Irrigation and Drainage Engineering (Agricultural Engineering)** of the College of Post-Graduate Studies, G. B. Pant University of Agriculture and Technology, Pantnagar, is a record of *bona fide* research carried out by **Mr. Sudhir Kumar Jain** Id. No. 25689, under my supervision, and no part of the thesis has been submitted for any other degree or diploma.

The assistance and help received during the course of this investigation have been acknowledged.

K K Singh 27.6.01

(K. K. Singh)
Chairman,
Advisory Committee

CERTIFICATE

We, the undersigned, members of the Advisory Committee of **Mr. Sudhir Kumar Jain**, Id. No. 25689, a candidate for the degree of **Doctor of Philosphy** with major in **Irrigation and Drainage Engineering (Agricultural Engineering)** agree that the thesis entitled **"Development of Design Methodology and Software for Microirrigation Subunits"** may be submitted in partial fulfilment of the requirements for the degree.

(K. K. Singh) 27.6.01
Chairman,

(K. N. Shukla)
Member

(R. P. Singh)
Member

(Manoj Kumar)
Member

ACKNOWLEDGEMENTS

No selective, artificial and melodious words can ever substitute my heartfelt gratitude and profound sense of appreciation to Dr. K. K. Singh, Professor and Head, Department of Irrigation and Drainage Engineering for his invaluable guidance, constructive and convincing criticism, keen interest and constant encouragement during the course of the investigation. I am highly indebted to him for which I can not even imagine of repaying in my whole life.

I express my gratefulness to Dr. K. N. Shukla, Professor, Dr. R. P. Singh, Associate Professor, Department of Irrigation and Drainage Engineering, and Dr. Manoj Kumar, Assistant Professor, Department of Mathematics, Statistics and Computer Science, members of my advisory committee, for their valuable counsel from time to time during the course of this study.

I wish to express my sincere gratitute to Dr. H. S. Chauhan, former Dean, College of Technology, and Emeritus Fellow (AICTE), for his invaluable suggestions and constant encouragement in identifying the research problem.

I feel happy to express my unqualified and unfailing allegiance to the authorities of the Rajendra Agricultural University, Bihar, Pusa, for deputing me to undergo the Ph. D. degree programme at this prestigious university.

Special regards and sense of gratitude goes to Dr. A. P. Mishra, Dean, College of Agricultural Engineering, R. A. U., Pusa, without whose inspiration and help, it would have been a different story.

I am thankful to Dean, Post Graduate Studies and, Dean, College of Technology, for providing necessary facilities for the investigation.

At this occasion, I remember and wish to express my gratitude to all my teachers who have taught me and with their assistance and blessings I am able to reach the present academic level.

My sincere thanks are due to Er. P. K. Singh, Junior Research Officer, Department of Irrigation and Drainage Engineering, Dr. S. R. Singh, Associate Professor, and Dr. M. C. Joshi, Assistant Professor, Department of Statistics, Mathematics & Computer Science for their cooperation and help during my stay at Pantnagar.

I am also thankful to Dr. R. K. Sohane, Mr. A. K. Gauraha, Er. R. K. Mehta, Er. S. P. Gupta, Er. P. K. Sigh, Er. O. P. Soni, Er. R. S. Rana, Dr. S. K. Shakya, Dr. U. P. Choudhary, Dr. P. S. Shekhawat, and all the friends who directly or indirectly helped me during my stay at Pantnagar.

Thanks are also due to all the staff members of the Department of Irrigation and Drainage Engineering, for their cooperation during the investigation and course work.

I shall be doing a great inservice to humanity if I do not take this opportunity to express my utmost and heartiest felicitation to all my family members Dr. Pratibha Jain (wife), Rubal (daughter) and Chetan (son) who cooperated and supported me to complete the course work and carry out research work for the degree.

Pantnagar

(Sudhir Kumar Jain)

CONTENTS

LIST OF FIGURES

LIST OF TABLES

LIST OF SYMBOLS

γ	=	a constant (= 0 for strip source and 1 for disc source)
ε	=	error
ψ	=	soil – water tension
θ	=	volumetric soil moisture content
θ_n	=	initial moisture content
θ_s	=	saturation moisture content
∇	=	vector gradient operator
∇^2	=	Laplacian operator
$\phi(h)$ or $\phi(\theta)$	=	matric flux potential
$\rho(t)$ or ρ	=	radius of saturated disc
cm	=	centimeter
C(h)	=	specific water capacity
C	=	clay content of the soil, %
D	=	diameter of lateral/submain
$D(\theta)$	=	soil-water diffusivity
D_r	=	diameter of riser tube
DU	=	lower quarter distribution uniformity
f	=	friction factor in Darcy-Weisbach formula
h or $h(\theta)$	=	matric potential or matric/capillary head
h	=	grid interval in space
h_r	=	height of riser tube
H	=	total head
H_{in}	=	pressure head at the inlet of the lateral/submain
H_{rin}	=	head required at the inlet of lateral/submain
L_r	=	length of riser
k	=	time increment
kPa	=	kilo Pascal
K_s	=	saturated hydraulic conductivity

$K(h)$ or $K(\theta)$	=	unsaturated hydraulic conductivity
LDE	=	lateral discharge equation
m	=	meter
mm	=	millimeter
min	=	minutes
M_o	=	maximum number of iterations allowed in Newtons procedure
P_{best}	=	best submain position
q	=	emitter discharge
q_{av}	=	average emitter discharge
q_{req}	=	required average emitter discharge
Q	=	discharge in the lateral/submain element
Q_{in}	=	discharge at the inlet of the lateral/submain
r	=	cylindrical coordinate
R_e	=	Reynolds number
s	=	second
S	=	slope
S	=	sand content of the soil, %
S_e	=	spacing of emitters along lateral
S_l	=	spacing of laterals along submain
T or t	=	time
UCC	=	Christiansens uniformity coefficient
V_H	=	effective pressure head variation at the emitters
V_{HM}	=	total emitter flow variation
V_M	=	manufacturing variation of emitters
x	=	emitter flow exponent
Z	=	elevation head

Chapter 1

Introduction

1. INTRODUCTION

1.1 General

Irrigation has played a key role in raising the food production and achieving self-sufficiency in India. The irrigation potential has increased from 22.6 mha in 1951, the starting year of I five year plan to about 90 mha at the end of VIII five year plan (1992-97). The actual area irrigated however is about 80 mha at the end of VIII five year plan (**India, 1999**) with a gap in irrigation of about 10 mha. One of the main reasons for this gap is the adoption of inefficient water application methods by majority of farmers. Surface irrigation methods are undoubtedly the most commonly used methods for applying water to fields and account for more than 95 per cent of 250 mha of land irrigated world wide and this is likely to remain so in the foreseeable future (**Kay, 1990**). The utilizable water resources in India are also not enough to irrigate the entire cultivable area of the country, hence concerted efforts are needed to use the irrigation water more efficiently. Irrigation water losses during application to the fields including deep percolation etc. are substantial and account for 25 to 27 per cent of water released at the canal head (**Sharma and Sarkar, 1994**).

Irrigation is one of the oldest known agricultural technologies, but improvements in irrigation methods and practices are still being made. The future will require even greater improvements as the demands on

water supplies are steadily increasing in the country and in many areas the ground water supplies are depleting rapidly. Creation of irrigation potential is an expensive process and at the same time there is a tremendous environmental concerns about the mega-irrigation projects. An investment of about Rupees one lac is required to create an additional water resource in order to bring only one hectare area under irrigation. The microirrigation systems have a great potential to increase the net irrigated area with the available water resources of the country. This method is an accepted system of irrigating many crops, yet microirrigation should not be expected to replace the other irrigation methods or in some areas to even compete with conventional irrigation methods.

Like other methods, this method of irrigation is not suitable to every crop or site. Presently, microirrigation has greatest potential where – water is expensive or scarce; soils are sandy, rocky or difficult to level; and high value crops are produced.

1.2 Microirrigation System

Microirrigation is a new approach compared to surface and sprinkler irrigation systems and offers unique agronomical, agro-technical and economical merits over the conventional irrigation methods. It is the frequent application of small quantity of water on or beneath the soil surface as drops, tiny streams or miniature sprays through the emitters or applicators placed along a water delivery line.

The main components of a microirrigation system are emitters, laterals, submains and main lines. A microirrigation system may consist of several subunits. Each subunit has a submain and number of laterals attached to the submain. The submain is provided with a control valve at its inlet, which facilitates regulation of pressure head in the subunit and operation of the subunit independent of other subunits. Microirrigation offers several potential advantages over other methods of irrigation, the primary one being the precise application of water from the emitter system.

1.3 Microirrigation in India

Microirrigation was commercially launched in India in the year 1986. The adaptation was low until 1990, the area has been increasing steadily since then. Presently, about 0.38 Mha are microirrigated in the country (**Jain, 2000a**) putting India as the second largest microirrigated country in the world, next to USA with coverage of 1.05 Mha. An area of about 15 Mha is under various horticultural crops throughout the country and it is expected that at least 1 Mha can be brought under microirrigation by 2005 (**Jain, 2000b**). Adoption of this method picked up rapidly in the States of Maharashtra, Karnataka, Tamil Nadu, Gujarat and Kerala. Maharashtra is the leading state in adoption of microirrigation, contributing almost half of the country's microirrigated area. The main driving factors being, accelerated horticultural development, dwindling groundwater resources, full fledged growth of

indigenous microirrigation industry, substantial financial support from the Government, progressive farming community and research support from various academic institutions. Microirrigation is adopted for fruit trees, vegetables, flowers, and other crops like sugarcane, cotton, and agro-forestry. Applied research on microirrigation is being carried out through 16 Plasticulture Development Centers (PDCs), sponsored by Ministry of Agriculture, Government of India, established at different regions of the country.

1.4 Microirrigation Hydraulics

Microirrigation systems normally wet only a portion of the horizontal cross sectional area of the soil. The movement of water in the soil depends on the physical properties of the soil and emitter discharge. If the emitter discharge exceeds basic infiltration rate of the soil, water starts ponding at the surface and a disc shaped saturated zone is formed around the point source. The radius of the saturated disc increases with time and also depends on emitter discharge. Higher the discharge, larger will be the radius of saturated disc, at any point of time. Due to wider spread of water at the surface, its movement will be faster in horizontal direction than in vertical direction. Therefore the shape of the wetted profile developed below the trickle source will depend on the emitter discharge.

A number of analytical and numerical models in cartesian and cylindrical coordinates, are available in literature to predict water

movement from different types of surface and subsurface trickle sources. The basic inputs to these models are the soil-water characteristic relationships. A good number of these relationships are also reported, but most of them are the empirical ones and needs their constants to be evaluated for the specific soils being studied. Determination of soil-water characteristics is a tedious job and requires a lot of time and efforts to get a reliable value.

The flow regime through a microirrigation system is hydraulically steady, spatially varied pipe flow with lateral outflows. Total discharge in the distribution network decreases with respect to distance from the inlet of the system. The lateral and submain have similar hydraulic characteristics and are designed to maintain a small pressure variation in order to achieve relatively uniform outflow from the emitters.

In microirrigation systems, laterals normally extend only on one side of the submain and they are known as the single laterals. The flow rate of emitters depends on their operating pressure head, which varies along the line due to the elevation differences and friction losses in the pipeline. The friction losses per unit length of pipe, in different segments of the pipeline are different because of decreasing flow rate. Hence, hydraulic analysis of a microirrigation pipeline becomes complicated because, both the parameters i.e. inlet pressure head and inlet discharge of the pipeline are unknown. In most of the methods and design charts, the outflow from the emitters is assumed to be uniform,

which leads to an error in estimation of inlet pressure head. Use of Hazen-Williams formula in these methods with a constant roughness factor multiplies the error. Analyzing the microirrigation lines, step by step (**Hathoot *et al.*, 1993**) can eliminate these errors. Thus, the methods based on this approach provide an accurate solution for single laterals.

When two laterals extend in opposite direction from a common submain outlet, they are referred to as paired laterals. With the use of such laterals of the permissible length of laterals can be increased for the same allowable pressure variation and hence the initial cost of the system may be reduced to some extent. The problem of design of such laterals is more complicated due to the position of inlet and opposite directions of slopes. The problem of design of paired laterals was solved by a new approach known as lateral discharge equation approach (**Kang and Nishiyama, 1995**) which is discussed in detail in chapter 3.

Normally, the laterals and submains in the microirrigation systems are used with uniform diameter. It can be understood that in the downstream segments of these pipelines, the discharge is very small and hence their contribution towards the head loss due to friction is very small. In large microirrigation systems where the difference in discharge of the upstream and downstream segments is very high, use of smaller pipe size for downstream segment may also reduce the cost of the system. But, design of such pipelines which are known as tapered

laterals/submains, is further complicated due to the use of different diameters in various segments of the line.

The procedures available for design of tapered pipelines are also based on the assumption of uniform outflow from emitters. Methods based on step by step analysis and lateral discharge equation approach, though are accurate, but can not be applied for design of tapered laterals.

1.5 Problems and Objectives

Several researchers have worked on different aspects of the microirrigation system design but, there remain many problems requiring further research. Presently, the emitter discharge is selected, keeping convenience in operation of the system in mind. With this discharge the applied water may not be distributed properly in the plants root zone and may result in poor irrigation efficiency. This creates a design problem for determination of emitter discharge based on different soil hydraulic properties. Due to complications in the procedures available for design, most of the microirrigation systems are designed with uniform single laterals only, using thumb rules. An important aspect of microirrigation system design i.e. uniformity of application, is neglected. Use of paired and tapered pipelines is avoided. These problems may lead to poor performance of the system and higher initial cost.

Keeping in view, the above stated problems related to microirrigation system design, the present study is undertaken with the following specific objectives:

1. To evolve an approach for determination of discharge of trickle emitters based on wetted soil profile.
2. To develop a methodology for the design of microirrigation laterals to obtain required average discharge from the emitters.
3. To develop a methodology for the design of submain of microirrigation subunit.
4. To develop a user friendly computer software for the design of a microirrigation subunit.

Chapter 2

Review of Literature

2. REVIEW OF LITERATURE

This chapter presents a brief review of literature available on models of soil-water distribution below trickle sources, emitter discharge, design of microirrigation laterals and submains, determination of friction losses in multioutlet pipelines, etc. The other aspects related to the modeling of unsaturated flow such as functional relationships of the two important parameters governing the unsaturated properties of the soil i.e. hydraulic conductivity and soil-water potential, with soil-water content are also reviewed.

2.1 General

A microirrigation subunit consists of a submain, laterals and emitters. Submain receives water from main line and delivers to the laterals. Emitters attached to the laterals distribute water to the field. The flow from submain to laterals and the outflow through each emitter is controlled by the pressure distribution along the submain and lateral lines, respectively. The pressure distribution along a submain or lateral line, which are considered as the multioutlet pipelines is controlled by the energy drop through friction and the gain or loss of energy due to slopes of pipeline. A pressure regulator provided at the inlet of the submain controls the pressure head in submain line. The friction losses in the pipelines are estimated using the Darcy-Weisbach or the Hazen-Williams formula.

Water delivered through emitters, infiltrate down to meet the water requirement of the crop. Due to slow application, water gets distributed within the root zone of the plant evenly and adequately. The distribution of water below the soil surface is controlled by the complicated soil physical parameters, application rate of water, and spacing of the emitters. The flow of water below a trickle source into the soil is a case of three-dimensional flow in an unsaturated media and is evaluated using the soil-water distribution models.

2.2 Soil-Water Distribution Models

Numerous analytical and numerical models have been developed to study the flow of water below trickle sources. These models are based on the Richards equation, which describes the three-dimensional flow of water in an unsaturated media. The knowledge of different hydraulic properties of soils viz. unsaturated hydraulic conductivity (K) and soil-water potential (h) and their relationships with soil-water content (θ) which govern the flow in an unsaturated media, is necessary for modeling unsaturated flow in soils.

2.2.1 Functional relationships for K, h and θ

To represent experimental data to develop analytical and numerical solutions of flow problems, simple relationships amongst K, h, and θ are useful. Some of the relationships available in literature are given in Table 2.1. **Brutsaert (1967)** reviewed the functional forms of K(h) or K(θ). **Burdine (1953)** and **Maulem (1976)** gave the integral type

Table 2.1 Empirical relationships between hydraulic conductivity (K), matric potential (h) and effective saturation (S_e)*.

Model No.	Given By	Relationship	Referred from
A. Matric potential (h) and effective saturation (S_e)			
1.	Brook and Coorey (1964)	$S_e = (h_e/h)^{\beta}$ $h \le h_e$ $= 1$ $h \ge h_e$	Russo (1988)
2.	Clapp and Hornberger (1978)	$h = -h_e m(S_e - n)(S_e - 1)$	Clapp and Hornberger (1978)
3.	Huston and Cass (1987)	$h = h_e m(1-S_e)^{1/2}$	Alessi *et al.* (1992)
4.	Van Genuchten (1980)	$h = (1/\beta)(S_e^{-1/m} - 1)^{1/n}$	Van Genuchten (1980)
B. Hydraulic conductivity (K)			
5.	Green and Ampt (1911)	$K = K_S$	Raats and Gardener (1971)
6.	Richards (1931)	$K = (1 - 2h/h_e)K_S$	Raats and Gardener (1971)
7.	Gardener (1958)	$K = K_S e^{\alpha h}$	Raats and Gardener (1971)
8.	Gardener (1958)	$K = K_S/[(h/h_k)_n + 1]$	Raats and Gardener (1971)
9.	Wind (1955) and Brook and Coorey (1964)	$K = K_S(h/h_e)^{-m}$	Raats and Gardener (1971) and Russo (1988)
10.	Burdine (1953)	$K = K_S S_e^2 \left[\int_0^{S_e} \frac{dS_e}{h^2} / \int_0^{1} \frac{dS_e}{h^2} \right]$	Van Genuchten (1980)
11.	Maulem (1976)	$K = K_S S_e^{1/2} \left[\int_0^{S_e} \frac{dS_e}{h} / \int_0^{1} \frac{dS_e}{h} \right]$	Maulem (1976)
12.	Van Genuchten (1980)	$K = K_S S_e^{1/2} [1 - (1 - S_e^{1/m})^m]^2$	van Genuchten (1980)

* $S_e = (\theta - \theta_r)/(\theta_S - \theta_r)$, where θ_r and θ_S are residual and saturated water content respectively. h_e is air entry value of h, K_S is the saturated hydraulic conductivity and α, β, k, m, and n are constants.

of relationships amongst K, h, and θ (model nos. 10 and 11). Substitution of any h-θ expression in the integrals will give the functional form of hydraulic conductivity e.g. **van Genuchtens** model (no. 12). Among the many other models available, the models (no. 7 and 12) proposed by **Gardener (1958)** and **van Genuchten (1980),** respectively are used extensively by different workers.

The functional relationships shown in Table 2.1, though gives sufficient accurate estimate of the properties, but involves very complicated procedure for determination of the constants. Keeping in view, these complications, **Gupta and Larsen (1979)** used multiple linear regression equation to predict the soil-water content given soil-water potentials. This equation relates the soil-water content with texture (sand, silt, clay and organic matter content) and bulk density of the soil.

Arya and Paris (1981) presented a model to predict the soil water tension curve from particle size distribution and bulk density data. This model calculates a pore size distribution from particle size distribution, bulk density, and particle density. Then the pore radii are converted to equivalent soil-water tensions using the equation of capillarity at the corresponding volumetric water content.

Rawls *et al.* (1982) also reported a multiple regression analysis of soil-water content with soil attributes using very extensive data sets. Using the stepwise regression, they correlated only the most statistically significant variables. The equations have a small sensitivity to organic

matter. **Cosby *et al.* (1984)** also clearly demonstrated that soil textures could be related to hydraulic characteristics, when they applied regression and descriminant analysis to these and other data.

Saxton *et al.* (1986) further simplified the regression equations of **Rawls *et al.* (1982)** by eliminating 3 variables viz. silt, organic matter and bulk density of the soil. These variables were found to have negligibly small regression coefficient and hence their influence on the h-θ and K-θ relationship was negligible. They proposed three equations to express the h-θ relationship for 3 ranges of soil-water potentials. An equation to predict the unsaturated hydraulic conductivity K(θ) was also proposed. The proposed equations are valid for the soil-water tensions in the range of 0-1500 kPa and for a wide range of soil textures (i.e. 5≤ %sand ≤30 with 8≤ %clay ≤58 and 30≤ %sand ≤95 with 5≤ %clay ≤60).

2.2.2 Trickle irrigation flow system

In trickle irrigation modeling, generally the flow is assumed to be axisymmetric. With this assumption, the three-dimensional flow may be studied in two dimensions only. In this section, a review of water flow boundaries considered in different modeling approaches is discussed.

2.2.2.1 Flow region

In general a semi-infinite flow region is assumed for analytical modeling of trickle irrigation flow from a single emitter i.e. in (x, z) coordinates, the flow region is defined in the range $-\infty \leq x < \infty$; $0 \leq z < \infty$

(**Lockington *et al.*, 1984; Ben-Asher *et al.*, 1986**, etc.). For numerical modeling a finite flow region with sufficient dimensions in x and z direction is considered (**Taghavi *et al.*, 1984** and **Healy and Warrick, 1988**). **Brandt *et al.* (1971)** considered $-X \leq x \leq X$, where 2X is the spacing between emitters.

2.2.2.2 Initial conditions

In most of the studies uniform initial moisture content (θ_n) is considered for the whole flow region. The value of θ_n taken is so small that $K(\theta)$ becomes negligibly small, and therefore, the initial water movement in the flow region is ignored. **Lockington *et al.* (1984)** used initial effective saturation, $Se_i = 0$ and $Se_i = 0.01$ was taken by **Healy and Warrick (1988)** to obtain numerical solution. **Warrick (1974a)** used matric flux potential, $\phi_n = 0$ for $h = -\infty$ as initial condition for analytical solution.

2.2.2.3 Boundary conditions

The general boundaries considered in various studies to simulate the axisymmetric water flow from surface trickle source are shown in Fig. 3.1. These are represented in cartesian (x, z) and cylindrical (r, z) coordinates.

a) Source boundary

For a single emitter simulation this boundary represents a disc of radius $\rho(t)$ which is a function of time (**Brandt *et al.*, 1971**). The condition applied to this boundary is

$$\theta = \theta_s; \qquad 0 \le r \le \rho(t); \qquad z = 0; \qquad 0 \le t \le T \qquad ...(2.1)$$

where, θ_s is saturated moisture content.

This condition can be represented for in terms of potential as h = 0 or H = 0 (**Lafolie *et al.*, 1989**). **Taghavi *et al.* (1984)** and **Angelakis *et al.* (1993)** considered constant radius of disc, ρ, and used a constant flux condition for this boundary that can be expressed as

$$V = \frac{Q}{2\pi\rho^2} = K - K\frac{\partial h}{\partial z}; \qquad 0 \le r \le \rho; \qquad z = 0; \qquad t > 0 \qquad ...(2.2)$$

Clothier and Scotter (1982) assumed the source boundary in the form of hemisphere and used constant flux condition (equation 2.6). **Healy and Warrick (1988)** and **Ben-Asher *et al.* (1986)** considered a point source and hence ρ = 0, and thus no condition specified for source boundary.

b) Non-wetted surface boundary

The boundary represents soil surface outside the wetted disc. The general condition applied to this boundary is no vertical flow across the boundary or vertical flow equals evaporation (**Brandt *et al.*, 1971** and **Ben-Asher *et al.*, 1986**). This can be written as

$$\left.\begin{aligned} K + E - K\frac{\partial h}{\partial z} &= 0 \\ K + E - \frac{\partial \phi}{\partial z} &= 0 \end{aligned}\right\} \qquad r > \rho; \qquad t > 0 \qquad ...(2.3)$$

c) Axis of symmetry

This is the vertical line drawn from the centre of the disc. Since this is the axis of symmetry, no flow occurs across this line in either

direction (Brandt *et al.*, 1971). The boundary condition may be expressed as

$$\frac{\partial h}{\partial x} = 0; \qquad r = 0; \qquad 0 \le z \le \infty; \qquad t < 0 \qquad \ldots(2.4)$$

d) Large distance from the source

For the analytical solutions, this boundary represents $r \rightarrow \infty$ and/or $z \rightarrow \infty$. Warrick and Lomen (1976) assumed ϕ to vanish as $r^2+z^2 \rightarrow \infty$. In other words, soil remains to be at initial moisture content (θ_n) at this boundary. For numerical analysis (Healy and Warrick, 1988), similar condition applies for $x = X$ and $z = Z$, where X and Z are finite, but sufficiently large values of coordinates (x,z), respectively, to represent the flow boundaries. Brandt *et al.* (1971), Angelakis *et al.* (1993), etc. considered no flow across these boundaries, which can be expressed as

$$\left.\begin{aligned} \frac{\partial h}{\partial r} &= 0; \quad r = R; \quad 0 \le z \le Z; \quad t > 0 \\ \frac{\partial h}{\partial z} &= 0; \quad 0 \le r \le R; \quad z = Z; \quad t > 0 \end{aligned}\right\} \qquad \ldots(2.5)$$

2.3 Solutions to Three-Dimensional Flow Problems

Various solutions reported in literature are grouped in two broad categories i.e. analytical solutions and numerical solutions. The discussion of these solutions includes point source, disc source, line source and strip source solutions and the experimental studies that are related to trickle irrigation.

2.3.1 Analytical solutions

Analytical solutions of Richards equation for flow below trickle sources have been developed for steady state as well as unsteady state conditions. The non-linear governing equation was linearized using the approach of **Garderner (1958)** by defining a matrix flux potential as

$$\phi = \int_{-\infty}^{h} K(h)dh = \frac{K}{\alpha} \qquad \ldots(2.6)$$

where,

h is the pressure head [L], and

K(h) is the hydraulic conductivity [LT^{-1}]

$$K(h) = K_s \exp(\alpha h) \qquad \ldots(2.7)$$

where, α is a coefficient commonly within the range 0.002 to 0.2 cm^{-1} **(Philip, 1969; Braester, 1973)** and K_s is commonly known as saturated hydraulic conductivity. Use of equations (2.10 and 2.11) in the non-linear moisture flow equation, gives

$$\frac{\partial \phi}{\partial t} = \nabla^2 \phi - \alpha \frac{\partial \phi}{\partial z} \qquad \ldots(2.8)$$

where

t is the time, θ the volumetric water content and ∇^2 the Laplacian space operator. The ordinate z is taken positive downward. For steady flows, equation (2.12) takes the form **(Philip, 1968, 1969, 1971; Raats, 1970, 1971, 1972)**

$$\nabla^2 \phi - \alpha \frac{\partial \phi}{\partial z} = 0 \qquad \ldots(2.9)$$

Assuming $d\theta/d\phi$ to be constant leads to the linearized form with time

$$\frac{\partial \phi}{\partial t} = \frac{\mathbf{k}}{\alpha}\nabla^2\phi - \mathbf{k}\frac{\partial \phi}{\partial z} \qquad \ldots(2.10)$$

where

$d\theta/d\phi = \alpha/k,$ $\qquad k = dK/d\theta$

The initial and boundary conditions used for different types of sources under steady state and unsteady state conditions are given in Table 2.2.

2.3.1.1 Steady state solutions

If trickle irrigation is applied frequently and water application periods are sufficiently long, the flow at some distance from the source approaches a steady state condition (**Merill *et al.*, 1978**). Of course a truly steady state flow can never be achieved during trickle infiltration, but it represents an asymptotic case which permits the use of a simple theory for the practical purposes of designing trickle irrigation (**Bresler, 1978**). In the following text, steady state models with point, disc and line sources are discussed.

a. Point source

When water is applied through emitters on the soil surface and the emitter discharge is not higher than the water intake rate of the soil, hemispherical flow geometry develops below the soil surface. At the point of application the matric suction is zero and outside the hemisphere $-\infty$.

Table 2.2. Initial and boundary conditions used for various trickle sources.

S. No.	Source	Initial Condition	Boundary Conditions
1.	Surface point source	$\phi(r,z,0) = 0$	$-\partial\phi/\partial z+\alpha\phi = 0,\ z = 0,\ r \neq 0$
2.	Surface point source with loss at surface	$\phi(r,z,0) = 0$	$-\partial\phi/\partial z+\alpha\phi = -(\alpha m/2)\ \phi,\ z = 0,\ r \neq 0$
3.	Surface line source	$\phi(x,y,z,0) = 0$	$-\partial\phi/\partial z+\alpha\phi = 0,\ z = 0,\ x \neq 0$
4.	Surface line source with loss at surface	$\phi(x,y,z,0) = 0$	$-\partial\phi/\partial z+\alpha\phi = -(\alpha m/2)\ \phi,\ z = 0,\ x \neq 0$
5.	Surface disc source	$\phi(r,z,0) = 0$	$-\partial\phi/\partial z+\alpha\phi = 0,\ z = 0,\ r > r_0$
6.	Surface strip source	$\phi(x,y,z,0) = 0$	$-\partial\phi/\partial z+\alpha\phi = 0,\ z = 0,\ \|x\| > x_0$

where m is the surface flux proportionality constant

Philip (1968) introduced the quasilinear approximation to unsaturated porous media and then obtained the first solution to single point source buried in an infinite three-dimensional media using the known results from **Carslaw and Jaeger (1959)**.

The partial differential equations for matric flux potential and Stokes stream function were derived by **Raats (1971)** using the approach similar to quasilinearization. The solution of **Philip (1968)** for buried point source was used to obtain an analogous solution for point source at surface after incorporating the boundary conditions at surface. Similar expression were given by **Philip (1971)** as a theorem that enables the solution of the quasilinearized steady infiltration equation for any distribution of surface sources to be found immediately from the corresponding solution for buried sources. **Raats (1972)** generalized this theorem to an arbitrary distribution of sources at arbitrary depths.

Raats (1976) investigated the steady flow from point and line sources to point and line sinks, as well as the steady vertical flow subject to distributed uptake by plant roots and water table.

Using Cauchy-Reimann condition **Raats (1977)** derived the partial differential equation in terms of stream function. The solution was obtained in terms of stream function using separation of variables. The results included expression describing flow pattern, the distribution of matrix flux potential, pressure head, water content and total head.

Warrick *et al.* (1980) discussed the radially symmetric flow from a surface point source with water uptake modeled by various combinations of disc and cylindrical sinks.

The point source solutions may serve as a reasonable approximation in some situations, but, they generally fall short of giving realistic representation of flow from physical sources of non-zero dimensions i.e. circular, semicircular, spherical and hemispherical sources (**Pullan, 1990**).

b. Disc source

When the emitter discharge is higher than the intake rate of the soil, water starts ponding around the source and a disc of saturated soil surface is formed. The radius of this disc increases with time and reaches equilibrium after some time. The flow geometry of the wetted front follows an oblate spheroidal geometry.

The first application of quasilinearization to a problem of disc source with constant matric flux potential specified on the source boundary was given by **Wooding (1968)**. The problem of mixed boundary conditions was reduced to a system of dual integral equations and solved by a modified Tranters method. The important discussion made in the paper regarding total flux through system and distribution of the unsaturated flow were explored in many subsequent studies (**Bresler, 1978; Philip, 1986; Weir, 1987; Warrick, 1992**, etc.). **Philip (1984)** stated that "Woodings work is a heroic piece of mathematics. It may be that the complications of Woodings study have discouraged

others from attempting problems of steady infiltration from finite supply surfaces with h fixed at such surfaces." This may be the reason that the literature remained devoid of any further studies on disc source for a long spell of time.

c. Line source

When the spacing of the emitters along the lateral is such that the flow geometry of the emitters are interacting with each other and emitter flow rate is not higher than the intake rate of the soil, a water saturated line is formed below the line of sources. In this case the flow may be considered to be two-dimensional.

Parlange (1972) included the time dependence and solved the problem of multi-dimensional infiltration by single perturbation technique. The case of a spherical cavity is treated explicitly as an illustrative example. **Parlange (1973)** again used the same technique and derived analytical expression for absorption of water when the flux of water at the cavity surface was imposed. It was noted that after a certain time the soil around the cavity may become saturated and the growth of the saturated region with time was examined.

Philip (1969) presented the quasilinear form of Richards equation in which diffusivity and $dK/d\theta$ were assumed to be constant.

Warrick (1974b) analyzed the water flow from a point source using quasilinear form of the Richards equation as governing equation. The analytical solution for buried point source was adopted from **Carslaw and Jaeger (1959)**. The solution for surface point source was

derived using theorem of **Philip (1971)**. **Warrick and Lomen (1976)** who obtained analytical solution for water flow from strip and disc sources also used similar approach. The results were compared with the point and line source solutions of **Warrick (1974a)**.

After the theories of **Raats (1971)**, **Parlange (1973)** and **Warrick (1974a)** describing constant flux infiltration, **Clothier and Scotter (1982)** re-examined the gravity free infiltration using a method based on flux concentration approach of **Philip and Knight (1974)**. Experimental verification of results and comparison with above theories concluded that the early stages of infiltration (up to 120 min) from a small cavity into a fine sandy loam were described by the simple absorption theory presented in the paper. In another paper, **Clothier *et al.* (1985)** further discussed the experimental (field and laboratory tests) comparisons of the theories (including **Wooding, 1968**). It was concluded that the Woodings theory is more applicable to trickle irrigation.

Ben-Asher *et al.* (1986) derived an analytical expression for the position of wetting fronts for infiltration (gravity free) from a point source in the presence of water extraction using an approximate hemispherical model. The results were compared and found consistent with available experimental data of **Roth (1974), Taghavi *et al.* (1984), Clothier and Scotter (1982), Bar-Yosef and Sheikolslami (1976)** and **Ben-Asher (1979)**.

Smetten *et al.* (1994) obtained an analytical solution for unconfined gravity free, three-dimensional flow from the disc infiltrometer into soils that are homogenous and isotropic over the depth of wetting. The results were tested against laboratory experimental data with Redland soils.

The solutions under various assumptions for steady state conditions are presented in Table 2.3.

2.3.1.2 Unsteady state solutions

The unsteady state solutions related to trickle irrigation may be classified into two categories: those with constant source dimensions or fixed boundary, and those with source dimensions changing with time or moving boundary. Most of the models with fixed boundary used flow velocity or flux specified at the supply surface, whereas, the models having moving boundary used more natural boundary conditions i.e. moisture potential/content specified at the supply surface.

The solutions under various assumptions for steady state conditions are presented in Table 2.4.

2.3.2 Numerical solutions

The Richards equation in its nonlinear form is difficult to solve analytical, and thus, numerical solutions are necessary to be developed to explore the non-dimensional behaviour of water flow in unsaturated media. Numerical solutions to the Richards equation under varying simplifications and various experimental soil properties were used to

Table 2.3 Steady state analytical solutions for infiltration below trickle sources.

Model No.	Source	Solution	Given by
1.	One dimensional step sink	$\phi_s(z)=\begin{cases}[m/(2+m)](a/\alpha^2)[1-\exp(-\alpha z_0)] \\ -(a/\alpha^2)\{(\alpha z+1)-\exp[\alpha(z-z_0)]\}, & 0<z<z_0 \\ [m/(2+m)](a/\alpha^2)[1-\exp(-\alpha z_0)]-az_0/\alpha, & z>z_0\end{cases}$	Warrick *et al.* (1979)
2.	Two dimensional line source	$\phi=\frac{q}{2\pi}\{\exp(Z-D)[Ko(\sqrt{X^2+(Z-D)^2})+K_o(\sqrt{X^2+(Z+D)^2})]-2(1+m)\exp(mD+(2+m)Z)\times\int_{Z+D}^{\infty}\exp(-(1+m)\eta)K_o(\sqrt{X^2+\eta^2})d\eta$	Lomen and Warrick (1978)
3.	Point source	$\phi=2\left\{\phi_B-e^{2Z}\int_Z^{\infty}e^{-2Z'}[\phi_B]_{Z=Z'}dZ'\right\}$ $\phi_B=(\alpha q/8\pi\rho)\exp(Z-\rho),\quad \rho^2=R^2+Z^2$	Warrick (1974)
4.	Disc source (or sink) at depth z_o	$\phi=(\alpha q/4\pi R_o)\int_0^{\infty}\frac{J_o(\lambda R)J_1(\lambda R_o)}{(1+\lambda^2)^{1/2}}\psi(Z,\lambda,Z_o)d\lambda$ $\psi(Z,\lambda,Z_o)=\exp(Z-Z_o)\{\exp[-\lvert Z-Z_o\rvert\sqrt{1+\lambda^2}]+\frac{(\sqrt{1+\lambda^2}-1)}{(\sqrt{1+\lambda^2}+1)}\exp[-(Z+Z_o)\sqrt{1+\lambda^2}]\}$	Warrick *et al.* (1980)
5.	Cylindrical source (or sink) with radius r_o and depth z_o	$\phi(R,Z)=(\alpha q/4\pi R_o)\int_0^{\infty}\frac{J_o(\lambda R)J_1(\lambda R_o)}{(1+\lambda^2)^{1/2}}\times\left\{\frac{b}{[1-\exp(-bZ_o)]}\frac{(\sqrt{1+\lambda^2}-1)\exp[Z(1-\sqrt{1+\lambda^2})]}{(\sqrt{1+\lambda^2}+1)(b+1+\sqrt{1+\lambda^2})}\times\left(1-\exp[-Z_o(b+1+\sqrt{1+\lambda^2}]+1\right)\right\}d\lambda$ where I $=\begin{cases}\frac{\exp[Z(1-\sqrt{1+\lambda^2})]\{1-\exp[-Z(b+1-\sqrt{1+\lambda^2})]\}}{[b+1-\sqrt{1+\lambda^2}]} \\ +\frac{\exp(-bZ)-\exp[-bZ_o+(Z-Z_o)(1+\sqrt{1+\lambda^2})]}{[b+1-\sqrt{1+\lambda^2}]}, & 0<Z<Z_o \\ \frac{\exp[Z(1-\sqrt{1+\lambda^2})]\{1-\exp[-Z_o((b+1-\sqrt{1+\lambda^2})]\}}{[b+1-\sqrt{1+\lambda^2}]}, & Z_o<Z\end{cases}$	Warrick *et al.* (1980)

Note: The suffix B stands for buried and the dimensionless coordinate are expressed as $X=\alpha x/2$; $R=\alpha r/2$; $Z=\alpha z/2$; $Z_o=\alpha z_o/2$; $D=\alpha d/2$; $R_o=\alpha r_o/2$.

Table 2.4 Unsteady state analytical solutions for infiltration below trickle sources.

Model No.	Type of source	Solution	Given by
1.	Surface point Source	$\phi = 2\left\{\phi_B - e^{2Z}\int_Z^\infty e^{-2Z'}[\phi_B]_{Z=Z'}dZ'\right\}$ $\phi_B = \frac{\alpha q e^{Z}}{16\pi\rho}\{e^{\rho}\text{erfc}\,[\rho/(2\sqrt{T}) + \sqrt{T}]$ $+ e^{-\rho}\text{erfc}\,[\rho/(2\sqrt{T}) - \sqrt{T}]\}$	Warrick (1974)
2.	Surface point Source with loss at surface	$\phi = \phi_B(X,Z-D,T) + \exp(-2D)\phi_B(X,Z+D,T) + F(R,Z,T)$ where, $F(R,Z,T) = -\frac{\alpha q}{8\pi}(1+m)\exp(mD + (2+m)Z)$ $\times \int_0^T \xi^{-1}\exp(m(m+2)\xi - R^2/4\xi)$ $\times \text{erfc}(1+m)\sqrt{\xi} + (Z+D)/2\sqrt{\xi})d\xi$ and ϕ_B from 1 above	Lomen and Warrick (1978)
3.	Surface line source	$\phi = 2\{\phi_B - \exp(2Z)\times\int_Z^\infty \exp(-2Z')[\phi_B]_{Z=Z'}dZ'\}$ $\phi_B = \frac{qe^{Z}}{4\pi}\int_0^T \xi^{-1}\exp[-\xi - (X^2+Z^2)/4\xi]d\xi$	Lomen and Warrick (1974)
4.	Surface line source with loss at surface	$\phi = \phi_B(X,Z-D,T) + \exp(-2D)\phi_B(X,Z+D,T)$ $-\frac{q(1+m)}{2\sqrt{\pi}}\exp(m(m+2)\xi - X^2/4\xi)\text{erfc}\left(\frac{Z+D+2(1+m)\xi}{2\sqrt{\xi}}\right)d\xi$ where and ϕ_B from 3 above	Lomen and Warrick (1978)
5.	Surface strip source	$\phi = 2\{\phi_{2B} - \exp(2Z)\times\int_Z^\infty \exp(-2Z')[\phi_{2B}]_{Z=Z'}dZ'\}$ $\phi_{2B} = \frac{qe^{Z}}{8X_o\sqrt{\pi}}\int_0^T \tau^{-1/2}\exp(-\tau - Z^2/4\tau)$ $\times[\text{erf}\{(X+X_o)/2\sqrt{\tau}\} - \text{erf}\{(X-X_o)/2\sqrt{\tau}\}]d\tau$	Warrick and Lomen (1976)
6.	Surface disc source	$\Phi = (2/R_0)\int_0^\infty J_0(\lambda R)J_1(\lambda R_0)$ $\left\{\frac{\exp[Z(1-\sqrt{1+\lambda^2})]\text{erfc}(Z/2\sqrt{T} - \sqrt{(1+\lambda^2)T})}{1+\sqrt{1+\lambda^2}}\right.$ $+\frac{\exp[Z(1+\sqrt{1+\lambda^2})]\text{erfc}(Z/2\sqrt{T} + \sqrt{1+\lambda^2 T})}{1-\sqrt{1+\lambda^2}}$ $\left.+\frac{2\exp(2Z - \lambda^2 T)\text{erfc}(Z/2\sqrt{T} + \sqrt{T})}{\lambda^2}\right\}d\lambda$	Warrick and Lomen (1976)

Note: Dimensionless coordinate are expressed as $X = \alpha x/2$; $R = \alpha r/2$; $Z = \alpha z/2$; $Z_o = \alpha z_o/2$; $D = \alpha d/2$; $R_o = \alpha r_o/2$; $T = \alpha kt/4$; $k = dK/d\theta$

check the assumptions included in analytical solutions. Finite difference, finite element and boundary element methods were usually used to obtain numerical solutions.

The first and most quoted numerical solution to partial differential equation (2.12) with Kirchaffs transformation was given by **Brandt *et al.* (1971)** for transient infiltration from a trickle source. Solutions were developed for two types of sources viz. strip source and disc source. The width/radius of saturation was considered as a function of time (i.e. moving boundary) with specified moisture content in the study. The three dimensional solution was obtained in cartesian coordinates for strip source and in cylindrical coordinates for disc source. Tabulated experimental values of $K(\theta)$ which was interpolated using cubic spline for intermediate values were used in the simulation. The solution was checked with **Wooding (1968)** results for steady infiltration that approached after 999 min for $\phi/\phi_s = 0.05$. **Bresler *et al.* (1971)** compared the results of this model with experimental data and found good agreement with some discrepancies observed for large trickle discharge rates.

Bresler (1978) again used the model of **Brandt *et al.* (1971)** to quantify the effect of soil hydraulic properties and trickle discharge on unsteady state infiltration from a trickle source. The results of **Wooding (1968)** to linearized steady infiltration were also used to derive surface distribution of matrix flux potential function and the expression for steady radius of saturated zone. The results were then employed to

estimate the emitter spacing. Hydraulic conductivity parameters were given for 17 different soils to be used for design purposes.

Ben-Asher *et al.* (1979) compared the analytical solution of **Warrick (1974b)** with numerical solution of **Brandt *et al.* (1971)**. For cyclic condition the results were approximately same with regards to change in values between the wettest and driest values.

Finite element method was used by **Taghavi *et al.* (1984)** to solve the nonlinear partial differential equation of infiltration from a trickle source and the results were compared with an experiment conducted on clay loam soil. For the simulation of trickle irrigation flow, disc of constant radius (r_o) was assumed as source for which flux was taken as constant. The disc radius was also considered as function of time, determined by the relationship $r(t) = t(r_o/t_o)$, where r_o and t_o were the maximum radius and irrigation time respectively. This did not improve the results. The model was again applied to steady state moisture flow in a heterogeneous medium by **Taghavi *et al.* (1985)** and was compared with the experimental results of **Merill *et al.* (1978)**.

Healy and Warrick (1988) presented a generalized empirical method for estimation of the time variant wetting front and wetted volume due to infiltration from a surface point source. The method is based on a finite difference solution. The results were empirically fitted to the following type of equation

$$D = At^{1/2} + Bt + Ct^{3/2} \qquad ...(2.11)$$

where D is distance of wetting fronts (diagonally, vertical down and horizontally away) from origin of wetted volume. The values of constants A, B and C were tabulated for different soil parameters and discharge. The method was compared with experimental data of **Clothier and Scotter (1982)** and the results of model given by **Bresler (1978)**.

Lafolie *et al.* (1989) presented a new method for finite difference approximation of partial differential equation governing the disc flow under trickle irrigation with moving boundary. It was claimed that the new method improved the prediction of the size of ponded area at the soil surface and was computationally efficient. The results were compared with the numerical solution of **Brandt *et al.* (1971)** and the experimental results given by **Ababou (1981)** and **Brandt *et al.* (1971)**. **Lafolie *et al.* (1989)** further confirmed the validity of the model by comparing it with experimental results for stratified and anisotropic soils.

Warrick (1992) compared the finite element solution for disc infiltration for large times with steady state models of **Wooding (1968)** and **Weir (1987)** and for small times with an approximation of the time dependent flow rate for linear diffusion from a disc presented by **Warrick *et al.* (1992)**. For these comparisons, K(h) function given by **Gardener (1958)** and **van Genuchten (1980)** were used.

Angelakis *et al.* (1993) conducted an experiment to measure soil-water distribution in homogeneous soil profile of Yolo clay loam and Yolo sand irrigated from a circular source of water. The experimental

results were then compared with the models given by **Warrick (1974b)**, **Taghavi *et al.* (1984)**, **Ben-Asher (1986)** and **Healy and Warrick (1988)**.

Bhatnagar *et al.* (1997) proposed a model in oblate spheroidal coordinate system to study the wetting pattern below a trickle (disc) source. Two types of boundary conditions viz. inflow through a saturated disc, and constant inflow through a disc were considered. The ADI finite difference method was used to solve the quasilinear governing equation. The model was validated with the analytical solution of **Warrick and Lomen (1976)** and the results were compared with the experimental results of **Clothier and Scotter (1982)**.

2.4 Other Studies Related to Emitter Discharge

In this section the studies which are related to trickle irrigation, but not included in above discussion are discussed.

Bar-Yosef and Sheikholslami (1976) conducted a laboratory experiment to study distribution of water from a trickle source. The data generated regarding hydraulic conductivity, water retention curve and soil water distribution (time dependent) were presented with the intention to enable verification of mathematical models against the experimental results obtained under various conditions.

The application of the known analytical solution to the design of trickle irrigation system was discussed by **Bresler (1977)**. **Amoozegar-Fard *et al.* (1984)** developed nomographs relating discharge rate, plant

uptake, and soil-water potential at a reference point for trickle irrigation system.

Russo (1983) used a geostatistical approach to investigate the spatial variability of two measured hydraulic parameters, K_s and α, for a heterogeneous soil. The results were applied to estimate the spatial distribution of the spacing between emitters required to achieve the prescribed value of h_c (soil-water pressure midway between the emitters), uniform through out the field. The analysis was based on recommendations of **Bresler (1978)**.

2.5 Design of Lateral Line

In drip irrigation systems the lateral lines are the pipes on which emitters are installed. They receive water from manifolds and are usually made of plastic tubing (LLDPE) ranging in diameters from 12 to 25 mm. A precise design of drip irrigation lateral is important because the allowable pressure variation or pressure head losses in a drip irrigation system are much smaller than in sprinkler irrigation laterals.

If the pressure distribution along the lateral line can be determined, uniform irrigation can be achieved by adjusting size of emitters (**Myers and Bucks, 1972**) length or diameter of microtube (**Kenworthy, 1972**) or slightly adjusting the spacing between emitters **(Wu and Gitlin, 1973)**. Although, the measures suggested above may yield a uniform distribution of water but, are not feasible from operation and maintenance point of view. Therefore, if the design allows certain

variation of emitter outflow along the lateral line, a single type of emitter or same size of microtubes can be used with uniform spacing which will eliminate the problem of installation, operation and maintenance of the drip irrigation system.

The variation of flow from emitters is from two sources viz. variation due to manufacturing error in emitters (manufacturing variation) and variation due to operating pressure head at the emitter (hydraulic variation). The manufacturing variation can be controlled only up to certain limits. But the hydraulic variation is a function of the total length of lateral and inlet pressure head, emitter spacing and total flow rate. This creates a design problem to select the right combination of length and inlet pressure in order to achieve an acceptable non-uniform pattern of irrigation.

Over the past, numerous researchers have developed design equations considering the flow in a microirrigation lateral to be steady, spatially varied flow with uniform lateral outflow. **Yitayew and Warrick (1988)** considered that the emitters are so close that the trickle lateral can be regarded as a homogeneous system of a main tube with a longitudinal slot.

2.5.1 Energy gradient line (EGL) approach

Wu and Gitlin (1974) presented a general shape of the energy gradient line (EGL) which can be applied to estimate the distribution and variation of emitter discharge along a lateral line. The flow in the lateral was considered to be turbulent flow in smooth pipes and

accordingly Blasius equation was used to determine the friction factor. The approach is applicable when the variation in emitter outflow is very small (less than 10 percent) and emitters are equally spaced. Discharge from the emitters was considered to be proportional to square root of the operating pressure at the emitter. Based on this dimensionless EGL, design charts were developed to determine a combination of lateral length and inlet pressure for a desirable or acceptable uniformity coefficient (Christiansens).

Wu and Gitlin (1975) derived a simplified equation for EGL

$$R_i = 1 - (1 - i)^{m+1} \qquad \ldots (2.12)$$

where,

i = l/L, a ratio of a given length (l) from the inlet to the total length (L)

R_i = $\Delta H_i/\Delta H$, energy drop ratio

ΔH_i = total friction drop at a given length ratio i

ΔH = total friction drop at the end of the pipeline

m = an exponent of total discharge in the friction drop equation

This equation can also be used with Williams-Hazen equation and has been found very useful in analyzing the hydraulics of irrigation systems (drip and sprinkler).

Wu and Yue (1993) developed an energy gradient line approach for design of drip lateral line. This approach provided direct calculation of all emitter flows along the lateral line by the equation

$$q_i = q_o\left(1 - R_i \frac{\Delta H}{H} + R'_i \frac{\Delta H'}{H}\right)^x \qquad \ldots (2.13)$$

where,

q_i = emitter at a given length ratio i

q_o = emitter flow at the inlet determined by operating pressure

R'_i = $\Delta H'_i / \Delta H'$

$\Delta H'_i$ = energy gain for down slope laterals at a given length ratio i

$\Delta H'$ = total energy gain for down slope laterals at the end of the pipeline

x = emitter flow exponent

The errors from this approach were evaluated and a revised approach was developed. Simple equations were derived for calculating emitter flows and can be used to develop computer-aided design for a drip irrigation lateral line.

2.5.2 Graphical approach

Wu and Gitlin (1974) presented design charts for determination of acceptable combination of lateral length and inlet pressure of drip irrigation system. The design charts were prepared considering the general slope of energy gradient line, which can be applied to estimate distribution and variation of emitter discharge along the lateral. For the purpose of estimation of friction losses in the pipeline the flow was considered to be turbulent flow in smooth pipes. The charts help in selecting a drip irrigation line based on a desirable or acceptable coefficient of uniformity.

Howell and Hiller (1974) conducted an study on the design of trickle irrigation laterals with the objectives to develop design methods

for trickle irrigation laterals with application to orchard crops; and to develop inputs necessary for precise engineering design based on the experimental data. They developed two design methods among which one involves a computer programme while the other is a simplified procedure that is applicable when reduction coefficients are known. The design was based on the balance between friction losses and optimum variation in head (20 per cent) which maintained a lateral uniformity coefficient of at least 95 per cent as suggested by **Wu and Gitlin (1974).** The water requirement of the crop was calculated by the equation

$$R = 0.623\ E.A.P \qquad (2.14)$$

where,

R is the design application rate per tree per day, lpd

E is the peak consumptive use rate, in/day

A is the tree spacing, ft^2

P is the dimensionless coverage factor.

The disadvantages of the study were the several assumptions required in analysis and the pressure gain cause by the dividing flow in the lateral was neglected. The computer programme utilized a single value of the lateral slope.

Pitts *et al.* (1986) formulated the design procedure including an estimation of the uniformity with which water is applied to the crop. A microcomputer model, using fundamental hydraulic relationships to simulate flow within a lateral line was developed. The Darcy-Weisbach formula was used to compute the head loss. The head loss due to

emitter barb was considered in terms of equivalent length of pipe, which was expressed as

$$L_e = 0.25 \times B_w(19D_l) \quad \ldots(2.15)$$

where,

L_e is the equivalent length of pipe, m

D_l is the diameter of lateral, mm

B_w is the diameter of emitter barb.

All the methods mentioned above are based on the assumption of uniform outflow from emitters.

2.5.3 Numerical approach

Kang and Nishiyama (1996a) presented a method for the design of microirrigation laterals based on the required average emitter discharge and the required uniformity of water application. The finite element method was used to analyze the hydraulics of a lateral. In order to save the computation time, the golden section search was employed to find the operating pressure head of the lateral that can produce the required average emitter discharge. In the paper it was also shown that the lateral length for the required uniformity of water application may have three solutions and the diameter may have two solutions when laterals are laid on sloped fields.

The finite element method has been used to analyze, the hydraulics of subunits of trickle irrigation systems (**Bralts and Segerlind, 1985**), the hydraulics of pipe networks (**Haghighi *et al.*, 1988**), the hydraulics of sprinkle irrigation systems (**Saldivia *et al.*,**

1990), and the hydraulics of microirrigation systems (**Kang and Nishiyama, 1994**). All of these methods used a large band matrix, which requires a large computer memory. Therefore, it is difficult to analyze a submain unit using a personal computer if the number of emitters is large.

Bralts *et al.* (1993) used virtual emitter system to reduce the width of the band matrix and expedite calculations. However, the method still has size limitations (band width = 15 and 27 when the seven node configuration is used for submain units with single and paired laterals, respectively) and reduces the calculation accuracy.

Kang and Nishiyama (1996b) presented a lateral discharge equation approach for designing single as well as paired laterals. The lateral discharge equation (polynomial of n^{th} order, n = 3 ~ 7) was used to express the relationship between the discharge and the pressure head at the inlet of a lateral. Based on this approach **Kang and Nishiyama (1996a)** developed a simple method for design of microirrigation laterals. Back step method was used to generate data sets of discharge and pressure head at the inlet of the lateral and forward step method to analyze the hydraulics of the lateral. Given one of the parameter of lateral (diameter or length), required average emitter discharge, and required uniformity of water application the other parameter of the lateral and operating pressure head of the lateral can be determined. This approach has been very accurate for designing single and paired laterals under uniform and variable slope conditions.

2.5.4 Statistical approach

Anyoji and Wu (1987) presented an approach based on statistical analysis for design of trickle laterals. The technique is based on the coefficient of variation of pressure head along a lateral line and the variations of emitter flow caused by manufacturer. Considering the coefficient (K) and pressure (H) in the emitter flow equation ($q = KH^x$) as two random variables, an equation for mean emitter was derived using Taylors theorem. The coefficient of variation of K indicates the manufacturers variation. The coefficient of variation of pressure head is determined statistically from the average and variance of pressure head, which is affected by friction and slope changes along the lateral line. Once a design criterion of an emitter flow variation is set and a type of emitter is selected, the required coefficient of variation of pressure head for the lateral line can be calculated and the design length can be determined.

2.5.5 Step by step analysis

Hathoot *et al.* (1993) presented a stepwise calculation method for analysis and design of trickle laterals laid along uniform field slopes with equally spaced emitters. In the method presented, a small increment of pressure head is given at the inlet of the lateral. Individual emitters were considered in discharge and pressure estimation along the lateral. The friction head loss between successive emitters is estimated by Darcy-Weisbach formula, taking into account the variation

of Reynolds number, the different zones of Moody diagram and friction coefficient formula corresponding to each zone. In addition, the change in velocity head was also taken into account. Based on the required average emitter discharge and the required uniformity of water application, a design chart similar to that presented by **Yitayew and Warrick (1988),** was developed. This method has the highest accuracy because only the basic equations of the hydraulics of steady pipe flow were used. These methods can be used to design a single lateral for flat and sloped field conditions. However, it is not possible with these methods to design paired laterals.

An important component of the designing paired laterals is to determine the best submain position. **Keller and Bliesner (1990)** reported that the best submain position is that location of submain where same pressure variation exists in uphill and downhill laterals. This concept has been very useful for design of paired laterals when methods presented by **Keller and Bliesner (1990)** and **Wu and Gitlin (1975)** are used. However, the determined location is an approximate solution of the best submain position in most cases when considering Christiansens uniformity coefficient (UCC), low-quarter distribution uniformity, and emitter flow variation (V_{HM}). It is far from the correct solution in many cases (**Kang and Nishiyama, 1996c**).

2.6 Design of Submain

Trickle irrigation submains are multi-outlet pipelines like laterals. They differ from laterals in their flow capacity. Due to high magnitude of

flow the head loss due friction in such pipelines is high and therefore, they are generally tapered with up to four different pipe sizes. To ensure adequate flushing, the smallest pipe should not be less than one-half the diameter of the largest pipe. The velocity in the manifolds should be limited to about 2 m/s (**Keller and Bliesner, 1990**). The methods developed for designing submain line and various optimization models developed for multi-outlet pipe network design are discussed briefly in this section.

Wu and Gitlin (1974) presented two simplified charts, one for submain slopes less than 0.5 per cent and the other for submain slope equal to or greater than 0.5 per cent. The main drawback of the design was that it fails to design the submain having high lengths and steep slopes.

Wu and Gitlin (1977) developed the submain design charts considering the maximum submain slope of 20 per cent. They also considered the geometry of the field for design of submain. The maximum slope for triangular shape of the subunit was 30 per cent and for rectangular and trapezoidal shapes of the subunit was about 20 per cent for the length and head ratio less than 5. The design chart was developed for rectangular subunit and when the field shape is not rectangular, the design can be made by adjusting the total discharge so that the design chart made for rectangular fields can be used directly.

Lopez (1985) developed the graphical and numerical procedures to calculate the friction head loss in manifolds feeding the lateral laid on

any shaped field. He considered shape factor for the geometry of the field and developed a formula for the multi-outlet factor, F, and based on this formula the friction head loss was calculated. Both the numerical and graphical solutions given by him make it possible to design tapered manifolds for almost any geometry or shape of the field. The method proposed neglects the slope of the slope of the submain, which was considered to be the main disadvantage of the method.

Wu (1985) presented a graphical method known as Uni-plot, for the design of drip irrigation laterals and submains. The technique was derived from the Poly-plot concept of **Herbert (1971).** The design was made by using the line slope and an allowable pressure variation to form a reference area and then fitting the energy gradient curve into the reference area.

Paco (1985) considered the shape of the areas to which a submain supplies water in a drip irrigation system. He considered the trapezoidal shape as a general and then developed the particular cases for rectangular or triangular shapes. He mainly considered the friction head losses in drip irrigation manifold and developed a general formula for the calculation of the reduction factor.

$$F = \int_0^1 \left(1 \mp \frac{u}{f}\right)^m (1-u)^m \, du \qquad \ldots (2.16)$$

where,

m = discharge exponent,

f = shape factor,

u = ratio of distance, up to which the head loss is to be calculated, and the total length of manifold,

F = reduction factor.

The negative sign (-) is for the laterals with decreasing length towards the end of the manifold and positive sign (+) is for the laterals with increasing length towards the end of the manifold.

Keller and Bliesner (1990) proposed graphical and numerical methods based on the universal economic pipe size selection chart and hydraulic grade line. The graphical design procedure proposed can be used for single pipe size or tapered submain on uniform as well as irregular topography. The method requires standard manifold curves. Using these standard curves, the approximate length and diameters of different segments of the tapered submain can be determined. They also developed an economic pipe size selection chart to select pipe size and the length of submain feeding the rectangular subunits and calculated equivalent annual cost of escalating energy per water horsepower.

Hozapfel *et al.* (1990) developed a nonlinear optimization model for the design and management of multiple subunit drip irrigation systems. In this model, the objective function represents the net benefit due to the sale of the crop and is a function of water application and the costs of implementation and operation of the drip irrigation system.

Mohtar *et al.* (1991) developed a finite element model for the optimization of complex pipe networks using life cycle costing technique. The model is applicable to a variety of practical design

situations including farm irrigation pipe networks and municipal water systems.

Zazueta and Smajstrala (1995) developed analytical expression to obtain the pipe diameter of a sloping tapered multiple outlet pipe. The expressions were based on the assumption that outflow from a multiple outlet pipe is continuous and constant along the pipe and that the friction coefficient is constant. An intermediate correction factor was developed that allows computation of head losses between any two points of a multiple outlet line.

Kang and Nishiyama (1996b) used finite element method to analyze the hydraulics of the lateral. The methodology used provides a symmetrical tridiagonal stiffness matrix, which is easy to solve, and requires minimum computer memory.

Dandy and Hassanli (1996) presented a nonlinear model for the optimum design and operation of drip irrigation systems on flat terrain. The design was based on dividing the field into subunits and evaluating various shift patterns and corresponding pipe and pipe sizes in order to identify a minimal cost solution. The optimization procedure involves a complete enumeration approach, which minimizes the sum of the capital cost of the system and present value of the operating cost.

Singh *et al.* (2000) presented a method for optimal design of a microirrigation submain. Based on the shortest route algorithm, the method is used to determine lengths of different pipe sizes that would result in minimal cost of the submain. Different route lengths were

represented by total annual costs of different pipe sizes between two successive laterals. The method was compared with graphical method of **Keller and Bliesner (1990)** through numerical example.

2.7 Determination of head loss due to friction

Determination of head loss due to friction in multioutlet pipes is different from that in plain pipes because of decreasing flow in the multioutlet pipelines.

2.7.1 Head loss due to friction in plain pipes

Hazen-Williams formula

This is the most commonly used formula for estimating friction head losses in sprinkler and microirrigation systems and mainlines of various pipe materials. The formula is given as:

$$\Delta H = k\left(\frac{Q}{C}\right)^{1.852} \times D^{-4.87} \times L \times 100 \qquad (2.17)$$

where,

Q = flow rate in pipe, l/s

ΔH = head loss due to friction in pipe, m

k = conversion constant, 1.212×10^{12} for metric units

C = friction coefficient (depends on pipe material characteristics)

L = length of pipe, m

D = inside diameter of the pipe, mm

Darcy-Weisbach formula

Darcy-Weisbach formula is a dimensionally homogeneous formula, which is used for estimating friction loss in pipes. The Moody diagram shows the relationship between the relative roughness of pipe and the Darcy-Weisbach friction factor (f) for different values of Reynolds number (R_e). The Darcy-Weisbach formula which relates the friction factor (f) to the head loss in pipes, due to friction (ΔH) is given as:

$$\Delta H = f \frac{L}{D} \frac{v^2}{2g} \qquad \ldots (2.18)$$

where

f = Darcy-Weisbach friction factor, dimensionless

v = velocity of flow in the pipe, m/s

g = acceleration due to gravity = 9.81 m/s^2

D = inside diameter of pipe, mm

Depending upon the flow conditions the Darcy-Weisbach friction factor (f) can be calculated as follows

(i) For laminar flow ($R_e < 2000$)

$$f = \frac{64}{R_e} \qquad (2.19)$$

(ii) For turbulent flow ($3000 < R_e \leq 10^5$), the Blasius equation can be used

$$f = \frac{0.316}{R_e^{0.25}} \qquad (2.20)$$

(iii) For fully turbulent flows ($10^5 < R_e \leq 10^7$), **Watters and Keller (1978)** equation can be used

$$f = \frac{0.13}{R_e^{0.172}} \tag{2.21}$$

In an experiment conducted by **Watters and Keller (1978),** it was demonstrated that the Darcy-Weisbach formula should be used for estimating friction head losses in smooth plastic pipes and tubings.

2.7.2 Head loss due to friction in multi-outlet pipes

The microirrigation lateral lines and submains are the pipes with multiple outlets discharging laterally. The flow conditions in such pipes are generally considered as steady, spatially varied with decreasing discharge. Flow of water through the length of a single outlet (plain) pipe of a given diameter causes more friction loss than does flow through a pipe with a number of outlets. This introduces complications in estimation of friction losses in multi-outlet pipes. The estimation of head loss caused by friction in pipelines with multiple outlets requires a stepwise analysis starting from most downstream outlet, working upstream and computing head loss caused by friction in each segment. **Christiansen (1942)** developed a friction factor known as F factor, to avoid the cumbersome stepwise analysis. Computing the head loss in a pipe considering the entire discharge to flow through the entire length and multiplying by factor F allows the head loss through a through a single diameter pipeline, with multiple outlets to be estimated. The derivation of factor F was based on the following assumptions:

i) No outflow at the downstream end of the pipeline,

ii) All outlets are equally spaced,

iii) All outlets have equal discharge, and

iv) The distance between the pipe inlet and the first outlet is equal to outlet spacing.

Christiansens factor F can be written as:

$$F = \frac{1}{m+1} + \frac{(m-1)^{0.5}}{6N^2} \qquad \ldots(2.22)$$

where,

m is the velocity or flow exponent in the head loss equation used, and

N is the number of outlets in the pipeline.

In many situations (generally in sprinkler irrigation systems) first outlet cannot be located in a full spacing from the pipe inlet. **Scaloppi (1986)** derived the adjusted factor F_α that allows for calculating head loss in single diameter pipelines with multiple equally spaced outlets and the first outlet at any distance from the pipeline inlet. This work also assumes zero outflow at the downstream end of the pipeline. The adjusted factor F_α may be expressed as:

$$F(\alpha) = \frac{NF - (1-\alpha)}{N - (1-\alpha)} \qquad \ldots(2.23)$$

where, F is the Christiansens factor.

For a single diameter pipeline with multiple outlets, factor F or the adjusted factor F_α allows rapid calculation of head loss caused by friction. However, if multi-diameter pipelines are used, these factors

cannot be applied directly to the entire length of the pipeline. If for analytical purposes the pipeline is divided into reaches based on pipeline diameter, then again factor F cannot be applied directly to any except the most downstream pipe reaches. Because other reaches of the pipeline would have outflow at their downstream ends. To resolve this problem, **Anwar (1999)** proposed a factor G to estimate the friction head losses in multi-outlet pipes or pipelines with outflow at the downstream end. The factor G can be written as:

$$G = \frac{1}{N^{m+1}(1+r)^m}\left[\frac{1}{m+1}\left\{(N(1+r)+1)^{m+1} - (Nr)^{m+1}\right\} - \frac{1}{2}\left\{(N(1+r)+1)^m + (Nr)^m\right\} + \frac{1}{12}\left\{m(N(1+r)+1)^{m-1} - m(Nr)^{m-1}\right\}\right] \quad \ldots (2.24)$$

where

r = Q_o/Nq

Q_o = outflow discharge at the downstream end of the pipe beyond the last outlet

q = discharge of each outlet

N = number of outlets

m = exponent of average flow velocity in the pipeline, (= 2)

The review of literature related to the three-dimensional soil-water flow indicates that the flow under a point trickle source occurs from a circular saturated area developed around the point source. In case of line trickle source the flow occurs from a saturated strip developed along the line of source. The radius of the saturated disc in case of

point source or width of the saturated strip in case of line source changes with time and hence use of moving boundary conditions is most appropriate for modeling the flow. An effort may be made for use of soil texture based soil-water characteristic relationships.

The literature related to the design of microirrigation laterals and submain indicates that the most of the design procedures developed are based on the assumption of uniform discharge from the emitters. Generally the single laterals have been in mind of the researchers and not much emphasis has been given for paired and tapered laterals. The hydraulics of the microirrigation submains is similar to the laterals and therefore their design principles are the same.

Chapter 3

Theoretical Development

3. THEORETICAL DEVELOPMENT

This chapter deals with the theoretical development of the model and the methodology used for determination of emitter discharge and design of lateral and the submain lines.

3.1 Emitter Discharge

The emitters of trickle irrigation system are the outlets, which supply water directly to the plants. The emitters are designed in such a way so that enough water is supplied to the plant root zone to meet the plant water requirement. Normally, one-third to as much as three-fourths of the plant rooting volume should be supplied with adequate water (**Nakayama and Bucks, 1986**). The design will be safer if the percentage of wetted rooting volume relative to the total rooting volume is larger. However, if the wetted volume becomes too large, many of the advantages of trickle irrigation are lost. The shape of the wetted soil volume, which is described by soil-water distribution within the root zone depends on emitter discharge, duration of irrigation, emitter spacing and soil texture. In microirrigation systems water is applied frequently and hence the effect of irrigation interval on the wetted soil volume may be neglected. In most orchard and vegetable crops the spacing of the emitters is decided according to the plant to plant and row to row spacing. Therefore, emitter flow rate and soil texture plays a vital role in deciding the distribution of water within the root zone.

The soil-water distribution is determined by the soil properties and the way water is added and withdrawn from the profile. Factors which generally differentiate the soil-water regime of trickle from other sources are (1) the flow regime is 2 or 3-dimensional rather than vertical only; (2) the water is added at a high frequency; and (3) soil-water is maintained within a relatively narrow range.

3.1.1 Unsteady state flow problem

Over the past, mathematical models have been developed which describe the soil water regime under a trickle source. But, only few have presented guidelines for the design and operation of trickle irrigation system. In the present investigation, two types of trickle sources (viz. strip source and disc source) have been considered. The problem has been formulated to describe the three dimensional axially symmetrical soil-water flows from trickle source.

The formulation of the problem is based on the following assumptions:

1. Soil is a stable, isotropic, homogeneous and non-swelling porous medium.
2. Both, the soil-water content (θ) and the unsaturated hydraulic conductivity (K) of the soil are single valued and continuos functions of soil-water matric potential (h).
3. Darcy law is applicable in both saturated and unsaturated zones.
4. Initial water content (θ_n) is sufficiently low and uniform so that the movement of water is negligible everywhere in the system.

5. Evaporation and plant water uptake during the course of irrigation is negligible from the flow region.

Under these assumptions, the non-linear Richards equation which describes the three dimensional transient flow through a porous medium is adopted as governing equation.

3.1.2 Governing equation:

The flow through an unsaturated porous media is governed by the Richards equation, which is expressed in cartesian coordinates as:

$$\frac{\partial \theta}{\partial t} = \frac{\partial}{\partial x}\left(K(\theta)\frac{\partial H}{\partial x}\right) + \frac{\partial}{\partial y}\left(K(\theta)\frac{\partial H}{\partial y}\right) + \frac{\partial}{\partial z}\left(K(\theta)\frac{\partial H}{\partial z}\right) - S \qquad \ldots(3.1)$$

Introducing the term of diffusivity equation (3.1) takes the form

$$\frac{\partial \theta}{\partial t} = \frac{\partial}{\partial x}\left(D(\theta)\frac{\partial \theta}{\partial x}\right) + \frac{\partial}{\partial y}\left(D(\theta)\frac{\partial \theta}{\partial y}\right) + \frac{\partial}{\partial z}\left(D(\theta)\frac{\partial \theta}{\partial z}\right) - \frac{\partial K(\theta)}{\partial z} \qquad \ldots(3.2)$$

where,

θ = volumetric soil water content, cm^3/cm^3

$D(\theta)$ = soil water diffusivity, cm^2/min

H = total head, cm

= h - z

h = capillary potential or matric potential, cm

z = elevation head (measured +ve downward), cm

$K(\theta)$ = unsaturated hydraulic conductivity, cm/min

t = time, min

S = sink or source term

Brandt *et al.* (1971) used a new function of water content, the matric flux potential (ϕ), to express the flow equation and relevant boundary conditions, which is defined as:

$$\phi = \int_{h_n}^{h} K(h)dh = \int_{\theta_n}^{\theta} D(\theta)d\theta \qquad \ldots(3.3)$$

where, $h_n = h(\theta_n)$

In case of a strip (or line) source the flow is axisymmetric along the line of source and hence it becomes a case of two-dimensional flow and the governing equation may be expressed in cartesian coordinates. For disc (or point) source the flow can be considered to be radially symmetric and the governing equation for two-dimensional flow may be expressed in cylindrical coordinates. The trickle irrigation flow system in both the coordinate systems is shown in Fig. 3.1. The governing equation and the relevant boundary conditions for both the trickle sources are presented in the following sections.

3.1.2.1 Strip source

If a set of trickle sources are spaced very close to each other at equal interval along an infinite straight line (lateral line), their ponding areas will overlap after only a short period of time and a strip of width $\rho(t)$ along the lateral line will be wetted. It may be assumed that there is a continuos lateral discharge from the line. When this strip is oriented along the y axis, and x is the horizontal coordinate normal to y, the flow becomes independent of the y coordinate. Substituting the new variable

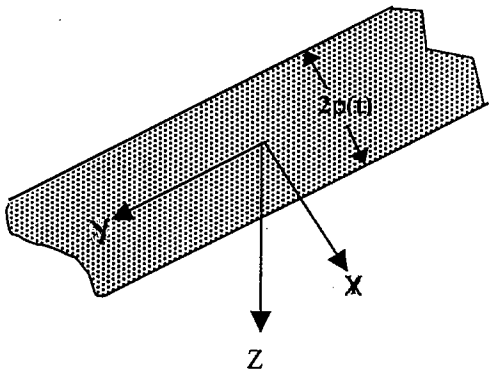

(a) strip source

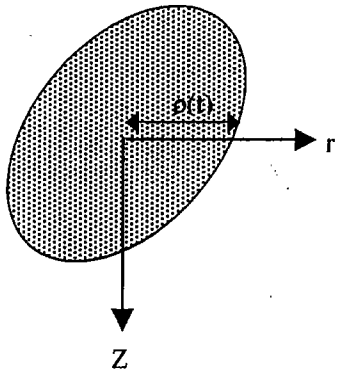

(b) disc source

Fig. 3.1 Trickle irrigation flow system in cartesian (strip source) and cylindrical (disc source) coordinate system.

ϕ from equation (3.3) into equation (3.2) and considering strip source the governing equation takes the form

$$\frac{\partial\theta}{\partial t}=\frac{\partial^2\phi}{\partial x^2}+\frac{\partial^2\phi}{\partial z^2}-\frac{\partial K(\theta)}{\partial z} \qquad \cdots(3.4)$$

The initial and boundary conditions can be written as:

$\theta = \theta_n;$ $0 \le x \le X;$ $0 \le z \le Z;$ $t = 0$ ...(3.5)

$\frac{\partial\theta}{\partial x} = 0;$ $x = 0, x = X;$ $0 \le z \le Z;$ $0 \le t \le T$ ...(3.6)

$\frac{\partial\theta}{\partial z} = 0;$ $0 \le x \le X;$ $z = Z;$ $0 \le t \le T$ ...(3.7)

$\theta = \theta_s;$ $0 \le x \le \rho(t);$ $z = 0;$ $0 \le t \le T$ ...(3.8)

$K - \frac{\partial\phi}{\partial z} = 0;$ $\rho(t) < x \le X;$ $z = 0;$ $0 < t \le T$ ...(3.9)

$\int_0^{\rho(t)}\left[K - \frac{\partial\phi}{\partial z}\right]dx = \frac{1}{2}q_e;$ $z = 0;$ $0 < t \le T$ ...(3.10)

where,

q_e = is the trickle discharge per unit length of the lateral, $cm^3/cm/min$

$\rho(t)$ = width of the saturated strip, cm

T = infiltration opportunity time, min

3.1.2.2 Disc source

In case a single trickle nozzle or a number of nozzles are spaced far apart to prevent interaction of the wetted soil volume, the source is said to be a disc source and the flow equations for such sources may be expressed in cylindrical coordinates. The water content (θ) is then a

function of the coordinates z, t and r = $(x^2+y^2)^{1/2}$. Due to the radial symmetry equation (3.2) takes the form

$$\frac{\partial\theta}{\partial t}=\frac{\partial^2\phi}{\partial r^2}+\frac{1}{r}\frac{\partial\phi}{\partial r}+\frac{\partial^2\phi}{\partial z^2}-\frac{\partial K}{\partial z} \qquad ...(3.11)$$

The initial and boundary conditions for the disc source are identical to those of equation (3.5) through equation (3.9) provided that $\rho(t)$ is the radius of saturated zone, r is substituted for x and R is substituted for X, and they should be sufficiently large. Equation (3.10) takes the form

$$2\pi\int_0^{\rho(t)}\left[K-\frac{\partial\phi}{\partial z}\right]rdr=q_e \qquad ...(3.12)$$

where,

q_e is the trickle discharge in cm^3/min.

3.1.3 Soil-water characteristics

Soil water potential and hydraulic conductivity varies widely and non-linearly with water content of the soil. These relationships are relatively difficult, time consuming and expensive to measure are not feasible for short term and remote investigations. It has been shown that soil texture predominately determines the water holding characteristics of most agricultural soils. The textural information is often either available or can be estimated by simple methods. Keeping all these facts in view the relationships developed by **Saxton *et al.* (1986)** and presented below, have been used with this model.

3.1.3.1 θ - h relationship

For the soil water tension, Ψ (i.e. the +ve value of soil-water potential, h) three different relationships have been given for different ranges of soil-water tension.

i) For 1500 to 10 kPa

$$\Psi = A\theta^{B} \qquad ...(3.13a)$$

ii) For 10 to Ψ_e kPa

$$\Psi = 10.0 - (\theta - \theta_{10})(10.0 - h_e)/(\theta_S - \theta_{10}) \qquad ...(3.13b)$$

iii) For Ψ_e to 0.0 kPa

$$\theta = \theta_S \quad \Rightarrow \quad \Psi = 0.0 \qquad ...(3.13c)$$

where,

$$A = \exp[a+b\mathbf{C}+c\mathbf{S}^2+d\mathbf{C}\mathbf{S}^2] \times 100 \qquad ...(3.14a)$$

$$B = e + f\mathbf{C}^2 + g\mathbf{S}^2 + g\mathbf{C}\mathbf{S}^2 \qquad ...(3.14b)$$

$$\theta_{10} = \exp[(2.302 - \ln A)/B] \qquad ...(3.14c)$$

$$\Psi_e = 100[m + n(\theta_S)] \qquad ...(3.14d)$$

$$\theta_S = h + j\mathbf{S} + k \log_{10}\mathbf{C} \qquad ...(3.14e)$$

Ψ = soil-water tension, kPa

Ψ_e = water tension at air entry, kPa

θ_S = water content at saturation, m^3/m^3

θ_{10} = water content at 10 kPa, m^3/m^3

$\mathbf{S}$ = sand content, %

$\mathbf{C}$ = clay content, %

Near saturation (h→0) the slope of θ - h curve is zero. This creates problem in finding the solution of equation (3.4 or 3.11). The problem may be eliminated if the θ - h relationship of **Angelakis *et al.* (1993)** is used in this zone

$$\theta = \theta_s + C(h).h \qquad \ldots(3.14f)$$

where, C(h) is the specific water capacity of the soil. A positive nonzero value of C(h) may be assumed in the saturation zone.

3.1.3.2 K - θ relationship

In case of hydraulic conductivity, K(θ), the relationship is continuous in the water tension range of 0 to 1500 kPa., and expressed as

$$K(\theta) = 1/60 \{\exp(p + qS + [r + tS + uC + vC^2] (1/\theta))\} \qquad \ldots(3.15)$$

where,

K = hydraulic conductivity, cm/min

and coefficients

a = - 4.396,	b = -0.0715,	c = -4.880×10^{-4},	d = -4.285×10^{-5},
e = - 3.140,	f = -2.22×10^{-3},	g = -3.484×10^{-5},	h = 0.332,
j = -7.251×10^{-4},	k = 0.1276,	m = - 0.108,	n = 0.341,
p = 12.012,	q = -7.55×10^{-2},	r = - 3.8950,	t = 3.671×10^{-2},
u = - 0.1103,	v = 8.7546×10^{-4}		

These relationships are valid over a wide range of soil textures (Fig. 3.2) which covers almost all the cultivable soils.

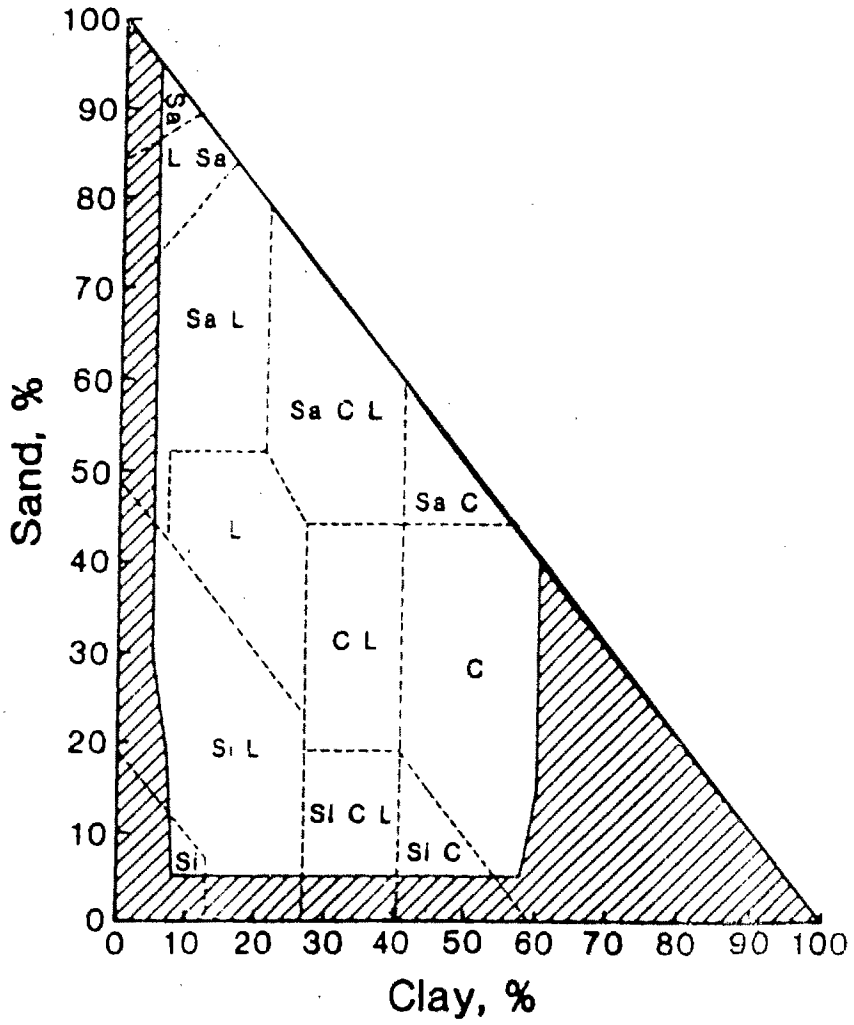

Fig. 3.2 Applicable textural region (clear) for soil-water characteristic equations of Saxton *et al.* (1986)

3.1.3.3 Matric flux potential (ϕ)

Using the $K(\theta)$ and $h(\theta)$ relationships expressed above, equation (3.3) which describes the relationship of matric flux potential with unsaturated hydraulic conductivity can also be written as

$$\phi = \int_{\theta_n}^{\theta} K(\theta)\frac{dh}{d\theta}d\theta \qquad \ldots(3.16)$$

Substituting the value of $K(\theta)$ from equation (3.15), equation (3.16) takes the form

$$\phi = C_1 \int_{\theta_n}^{\theta} \exp\left(C_2 + \frac{C_3}{\theta}\right)\frac{dh}{d\theta}d\theta \qquad \ldots(3.17)$$

where,

$C_1 = 1/60$

$C_2 = p + qS$

$C_3 = r + tS + uC + vC^2$

The slope of the θ - h curve (i.e. $dh/d\theta$) can be obtained from equation (3.13). The integral in equation (3.17) can be solved using a numerical method (like Simpson's $1/3^{rd}$ or $3/8^{th}$ rule).

3.1.4 Numerical procedure

Numerical method as used by **Brandt *et al.* (1971)** was applied to solve the equations (3.2, 3.4 and 3.11) together with associated boundary conditions. The method combines use of the non-iterative alternating directions implicit (ADI) finite difference method with

iterative method of Newton. This results in a numerical technique that is highly efficient and accurate.

The flow system was divided into network of squares. Each point on the grid is designated by two subscripts i and l, indicating that the point is located at the coordinates (ξ_i, z_l). To discuss the two models (strip and disc source) simultaneously, ξ represents x when dealing with strip source and for r when dealing with disc source. The space time continuum (ξ, z, t) is covered by grid points (ξ_i, z_l, t^j), where

$$\xi_i = (i - \tfrac{1}{2})\boldsymbol{h} \qquad i = 0, 1, 2, \ldots\ldots, N+1$$

$$z_l = l\boldsymbol{h} \qquad l = 0, 1, 2, \ldots\ldots, M+1$$

$$t^j = \sum_{p=1}^{j} k_p \quad \text{for} \quad j \geq 1 \quad \text{and} \quad t^0 = 0$$

where,

k_p is a changing time step and

$\boldsymbol{h}$ is a fixed space step satisfying X (or R) = N$\boldsymbol{h}$ and Z = M$\boldsymbol{h}$.

The points with ξ_0, ξ_{N+1}, or ξ_{M+1} have been extended beyond the physical boundary of the system to facilitate the treatment of the boundary conditions.

The finite difference approximation to $\theta(\xi_i, z_l, t^j)$ will now be denoted as θ^j_{il} and ϕ and K can also be written as

$$\phi^j_{il} = \phi(\theta^j_{il}), \qquad K = K(\theta^j_{il})$$

From the initial data $\theta^0_{il} = \theta_n$ the solution is advanced in time by ADI procedure. In this procedure each time step is further subdivided into two different stages.

First stage

During the first stage the solution is advanced from time t^j to an intermediate time $t^{j+1/2}$ by the finite difference equation (FDE)

$$\frac{\theta_{il}^{j+1/2} - \theta_{il}^{j}}{(k_j/2)} = \frac{\phi_{i+1,l}^{j} - 2\phi_{il}^{j} + \phi_{i-1,l}^{j}}{h^2} + \gamma\left[\frac{\phi_{i+1,l}^{j} - \phi_{i-1,l}^{j}}{(2i-1)h^2}\right] + \frac{\phi_{i,l+1}^{j+1/2} - 2\phi_{il}^{j+1/2} + \phi_{i,l-1}^{j+1/2}}{h^2} - \frac{K_{i,l+1}^{j+1/2} - K_{i,l-1}^{j+1/2}}{2h} \qquad (i = 1,2,\ldots,N;\ l = 1,2,\ldots,M) \qquad \ldots(3.18)$$

where, $\Upsilon = 0$ for strip source and 1 for disc source.

The boundary conditions to be satisfied at the time $t^{j+1/2}$ are equations (3.7, 3.8, 3.9, and 3.10 or 3.12). In finite difference form these become, respectively,

$$\theta_{i,M+1}^{j+1/2} = \theta_{i,M}^{j+1/2} \qquad i = 1,2,\ldots,N \qquad \ldots(3.19)$$

$$\theta_{i0}^{j+1/2} = \theta_S \qquad i = 1,2,\ldots,i_S - 1 \qquad \ldots(3.20)$$

$$F_i = 0 \qquad i = i_S + 1, i_S + 2,\ldots,N \qquad \ldots(3.21)$$

$$F_{i_S} = q_e - \sum_{i=1}^{i_S-1} F_i \qquad \ldots(3.22)$$

where, i_s is approximated as $\rho(t)/h$;

$$F_i = 2h(1 - \gamma + \gamma\pi\xi_i)\left(K_{i0}^{j+1/2} - \frac{\Delta_z\phi_{i0}^{j+1/2}}{2h}\right) \qquad \ldots(3.23)$$

where, $\Delta_z\phi_{i0}^{j+1/2} = -3\phi_{i0}^{j+1/2} + 4\phi_{i1}^{j+1/2} - \phi_{i2}^{j+1/2}$

The above FDE is implicit, but only in z direction.

The set of equation (3.18), together with appropriate boundary conditions can be written for i^{th} column in a compact manner as:

$$\Phi_i(\Omega_i) = 0 \qquad \ldots(3.24)$$

where, Φ_i is a vector representing the equations,

$$\Phi_i = (\zeta_{i0}, \zeta_{i1}, \ldots, \zeta_{iM}, \zeta_{i,M+1}) \qquad \ldots(3.25)$$

The procedure for obtaining ζ_{i1} is described in section 3.1.5.

Starting with the first approximation $\Omega_i^{(1)} = (\theta^1_{i0}, \theta^1_{i1}, \ldots, \theta^1_{i,M+1})$, rapidly improved approximations $\Omega_i^{(2)}$, $\Omega_i^{(3)}$, ... can be successively computed, using Newton's formula

$$A_i^{(\upsilon)} w_i^{(\upsilon)} = - \Phi_i(\Omega_i^{(\upsilon)}) \qquad \ldots(3.26)$$

$$\Omega_i^{(\upsilon+1)} = \Omega_i^{(\upsilon)} + w_i^{(\upsilon)} \qquad \ldots(3.27)$$

where, $A_i^{(\upsilon)}$ is the (M+2) × (M+2) Jacobian matrix, i.e., its element in the p^{th} row and q^{th} column is $\partial\zeta_{ip}/\partial\theta_{iq}$, (p,q = 0,1, ... ,M+1) these partial derivatives being evaluated at $\Omega_i^{(\upsilon)}$. The matrix is tridiagonal when $i < i_s$ and nearly tridiagonal when $i \geq i_s$.

To determine i_s, which may vary with time, the equations (3.18, 3.19 and 3.20) are solved in order of increasing i. Before passing to i+1 the following condition is checked

$$\sum_{j=1}^{i} F_j \leq q_e \qquad \ldots(3.28)$$

If this inequality fails the quantity F_{is}, which thus turned out to be too large, is stored as $\bar{F}_{is}$ and the equations for $i = i_s$ are solved again, with equation (3.22) serving as boundary condition instead of equation

(3.20). The ratio $F_{is}/\ \bar{F}_{is}$ is a good measure to the fraction of the interval $[(i_s - 1)h,\ i_s h]$ which is in the saturated zone. The radius/width of the saturated zone may be approximated by

$$\rho(t) \approx (i_s - 1 + F_{is}/\ \bar{F}_{is})h. \qquad \ldots(3.29)$$

Then the equations (3.18, 3.19, 3.21) are solved for $i = i_s+1,\ i_s+2,\ldots,N$.

Second Stage

During the second stage of each ADI time step, the solution is advanced from time $t^{j+1/2}$ through the FDE

$$\frac{\theta_{il}^{j+1} - \theta_{il}^{j+1/2}}{k_j/2} = \frac{\phi_{i+1,l}^{j+1} - 2\phi_{i,l}^{j+1} + \phi_{i-1,l}^{j+1}}{h^2} + \gamma \frac{\phi_{i+1,l}^{j+1} - \phi_{i-1,l}^{j+1}}{(2i-1)h} + \frac{\phi_{i,l+1}^{j+1/2} - 2\phi_{i,l}^{j+1/2} + \phi_{i,l-1}^{j+1/2}}{h^2} - \frac{K_{i,l+1}^{j+1/2} - K_{i,l-1}^{j+1/2}}{2h} \qquad \ldots(3.30)$$

supplemented by the boundary condition

$$\phi_{0l}^{j+1} = \phi_{1l}^{j+1}; \qquad \phi_{Nl}^{j+1} = \phi_{N+1,l}^{j+1}, \qquad l = 1,2,\ldots,M \qquad \ldots(3.31)$$

These equations, approximating again the differential equation (3.4 or 3.11), and the boundary conditions (equation 3.6) are implicit in the ξ direction. The set of equations (equation 3.30), together with equation (3.31) can again be written in a compact manner as

$$\Phi_l(\Omega_l) = 0 \qquad \ldots(3.32)$$

where,

$$\Omega_l = \left(\theta_{0l}^{j+1}, \theta_{1l}^{j+1}, \ldots, \theta_{N+1,l}^{j+1}\right) \qquad \ldots(3.33)$$

$$\Phi_l = \left(\zeta_{0l}, \zeta_{1l}, \ldots, \zeta_{N+1,l}\right) \qquad \ldots(3.34)$$

ζ_{il} are obtained explicitly as explained in section 3.1.5. The method of solution is similar to that described earlier except that now $\theta_{il}^{j+1/2}$ provides the first approximation for $\Omega_i^{(1)}$. Unlike explicit schemes this implicit procedure can be shown to be unconditionally stable (**Brandt *et al.*, 1971**). Starting with the first approximation $\Omega_i^{(1)}=(\theta^1_{i0},\theta^1_{i1},\ldots,\theta^1_{i,M+1})$, rapidly improved approximations $\Omega_i^{(2)}$, $\Omega_i^{(3)}$, ... can be computed successively, using the Newton's formula

$$\mathbf{A}_i^{(\upsilon)} \cdot \mathbf{w}_i^{(\upsilon)} = -\Phi_i(\Omega_i^{(\upsilon)}) \qquad \ldots(3.35)$$

$$\Omega_i^{(\upsilon+1)} = \Omega_i^{(\upsilon)} + \mathbf{w}_i^{(\upsilon)} \qquad \ldots(3.36)$$

3.1.5 Computational procedure

The procedure for computing θ_{il}^{j+1}, when the values of θ^j_{il} are known, consists of the following steps:

A. First stage

1. Initializing $i = 1$, $\sigma_o = 0$, $i_S = N+1$, and
2. $\nu = 1$, $\Omega_i^{(1)} = (\theta^j_{i0},\theta^j_{i1}, \ldots, \theta^j_{i,M+1})$
3. Compute $\left[\Phi_i^{(\upsilon)}\right]_p = \zeta_{ip}(\Omega_i^{(\upsilon)})$ and $[A_i^{(\upsilon)}]_{p,q} = \left.\dfrac{\partial \zeta_{ip}}{\partial \theta_{iq}}\right|_{\Omega_i=\Omega_i^{(\upsilon)}}$,

   (p,q = 0,1,...,M+1) where ζ_{ip} are given as functions of $\theta_{iq} = \theta_{iq}^{j+1/2}$ by

$$\zeta_{i0} = \begin{cases} \frac{k}{2}(\theta_{i0}^{j+1/2} - \theta_S) & \text{for } i < i_S \\ -\frac{k}{2}[(2hK_{i0}^{j+1/2} + 3\phi_{i0}^{j+1/2} - 4\phi_{i1}^{j+1/2} + \phi_{i2}^{j+1/2}) & \\ \qquad (1-\gamma+\gamma\pi\xi_i) - q_e + \sigma_{i-1}] & \text{for } i = i_s \\ -\frac{k}{2}(2hK_{i0}^{j+1/2} + 3\phi_{i0}^{j+1/2} - 4\phi_{i1}^{j+1/2} + \phi_{i2}^{j+1/2}) & \\ \qquad (1-\gamma+\gamma\pi\xi_i), & \text{for } i_S < i \le N \end{cases}$$

$$\zeta_{il} = h^2(\theta_{il}^{j+1/2} - \theta_{il}^{j}) - \frac{k}{2}[\phi_{i,l+1}^{j+1/2} - 2\phi_{il}^{j+1/2} + \phi_{i,l-1}^{j+1/2} - \frac{h}{2}(K_{i,l+1}^{j+1/2} - K_{i,l-1}^{j+1/2})] - \frac{k}{2}[\phi_{i+1,l}^{j} - 2\phi_{il}^{j} + \phi_{i-1,l}^{j} + \frac{\gamma}{2i-1}(\phi_{i+1,l}^{j} - \phi_{i-1,l}^{j})], \quad \text{for } l = 1,2,\ldots,M;\ i = 1,2,\ldots,N$$

$$\zeta_{i,M+1} = -\frac{k}{2}(\phi_{iM}^{j+1/2} - \phi_{i,M+1}^{j+1/2}), \quad \text{for} \quad i = 1,2,\ldots,N$$

where, $k = k_j$. Then by elimination the system is solved as below

$A_i^{(\upsilon)} \cdot w_i^{(\upsilon)} = -\Phi_i^{(\upsilon)}$ and $\Omega_i^{(\upsilon+1)} = \Omega_i^{(\upsilon)} + w_i^{(\upsilon)}$

4. If components of the correction $w_i^{(\upsilon)}$ are smaller in magnitude than ε, step 6 is followed skipping step 5.

5. If $\upsilon < M_o$ (maximum number of iterations allowed), υ is increased by 1 and steps 3 – 4 are repeated. If $\upsilon = M_o$, the size of k_j is reduced and steps 1 – 4 are repeated.

6. The final iterant $\Omega_i^{(\upsilon+1)}$ is identified as $(\theta_{i0}^{j+1/2}, \theta_{i1}^{j+1/2}, \ldots, \theta_{i,M+1}^{j+1/2})$. If $i < i_s$, step 7 is followed. If $i \le i_s < N$, i is incremented by 1 and steps 2 – 5 are repeated. If $i = N$, step 8 is followed skipping step 7.

7. F_i is computed according to equation (3.23) and σ_i is obtained by $\sigma_i = \sigma_{i-1} + F_i$. If $\sigma_i < q_e$, i is increased by 1and steps 2–6 are repeated. If $\sigma_i \geq q_e$, assigning $is = i$, $\bar{F}_{is} = F_i$, steps 2–6 are repeated.

B. Second stage

8. Initializing $l = 1$, and

9. $\nu = 1$, $\Omega_l^{(\upsilon)} = (\theta_{0l}^{j+1/2}, \theta_{1l}^{j+1/2}, \ldots, \theta_{N+1,l}^{j+1/2})$

10. Compute $\left[\Phi_l^{(\upsilon)}\right]_p = \zeta_{pl}(\Omega_l^{(\upsilon)})$ and $[A_l^{(\upsilon)}]_{p,q} = \left.\frac{\partial \zeta_{pl}}{\partial \theta_{ql}}\right|_{\Omega_l = \Omega_l^{(\upsilon)}}$,

(p,q = 0,1, ... , N+1), where ζ_{pl} are given as functions of

$\theta_{ql} = \theta_q{}^{j+1/2}$ by

$$\zeta_{0l} = -\frac{\mathbf{k}}{2}(\phi_{1l}^{j+1} - \phi_{0l}^{j+1})$$

$$\zeta_{il} = \boldsymbol{h}^2(\theta_{il}^{j+1} - \theta_{il}^{j+1/2}) - \frac{\mathbf{k}}{2}[(1 + \frac{\gamma}{2i-1})\phi_{i+1,l}^{j+1} - 2\phi_{il}^{j+1} + (1 - \frac{\gamma}{2i-1})\phi_{i-1,l}^{j+1}$$
$$+ \phi_{i,l+1}^{j+1/2} - 2\phi_{i,l}^{j+1/2} + \phi_{i,l-1}^{j+1/2} - \frac{\boldsymbol{h}}{2}(K_{i,l+1}^{j+1/2} - K_{i,l-1}^{j+1/2})],$$
$$\text{for } i = 1,2,\ldots,N;\ l = 1,2,\ldots,M.$$

$$\zeta_{N+1,l} = -\frac{\mathbf{k}}{2}(\phi_{Nl}^{j+1} - \phi_{N+1,l}^{j+1}), \qquad \text{for } l = 1,2,\ldots,M$$

where, k = k_j. Then by elimination the linear system is solved as below

$A_l^{(\upsilon)} \cdot w_l^{(\upsilon)} = -\Phi_l^{(\upsilon)}$ and $\Omega_l^{(\upsilon+1)} = \Omega_l^{(\upsilon)} + w_l^{(\upsilon)}$

11. If components of the correction $w_i^{(\upsilon)}$ are smaller in magnitude than ε, step 13 is followed skipping step 12.

12. If $\upsilon < M_o$, υ is increased by 1 and steps 10 – 11 are repeated. If $\upsilon = M_o$, the size of k_j is reduced and steps 1 – 11 are repeated.

13. The final solution of $\Omega_l^{(\upsilon+1)}$ is obtained as $(\theta_{0l}^{j+1}, \theta_{1l}^{j+1}, \ldots, \theta_{N+1,l}^{j+1})$. If $l < M$, l is increased by 1 and steps 9 – 12 are repeated. If $l = M$, the entire time step has been completed. Selecting a new value of k and increasing j by 1 the whole procedure, starting with step 1, is repeated.

3.1.6 Determination of emitter discharge

It has been established that the wetting diameter of a trickle source is a function of the emitter discharge and the soil type only. Therefore, the emitter discharge is the only parameter that determines the profile of wetted volume for a given soil type, if the total volume of water applied is known.

If, the coordinates of a point, P, located in the plant root zone or at the surface are known and the required soil-water content at this point, after irrigation can be fixed. The application rate from the emitter can be determined, which will distribute the water in such a way that the moisture content at this point, P, are obtained with a specified accuracy. It is known that the wetting front moves faster in horizontal direction when discharge (or application rate) is higher. Starting with minimum discharge and then increasing it gradually the moisture content at the point P are determined until the required moisture

content is not obtained. To save the computation time golden section search method can be used to obtain the required emitter discharge.

3.1.7 Golden section search for determination of emitter discharge

This technique is used to find the exact estimate of discharge from the source (emitter) so as to obtain the required moisture level at the point P. The steps involved can be described as follows:

1. The discharge range $[Q_A, Q_B]$ is selected for the emitter that will result in the required moisture level (θ_r) at P. Here, H_A and H_B are the minimum and maximum discharge available from the emitter, respectively.
2. Initialize $a_1 = Q_A$, $a_3 = Q_B$, $a_2 = \lambda a_3$,

   $A_1 = a_1$, $A_4 = a_3$, where $\lambda = 0.618$

   If $|(a_3 - a_2)| > |(a_2 - a_1)|$ then

   $A_2 = a_2$, and

   $A_3 = a_2 + (1-\lambda)(a_3 - a_2)$

   Otherwise,

   $A_3 = a_2$, and

   $A_2 = a_2 - (1-\lambda)(a_2 - a_1)$
3. Assuming the discharge of the emitter as A_2, the moisture content (θ) at P is determined using the finite difference procedure, and the associated error (ε) as:

$$\varepsilon = \frac{|(\theta_r - \theta)|}{\theta_r}$$

4. If $\varepsilon \leq$ ERR (error allowed in computations), then A_2 is the required emitter discharge.

5. If $\varepsilon >$ ERR and

   If, $\theta < \theta_r$, then

   $A_1 = A_2$, $A_2 = A_3$, and $A_3 = \lambda A_2 + (1-\lambda) A_4$

   Otherwise,

   $A_4 = A_3$, $A_3 = A_2$, and $A_2 = \lambda A_3 + (1-\lambda) A_1$

   Now the discharge range is reduced and steps 3 – 4 are repeated.

3.2 Lateral Design

In microirrigation systems the lateral lines are pipes on which the emitters are installed. The design of a single lateral includes determining the lateral characteristics such as length or diameter of the lateral, location of the submain (in case of paired laterals), pressure head required at the inlet of the lateral. Usually constant diameter laterals are used because they are easy to install and maintain, but tapered laterals may be less expensive. Tapered laterals are sometimes needed on steep slopes also. However, it is impractical to use tapered laterals with more than two diameters **Keller and Bliesner (1990)**. In the design of tapered laterals the additional parameters to be determined are the length and diameter of different sections.

3.2.1 Lateral discharge equation

For designing microirrigation laterals **Kang *et al.* (1995)** and **Kang and Nishiyama (1995; 1996a, b)** have recommended the use of a

lateral discharge equation due to simplicity in calculations and high accuracy. They used a polynomial to express the relationship between inlet flow rate and inlet pressure head of a lateral

$$q_L = C_0 + C_1H + C_2H^2 + \cdots\cdots + C_nH^n \qquad \ldots(3.37)$$

where, C_0, C_1, . . . C_n are coefficients; H is the inlet pressure head, q_L is the lateral discharge and n = 3~7, depending on lateral parameters, emitter types and field slopes.

The lateral discharge equation is simulated using the least squares method by assuming pressure head (within a selected range) at closed end of the lateral of known diameter and length. The pressure required at the inlet of the lateral for maintaining the required flow at inlet is calculated from equation (3.37).

The lateral discharge equation thus simulated may have an error less than 0.1% if range of pressure heads is chosen well in simulation and the correlation coefficient (r^2) is higher than 0.999 at any condition (**Kang *et al.*, 1995**). But, in case of long laterals with relatively smaller diameter it becomes very difficult to predict this range of pressure heads. Under such situations the desired inlet flow rate may not fall within the range of pressure heads used and hence the lateral discharge equation will have to be extrapolated for required inlet flow rate. Since the lateral discharge equation is valid strictly for the input pressure range only, a severe error may be introduced in extrapolation of the lateral discharge equation. The situation in which such errors are

encountered is discussed in detail through a numerical example in chapter 5.

The hydraulics of lateral and submain are similar in the way that laterals attached to a submain behave similar to the emitters fitted on a lateral. Therefore, the flow equation for a lateral may be taken similar to the emission equation of the emitter. As an alternative to polynomial (equation 3.37) a simple power equation may be used as the lateral discharge equation to describe the flow behaviour of a microirrigation lateral. The proposed lateral discharge equation for a single microirrigation lateral (Fig. 3.3) may be expressed by:

$$q_L = aH^b \qquad \ldots(3.38)$$

where,

a and b are lateral flow coefficient and exponent, respectively.

For paired laterals (Fig. 3.4), the lateral discharge equation can be expressed separately for lateral on left and right side of the submain as:

$$q_{L_1} = a_1 H^{b_1} \qquad \ldots(3.39a)$$

$$q_{L_2} = a_2 H^{b_2} \qquad \ldots(3.39b)$$

where,

q_{L_1} = discharge at inlet of the lateral left to submain

q_{L_2} = discharge at inlet of the lateral right to submain,

a_1, b_1 are flow coefficient and exponent, respectively, for lateral at left side of submain, and

a_2, b_2 are flow coefficient and exponent, respectively, for lateral at right side of submain.

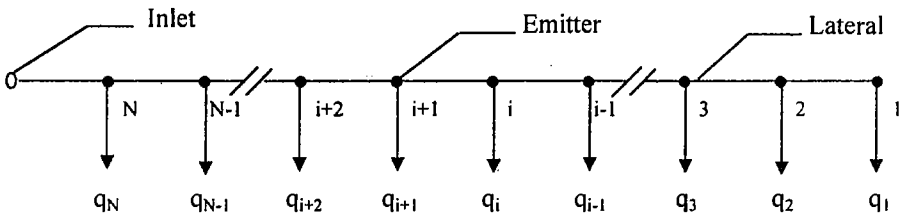

Fig. 3.3. A single lateral in microirrigation.

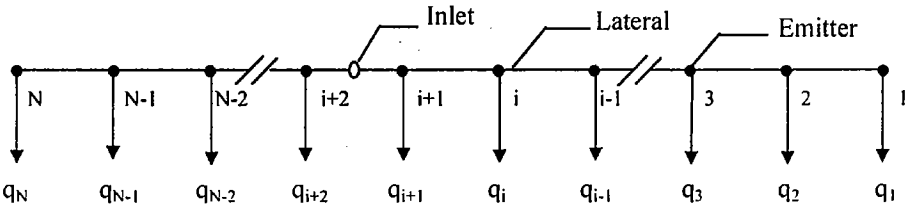

Fig. 3.4 Paired laterals in microirrigation.

3.2.2 Hydraulic analysis

Data sets of flow rate and pressure head at inlet are obtained by assuming a group of pressure heads, within the specified range, at the closed end of the lateral. The flow in the first element of the lateral is considered equal to the flow from first emitter. Using back step method the flow rate and pressure head at the inlet is determined.

3.2.2.1 Back step analysis

The general equation of back step method may be expressed by:

$$H_i = H_{i-1} + (Z_{i-1} - Z_i) + f_{i-1} \frac{8 S_e Q_{i-1}^2}{g\pi^2 D^5} \qquad \ldots(3.40)$$

where,

S_e = lateral element length (emitter spacing)

D = inside diameter of the lateral

H_i = pressure head at the inlet of emitter i

H_{i-1} = pressure head at the inlet of emitter i-1

Z_i = elevation head at the inlet of emitter i

Z_{i-1} = elevation head at the inlet of emitter i-1

g = acceleration due to gravity

f_{i-1} = friction factor of lateral element i-1.

For laminar flow (Reynold's number $R_e \leq 2000$)

$$f = \frac{64}{R_e} \qquad \ldots(3.41a)$$

For turbulent flow in a smooth pipe ($2000 < R_e \leq 10^5$) the Blasius equation for friction factor (f) can be used (**Keller and Bliesner, 1990**) in the transition zone.

$$f = \frac{0.316}{R_e^{0.25}} \qquad \ldots(3.41b)$$

For the fully turbulent flow ($10^5 < R_e \leq 10^7$) **Watters and Keller (1978)** formula can be used

$$f = \frac{0.130}{R_e^{0.172}} \qquad \ldots(3.41c)$$

The discharge in lateral elements is determined by

$$Q_i = Q_{i-1} + q_{i-1} \qquad \ldots(3.42)$$

$$q_{i-1} = KH_{i-1}^x \qquad \ldots(3.43)$$

where,

q_{i-1} = discharge of emitter i-1

Q_i = discharge in lateral element i

Q_{i-1} = discharge in lateral element i-1, and

K is emission coefficient and x is the emission exponent.

The pressure head at the inlet of the lateral is obtained by

$$H_{in} = H_N + (Z_N - Z_{in}) + f_N \frac{8S_{el}Q_N^2}{g\pi^2 D^5} \qquad \ldots(3.44)$$

where,

N = the number of emitters along the lateral

H_{in} = pressure head at inlet of the lateral

H_N = pressure head at inlet of emitter N

S_{el} = length from the inlet of lateral to the emitter N

Z_N = elevation head at inlet of emitter N

Z_{in} = elevation head at inlet of the lateral

3.2.2.2 Estimation of required head at inlet

The data sets thus obtained are used for simulating lateral discharge equation using the method of least squares. The correlation coefficient (r^2) has been found to be higher than 0.999 for any case. If the range chosen for closed end pressure head is not in accordance with the actual pressure head, the degree of error may be relatively higher. However, there are no chances for the severe error as may be encountered in case of polynomial (equation 3.37).

Pressure head required at inlet of a single lateral to cause a flow such that the average required emitter flow rate is maintained, is calculated by:

$$H_{rin} = \left(\frac{1}{a} N q_{req}\right)^{\frac{1}{b}} \qquad \ldots(3.45)$$

where,

H_{rin} is the pressure head required at inlet of the lateral.

In case of paired laterals total discharge through the lateral is obtained by combining discharges of laterals on left and right sides of the submain. Therefore, total discharge at the inlet of a paired lateral may be expressed by

$$q_L = q_{L_1} + q_{L_2} = a_1 H_{rin}^{b_1} + a_2 H_{rin}^{b_2} \qquad \ldots(3.46)$$

The total discharge through the lateral required for maintaining average required discharge in the lateral is obtained as

$$q_L = q_{req}(N_1 + N_2) \qquad \ldots(3.47)$$

where,

N_1 = number of emitters along the lateral located on left side of the submain

N_2 = number of emitters along the lateral located on right side of the submain.

Equation (3.46) can be evaluated using Newton-Raphson method as below.

1. The initial estimate of the head required at inlet of the lateral $(H_{rin})_1$ is obtained by:

$$(H_{rin})_1 = \left(\frac{q_{req}}{K}\right)^{\frac{1}{x}} \qquad \ldots(3.48)$$

2. The fresh estimate of H_{rin} is obtained as:

$$(H_{rin})_2 = (H_{rin})_1 - \frac{a_1(H_{rin})_1^{b_1} + a_2(H_{rin})_1^{b_2} - q_{req}(N_1 + N_2)}{a_1 b_1 (H_{rin})_1^{b_1 - 1} + a_2 b_2 (H_{rin})_1^{b_2 - 1}} \qquad \ldots(3.49)$$

3. If ε is the acceptable error in calculation of H_{rin}, the following condition is tested.

$$\frac{\left|(H_{rin})_1 - (H_{rin})_2\right|}{(H_{rin})_1} < \varepsilon \qquad (\varepsilon > 0) \qquad \ldots(3.50)$$

$(H_{rin})_1$ would be the final solution of H_{rin} if above condition is true otherwise, $(H_{rin})_1$ is set equal to $(H_{rin})_2$ and step 2 - 3 are repeated.

3.2.2.3 Forward step analysis

The pressure head and flow rate distributions along the lateral can be obtained by forward step method. For a single lateral the pressure head at the inlet of emitter N can be obtained by:

$$H_N = H_{rin} + (Z_{in} - Z_N) - f_N \frac{8S_{el}Q_N^2}{g\pi^2 D^5} \quad \ldots(3.51)$$

Pressure head and discharge at different emitter locations can be found by equation:

$$H_i = H_{i+1} + (Z_{i+1} - Z_i) - f_i \frac{8S_e Q_i^2}{g\pi^2 D^5} \quad \ldots(3.52)$$

$$Q_i = Q_{i+1} - q_{i+1} \quad \ldots(3.53)$$

The minor head losses due to emitter or other fittings can be obtained as equivalent length of lateral. This equivalent length is added to the lateral element for calculation of friction loss in the element.

$$S_i' = \frac{K_{fit}}{f_i} \quad \ldots(3.54)$$

where,

S_i' is the equivalent length due to fitting loss at emitter i, and

K_{fit} is the fitting loss factor to the length of lateral element i.

According to the mass conservation of energy principle, the flow in the first downstream lateral element should be equal to the outflow of first downstream emitter, obtained from equation (3.43). But, due to error in estimation of H_{rin} from lateral discharge equation, these may not be equal. If the discharge in lateral element 1 is negative the

pressure head at inlet of emitter 1 can be set equal to the pressure head at emitter 2. The discharge of emitter 1 can then be determined. The error caused by doing so is less than 1 per cent (**Kang and Nishiyama, 1995**).

3.2.3 Calculations with risers

In some of the microirrigation systems the emission devices are connected to the lateral lines through the riser tubes. These risers hold the emitters/spray nozzles vertically up in the air above the ground level. The discharge through the emitter is dependent on the friction losses in the riser tube and the friction loss in the riser tube can be estimated only when the flow rate in the tube is known. Therefore, a trial and error method can be used to calculate the discharge from a emitter with riser. Considering that the friction losses in the riser tube are significant, procedure of calculation is described as below:

1. Initially the discharge q_1 is calculated using equation (3.43) assuming that the friction loss in the riser tube is negligible

$$q_1 = K(H - h_r)^x \qquad \ldots(3.55)$$

where,

H is the pressure head at the inlet of the riser, and

h_r is the height of riser above the lateral.

2. Friction loss in the riser tube (ΔH_r) is determined using the Darcy-Weisbach formula as

$$\Delta H_r = 8f \frac{L_r}{D_r^5} \frac{q_1^2}{\pi^2 g} \qquad \ldots(3.56)$$

where,

L_r is the length of riser tube, and

D_r is the diameter of the riser tube.

The friction factor f is calculated using equation (3.41).

3. Again the discharge (q_2) from the emitter is calculated now considering ΔH_r to be significant, by

$$q_2 = K(H - h_r - \Delta H_r)^x \quad \ldots(3.57)$$

If, difference between q_1 and q_2 is acceptable then, q_2 is the discharge from the emitter otherwise, q_1 is set equal to q_2 and steps 2 – 3 are repeated.

3.2.4 Evaluation of uniformity of water application

After the pressure head distribution and emitter flow rate distribution along the lateral is obtained water application uniformity is evaluated using Christiansens uniformity coefficient (UCC) or the lower quarter distribution uniformity (DU) or emitter flow variation (V_{HM}), which are expressed as below

$$UCC = 1 - \frac{1}{Nq_{req}} \sum_{i=1}^{N} |q_i - q_{req}| \quad \ldots(3.58)$$

$$DU = \frac{4}{Nq_{req}} \sum_{i=1}^{N/4} (q_{low})_i \quad \ldots(3.59)$$

$$(V_{HM})^2 = V_H^2 + V_M^2 \quad \ldots(3.60)$$

where,

$(q_{low})_i$ = discharge of low-quarter emitter i

V_H = effective pressure head (H^x) variation at the emitters

V_M = manufacturing variation of emitters

3.2.5 Golden section search for designing tapered lateral

With the help of theories presented above one of the parameter, namely length or diameter, of a single and paired lateral can be designed. The diameter of lateral designed may not be the standard diameter of pipeline available and hence the next larger diameter has to be considered for the lateral. This will increase cost of the lateral. The cost can be minimized to some extent by using a next smaller diameter available for the down stream section of the lateral without compromising with the desired uniformity criteria used for design of the lateral. Here the parameter to be designed is the length of down stream section of the lateral, tapered with smaller lateral diameter. A typical tapered microirrigation lateral is shown in Fig. 3.5.

The smaller pipe size is used for downstream elements of the lateral. Considering 1, 2, ..., N-1 lateral elements with smaller pipe size, uniformity of water application is evaluated for each case, using the theories presented in previous sections. Golden section search is used to find quickly the number of elements with smaller pipe size.

In the procedure outlined below the standard golden section search is used with some modification. The three bracketing variables (n_0, n_1 and n_2) are used which can take only integer values. These

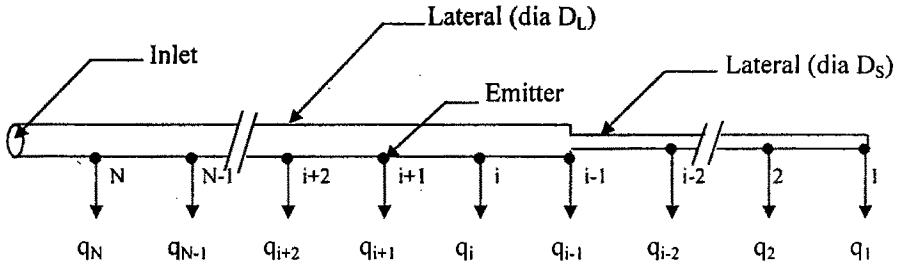

Fig. 3.5 A tapered (two pipe size) lateral in microirrigation.

variables denote the number of elements of the pipeline, which are to be used with the smaller diameter.

The minimum [N_A) and maximum (N_B] number of lateral element that can be on the tapered section are obtained. Generally, the value of N_A is kept zero which means that there is no element with smaller diameter i.e. the pipeline is uniform and N_B is assigned the value N-1, which means that all the elements of the pipeline are of smaller size except the element next to the inlet of the pipeline.

2. Initializing, $n_0 = N_A$, $n_2 = \lambda N_B$, and $n_1 = N - n_2$

3. Considering n_2 number of elements with smaller diameter and n_1 with larger diameter simulate the lateral discharge equation for this setup of the tapered pipeline. Determine H_{rin} and uniformity of application (UCC_o).

4. If, $UCC_o = |UCC_r + \varepsilon|$, (where ε is the acceptable error in UCC) then n_2 is the number of elements of the lateral with smaller diameter.

5. If $UCC_o < UCC_r$, then

   $n_1 = n_2$, and

   $n_2 = n_1 - \lambda (n_1 - n_0)$

   Otherwise,

   $n_0 = n_2$, and

   $n_2 = n_0 + \lambda (n_1 - n_0)$

6. Steps (3 – 5) are repeated until condition of step 4 is fulfilled.

3.3 Submain Design

Microirrigation submains are multioutlet pipelines like laterals. They differ from laterals in flow rate, which is much higher in submains and usually submains are tapered. This is done to economize on pipe costs keeping the pressure head variation within the desired limits. The submain design includes determining the following submain characteristics: flow rate, pipe sizes to keep within desired pressure head variation or uniformity of water application, and inlet pressure needed to give desired average emitter discharge.

With the introduction of lateral discharge equation approach the submains can be treated as laterals and laterals as emitters (**Karmeli *et al.*, 1985** and **Kang and Nishiyama, 1996b)**

3.3.1 Hydraulic analysis

The flow at the inlet of a single and paired lateral may be obtained by equation (3.38) and equation (3.39), respectively (lateral discharge equations). For paired laterals the discharge through both sides of the lateral is expressed separately.

One of the two parameters of the lateral i.e. length or diameter, can be designed for the desired average emitter discharge and uniformity of flow (like Christiansens uniformity coefficient), provided that the other parameter is known.

After the lateral is designed, length and diameter of lateral are known and the flow characteristics can be evaluated by the lateral

discharge equation simulated. Selecting proper dimensions of the laterals of a subunit facilitates minimum flow/pressure head variation through them and hence higher uniformity. With minimized flow/pressure head variation along laterals, the submain gets opportunity to allow more variation within it for the desired overall (global) uniformity of application. Now, one of the two parameters (length and diameter) of submain is to be designed for the known value of the other parameter. The equations (3.40-3.44) used for design of a lateral may also be used for design of a submain.

The general layout of a submain is shown in Fig. 3.6. The submain elements and the laterals are numbered (1,2, ... ,M) from downstream end of the submain. Pressure head at closed end of the submain is assumed and distribution of pressure head and flow rate along the submain can be determined using back step method. With the assumed pressure head at the downstream end of the submain the flow in the first lateral is obtained using the lateral discharge equation (equation 3.38 or 3.39). The discharge in the first element of the lateral is taken equal to the discharge of the first downstream lateral. The equation of back step method with submain parameters can be rewritten as:

$$H_i = H_{i-1} + (Z_{i-1} - Z_i) + f_{i-1} \frac{8 S_1 Q_S (i-1)^2}{g \pi^2 D_S^5} \qquad \ldots(3.61)$$

where,

D_S = diameter of submain,

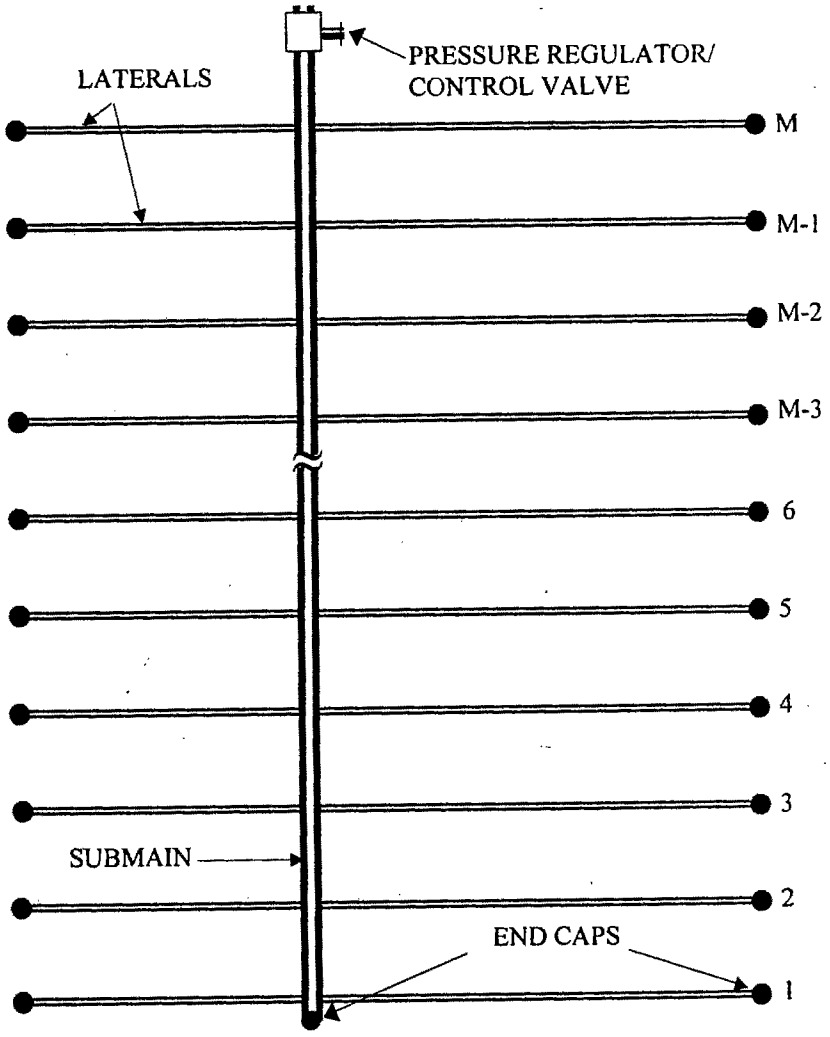

Fig.3.7. General layout of a microirrigation subunit with M number of paired laterals.

$Q_S(i-1)$ = discharge in submain element i-1,

S_l = length of submain element (lateral spacing), m

Other parameters have already been defined. The discharge from the lateral corresponding to the pressure head at their inlet is obtained using lateral discharge equation. This saves a lot of time required for computations. The flow in successive submain elements is obtained from

$$Q_S(i) = Q_S(i-1) + Q_L(i) \qquad \ldots(3.62)$$

where,

$Q_L(i)$ is the discharge at the inlet of lateral i.

The pressure head at the inlet of the submain can be calculated from equation (3.44) rewritten as:

$$H_{in} = H_N + (Z_N - Z_{in}) + f_N \frac{8S_l Q_S(N)^2}{g\pi^2 D_S^5} \qquad \ldots(3.63)$$

If the spacing of the first lateral is different from the normal spacing of laterals, actual length of submain element is used in equation (3.63) for computation of H_{in}.

If the average emitter discharge obtained differs significantly from the desired value, a fresh estimate of pressure head is obtained at the closed end of the submain using golden section search method, and entire process of back step calculation is repeated.

3.3.2 Golden section search for submain design

This technique is used to find the exact estimate of pressure head at the downstream end of the submain so as to obtain the required

average emitter discharge (q_{req}) from the subunit. The method can be described as follows:

1. The pressure head range [H_A, H_B] for the closed end of the submain that will produce q_{req} is selected. Where, H_A and H_B are the minimum and maximum pressure heads at the closed end of the submain, respectively.

2. Initializing,

   $a_1 = H_A$, $a_3 = H_B$, $a_2 = \lambda a_3$, and

   $A_1 = a_1$, $A_4 = a_3$

3. If, $|(a_3 - a_2)| > |(a_2 - a_1)|$

   $A_2 = a_2$

   $A_3 = a_2 + (1-\lambda)(a_3 - a_2)$

   Otherwise,

   $A_3 = a_2$

   $A_2 = a_2 - (1-\lambda)(a_2 - a_1)$

   Assuming the pressure head at the downstream end of the submain as A_2, the pressure head at the inlet of submain (H_{in}) and average emitter discharge (q_{av}) are determined.

4. If $q_{av} = q_{req}$, then H_{in} determined is the required pressure head at the inlet. Otherwise

   If, $q_{av} < q_{req}$, then

   $A_1 = A_2$, $A_2 = A_3$, and $A_3 = \lambda A_2 + (1-\lambda) A_4$

Otherwise,

$$A_4 = A_3, \qquad A_3 = A_2, \qquad A_2 = \lambda A_3 + (1-\lambda)\, A_1$$

Now the pressure head range is reduced. Step 3 - 4 are repeated until required average emitter discharge is obtained. In every iteration, the pressure head range is narrowed down. The correct estimate of pressure head at the downstream end of the submain, which will give the required average emitter discharge, is obtained quickly.

Chapter 4

Design Methodology

4. DESIGN METHODOLOGY

This chapter presents the procedures developed for designing the three major components viz. emitter, lateral and submain of a microirrigation subunit. The emitter discharge is determined as design emitter discharge, which is considered as required average emitter discharge for design of lateral and submain lines. Subunit of the system is designed to meet this required average emitter discharge. The single (uniform and tapered) and paired laterals have been dealt separately. However, the basic approach for their design is the same. The design of single lateral includes determination of diameter or length of lateral and the pressure head required at the inlet of the lateral so as to meet the required average emitter discharge and uniformity. For design of paired laterals an additional parameter i.e. best submain position, is to be determined.

Design procedures have been developed on the basis of theories, presented in chapter-3. The flowcharts (Appendix-A) prepared for the design of different components of microirrigation subunit are based on the design methodology developed. Interactive, user-friendly computer programmes have been developed for determination of emitter discharge and design of microirrigation subunit (lateral and submain), separately. The programmes were developed in C++ language.

4.1 Emitter Discharge

The mathematical model developed in section 3.1, to evaluate the soil water distribution below a trickle source and position of wetting front after application of a fixed volume of water, has been used to determine the discharge from the trickle source.

Two types of trickle sources viz. disc source and strip sources, have been considered for analysis of the movement of water below the source. The procedure used for analyzing the movement of water below the trickle sources is described in the following section.

4.1.1 Soil-water distribution model

The algorithm given by **Brandt *et al.* (1971)** has been used to solve the two-dimensional flow of water below the trickle source. The procedure combines the ADI finite difference procedure with Newtons iterative method. The equations proposed by **Saxton *et al.* (1986)** which describe the soil-water characteristics as function of soil texture, have been used in the model. The procedure used in solving the two-dimensional flow problem is presented in section 3.1.5. The problem of determination of discharge from the emitters is to find that discharge from the emitters, which will distribute water in the plants root zone in a desired manner. The desired distribution pattern may be indicated by specifying the moisture content at a point situated away from the source but in the root zone of the plant. The stepwise procedure for determination of emitter discharge is described in the following section.

4.1.2 Procedure for determination of emitter discharge

The emitter discharge to obtain desired distribution pattern of water, is determined by using the following steps.

1. Information on texture of the soil (sand and clay contents), moisture content of the root zone before irrigation (θ_n), minimum and maximum permissible emitter discharge, total volume of water to be applied (V) in a single application, and root zone width and depth to be evaluated are collected.
2. Coordinates (x, z) or (r, z) of a critical point, P, in the root zone of the plant are selected.
3. The moisture content required (θ_r) at the point P, after irrigation is obtained. This may be the minimum moisture content allowable at any point in the root zone.
4. A value of emitter discharge between minimum and the maximum allowable emitter discharge is selected and corresponding duration of irrigation is determined to supply V volume of water.
5. The moisture content at P is determined using the soil-water distribution model.
6. If, the obtained moisture content at P is not equal to θ_r, golden section search is applied as described in section 3.1.7 for selection of next emitter discharge.
7. The process is repeated till required moisture (θ_r) is obtained at the point P.

4.2 Lateral Design

The procedures developed for the design of microirrigation laterals are based on lateral discharge equation approach as discussed in section 3.2.1. The lateral discharge equation is simulated by assuming pressure head at the down stream end of the lateral and determining inlet flow rate and inlet pressure head (by back step calculations). The discharge required at the inlet of the lateral is obtained from number of emitters on the lateral and known required average emitter discharge (q_{req}). The pressure head required at the inlet of the lateral is obtained from the lateral discharge equation. Now, the uniformity of emission from the lateral can be evaluated. Different lengths (or diameters) of the lateral are evaluated in this way and the length or diameter which meets the design criteria is selected as the designed length or diameter.

With this approach, both single as well as paired laterals can be designed on uniform or nonuniform slope conditions.

4.2.1 Single lateral

Two types of problems of design are encountered in single laterals. Due to the restrictions imposed by geometry of the field, the length of lateral may be pre-decided and hence the diameter of the lateral is to be determined. When the diameter of the lateral is pre-decided the length of lateral is designed. Generally, the diameter of a single microirrigation lateral is uniform but in some cases the lateral may be tapered with two diameters.

4.2.1.1 Diameter of single lateral

The steps for designing the diameter of a single lateral are as below:

Uniform lateral

1. A series of values, D_1, D_2, D_3, ... , D_m for standard diameters available are selected, from smallest to largest.
2. The data samples $(H)_1 \sim (q_L)_1$, $(H)_2 \sim (q_L)_2$, ... ,$(H)_k \sim (q_L)_k$ for each given value of diameters D_1, D_2, D_3, ... ,D_m are obtained using back step method (equations 3.40-3.44).
3. The lateral discharge equation (equation 3.38) is simulated for each lateral diameter using least squares method.
4. Required pressure head at inlet, H_{rin}, for each lateral diameter is obtained from the corresponding lateral discharge equation (equation 3.45).
5. The pressure head and flow rate distribution along the lateral are determined for each lateral diameter using equations (3.51–3.53).
6. Uniformity of water application is determined for each lateral diameter.
7. The smallest lateral diameter that gives the desired uniformity is selected as the design diameter of the lateral.

Tapered lateral

Initially, the lateral is designed as uniform lateral using the procedure described above. If the uniformity criteria permit, the lateral

is considered for tapering and length of tapered section is designed. The procedure for design of length of tapered section is as below:

1. If the designed lateral diameter (from step 7, above) is D_L, the next lower diameter (D_S) is selected for tapered section of the lateral.
2. Considering the lateral with two sizes with the first lateral element having diameter D_S and rest of the lateral diameter D_L, steps 1–5 (of uniform size) are repeated. Similarly, the process is repeated considering the last 2, 3, 4, ... , N-1 elements having lateral diameter D_S and rest of the elements diameter D_L. To save the computation time golden section search is applied as explained in section 3.2.5.
3. Uniformity of water application is determined for each option considered in step 2, above. The largest number of elements with diameter D_L giving the desired uniformity are selected as the length of tapered section.

4.2.1.2 Length of single lateral

The procedure of designing length of lateral is similar to the procedure of designing diameter. When the diameter of lateral, emitter spacing, minimum and maximum feasible length of lateral, slope along the lateral, required average emitter discharge, emitter discharge equation etc. are known the length of a lateral can be designed. The knowledge of maximum feasible length may be necessary because of the geometrical restrictions of the field and the minimum length is specified

for saving the computational time. Number of emitters corresponding to the minimum and the maximum length of the lateral are calculated for the given emitter spacing. Starting with minimum number of emitters (or minimum length), the required parameters (UCC and H_{rin}) are calculated using steps 1-6 of the procedure for design of diameter (section 4.2.1.1). Similarly, the required parameters (UCC and H_{rin}) are obtained for each option of the lateral length (in one spacing incremental length). A lateral may have as many as three options for length with the same value of UCC. Therefore, the maximum length of lateral that gives the desired uniformity is selected as the designed length.

The flowcharts developed for the design of single laterals are appended (Fig. A-1 and Fig. A-2).

4.2.2 Paired lateral

The principle of design for paired lateral is similar to that for single lateral. The difference in the procedure is that two lateral discharge equations are simulated, one each for laterals on left and right sides of the submain. The best submain position (P_{best}) which is defined as the lateral length from the upper end of the paired laterals (**Kang and Nishiyama, 1996c**), is an additional parameter to be determined. (**Kang and Nishiyama, 1996a**) reported that P_{best} is unique for fixed lateral parameters and field conditions. On a level field, P_{best} is located at the centre of paired lateral but, on sloping field it will be located between centre and the upper end of the lateral. P_{best} shifts

toward upper end of the paired lateral when the length of the lateral decreases or the diameter of the lateral increases. P_{best} is located at or near the centre of the lateral when the lateral diameter is relatively small and the lateral length is too long.

To simplify the procedure it is assumed that the submain can be placed only at the centre of an emitter spacing. Therefore, when designing a paired lateral it is necessary that at least one emitter is placed on each side of the lateral. Contrary to the single laterals, paired laterals have emitters on both the ends (i.e. a 100 m long lateral will have 101 emitters place at 1 m spacing) and emitters adjacent to the inlet in both the directions are placed at half of the normal emitter spacing (S_e).

Similar to the single laterals the design problem of paired laterals may also be classified as design of diameter when length is known and design of length when diameter is known.

4.2.2.1 Diameter of paired lateral

The sequence of calculations for designing the diameter of paired laterals can be described in the following steps. The information required is - length of lateral, slope along the lateral, required average emitter discharge (q_{req}), emitter flow equation, etc.

1. A series of values, D_1, D_2, D_3, ... , D_m for standard diameters available are choosen from largest to smallest. Initially, the largest diameter (D_1) is selected as the lateral diameter.

2. Initially, the submain is assumed to be at the centre of the lateral.
3. The data sample of pressure head and flow rate at the inlet of the lateral i.e. $(H)_1 \sim (q_L)_1$, $(H)_2 \sim (q_L)_2$, ... ,$(H)_k \sim (q_L)_k$, are obtained for the selected value of lateral diameter (D), using back step method (equations 3.40 – 3.44).
4. After simulating lateral discharge equation (equation 3.39) the required pressure head at the inlet, H_{rin}, is determined using Newton-Raphson method (equations 3.48-3.50).
5. The pressure head and flow rate distribution along the lateral is obtained by forward step method (equations 3.51 – 3.53).
6. Uniformity of water application is evaluated.
7. The submain position is shifted by one emitter spacing in upward slope direction and steps 3 - 6 are repeated. Thus, uniformity of application is evaluated for all the possible positions of the submain for the selected lateral diameter.
8. The submain position that gives highest value of uniformity (UCC) is the P_{best} for the selected diameter of the lateral. Corresponding to this lateral diameter, P_{best}, UCC and H_{rin} are recorded.
9. The next diameter is chosen and steps 3 - 8 are repeated. To save computation time, initially, the submain is assumed to be located at the P_{best}, obtained for the previous diameter.
10. The smallest diameter that gives the desired UCC is considered as the designed diameter with the corresponding P_{best} and H_{rin}.

4.2.2.2 Length of paired lateral

The procedure for designing the length of paired lateral is same except that instead of various options for diameter, options for lateral length are evaluated. The information required is - lateral diameter, slope along the lateral, required average emitter discharge (q_{req}), emitter discharge equation, maximum permissible length of lateral, etc. The design procedure can be presented in the following steps.

1. Considering the maximum permissible length of lateral is as the length of the lateral, number of emitters on the lateral are determined for the known emitter spacing.
2. The submain is assumed to be located at the centre of the lateral, initially.
3. The data sets of pressure head and flow rate at the inlet of the lateral i.e. $(H)_1 \sim (q_L)_1$, $(H)_2 \sim (q_L)_2$, ... ,$(H)_k \sim (q_L)_k$ are obtained using back step method (equations 3.40 – 3.44).
4. After simulating lateral discharge equations (equation 3.39) required pressure head at the inlet, H_{rin}, is determined using Newton-Raphson method (equations 3.48 - 3.50).
5. The pressure head and flow rate distribution along the lateral is determined by forward step method (equations 3.51 – 3.53).
6. Uniformity of water application is evaluated for the lateral length and P_{best} considered in steps 9 and 7, respectively.
7. Shifting the submain by one emitter spacing in up slope direction steps 3 - 6 are repeated (if end of the lateral is encountered follow

step 8). Thus, uniformity of application is obtained for all the probable positions of submain for the selected lateral length.

8. The submain position that gives highest value of uniformity (UCC) is considered as P_{best} for the selected length of the lateral. Corresponding to this lateral length, P_{best}, UCC and H_{rin} are recorded.

9. Increasing the lateral length by one emitter spacing steps 3 – 8 (if lateral length is equal to the minimum allowable length, follow step 10) are repeated. To save computation time, initially, the submain is assumed to be located at the P_{best} determined for previous length.

10. The largest length that gives the desired UCC is selected as the designed lateral length with the corresponding P_{best} and H_{rin}.

The flowchart for design of the length of a paired lateral is appended in Appendix-A (Fig. A-3). This flowchart can also be used for design of diameter of the paired lateral with slight modifications.

4.3 Submain Design

With the introduction of lateral discharge equation approach, the analysis of the hydraulics of a microirrigation submain in a rectangular field is much simplified. When slope along the submain; spacing of laterals on the submain; diameter and length of the laterals; and the lateral discharge equation is known, the length or diameter of the

submain can be designed. The procedure for design of the submain is presented in the following sections.

4.3.1 Diameter of submain

The diameter of a submain may be uniform (single pipe size) or tapered (two pipe sizes). Theories presented in section 3.3 have been used for development of the design procedures. For designing diameter of a submain the information required are - field slope along lateral, spacing of emitters, length of lateral, diameter of lateral, spacing of laterals along the submain, field slope along the submain, required average emitter discharge, required uniformity of application, emission equation for emitters selected, and the lateral discharge equation for the laterals used.

The procedures for designing uniform and tapered diameter of a submain are explained in the following sections.

4.3.1.1 Uniform submain

The procedure for the design of uniform diameter of the submain is as below:

1. According to the lateral spacing the number of laterals along the submain are determined.
2. The diameters available for the submain are obtained. Initially, the smallest diameter is selected as diameter of the submain.

3. A range of pressure heads for the downstream end of the submain is selected and pressure head at the downstream end of submain is chosen within the selected range.
4. Discharge in the first lateral (from closed end) is obtained, using lateral discharge equation. This will also be the discharge in the first element of the submain.
5. The friction head loss in the first submain element is determined (using equations 3.61) and pressure head at the inlet of second lateral is obtained.
6. Similarly, the discharges from all the laterals are determined, step by step, using the same lateral discharge equation and back step analysis. In this way the pressure head and discharge at the inlet of the submain are obtained.
7. The average emitter discharge (q_{av}) is determined by dividing the inlet flow rate with the total number of emitters in the subunit.
8. If, q_{av} obtained is not equal to q_{req}, a fresh estimate of pressure head at the downstream end of the submain is obtained using golden section search method and steps 2 – 7 are repeated.
9. If, q_{av} obtained equals q_{req} with the acceptable error, the uniformity of application (UCC) is evaluated by forward step analysis and recorded against the diameter of the submain considered.
10. Next larger diameter is selected and steps 4 – 9 are repeated.

11. The smallest diameter that gives uniformity greater than or equal to the required uniformity of application is considered as the designed diameter of the submain.

4.3.1.2 Tapered submain

For designing the tapered submain the procedure is similar to that of tapered lateral design. After finding the diameter of uniform submain, the next smaller diameter of the submain (if available) is considered for tapering the submain. The procedure given below considers two pipe sizes (diameters) for determination of q_{req} and UCC and length of the tapered section of the submain is determined.

1. Considering the first element (downstream) of the submain of smaller diameter and rest of the submain of the designed diameter (obtained in the previous section), steps 4 - 9 of section 4.3.1.1, are repeated.
2. If, uniformity determined is greater than the desired UCC, the number of elements with smaller diameter, are increased and steps 4 - 9 (section 4.3.1.1) are repeated. To minimize the computation time golden section search method (as explained in section 3.2.5) is followed to determine the number of submain elements that can be used with smaller diameter.

4.3.2 Length of submain

When diameter of the submain is known the procedure given for design of diameter (section 4.3.1.1) is also used for designing length of

the submain. In step 2, starting from minimum length different length options in an interval of lateral spacing are considered and the q_{av} is compared with q_{req}. The maximum length, which gives UCC greater than or equal to the desired value, is considered as the designed length.

The flowchart developed on the basis of procedure described above for the design of length of submain is appended in Appendix-A (Fig. A - 4).

Chapter 5

Results and Discussion

5. RESULTS AND DISCUSSION

This chapter presents the results obtained from the procedures developed in chapter 4, for designing three major components of a microirrigation subunit viz. emitter discharge, lateral and submain. Numerical examples have been used for illustration of the procedures and comparison of the results with existing methods.

5.1 Emitter Discharge

Before use, the model presented in section 3.1 for determination of emitter discharge was validated with the results of **Bresler *et al.* (1971)** and **Bresler (1978)**. The procedure presented in section 3.1.5 was used for solving the two-dimensional flow problem.

5.1.1 Validation of the model

The accuracy of the model was evaluated by comparing the position of wetting fronts obtained at different volumes of infiltration for both, strip and disc trickle sources used, with the experimental and predicted results of **Bresler *et al.* (1971)** and **Bresler (1978)**. The soil-water characteristic relationships used in the model were also compared with the relationships used by **Bresler *et al.* (1971)**.

The θ - h and K - θ relationships for the Gilat loam soil (sand 48% and clay 20%) obtained from equation (3.13) of **Saxton *et al.* (1986)** were compared (Fig. 5.1 and Fig. 5.2) with the relationships obtained by **Bresler *et al.* (1971)**. It is evident from Fig. 5.1 that the slope of the θ -

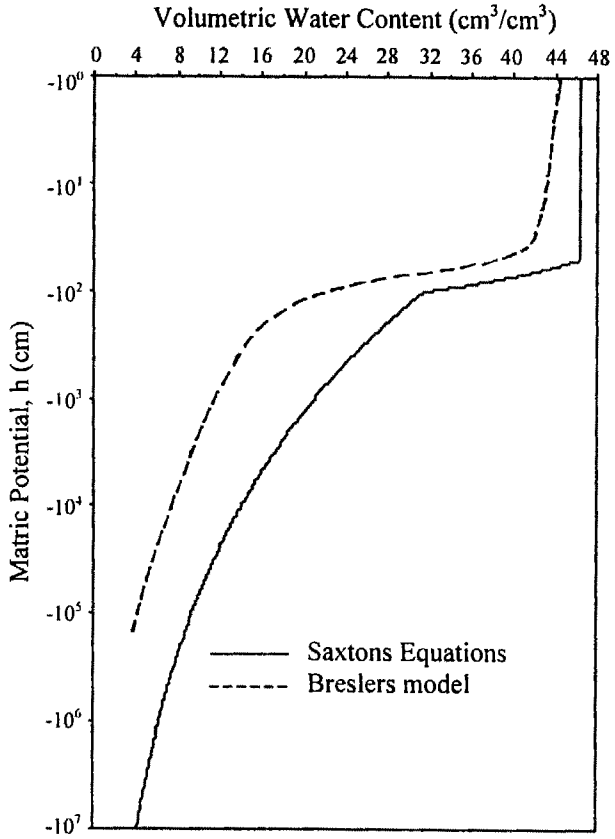

Fig. 5.1 Comparison of θ - h relationship obtained from Saxtons equations with Bresler et al. (1971) for Gilat loam soil.

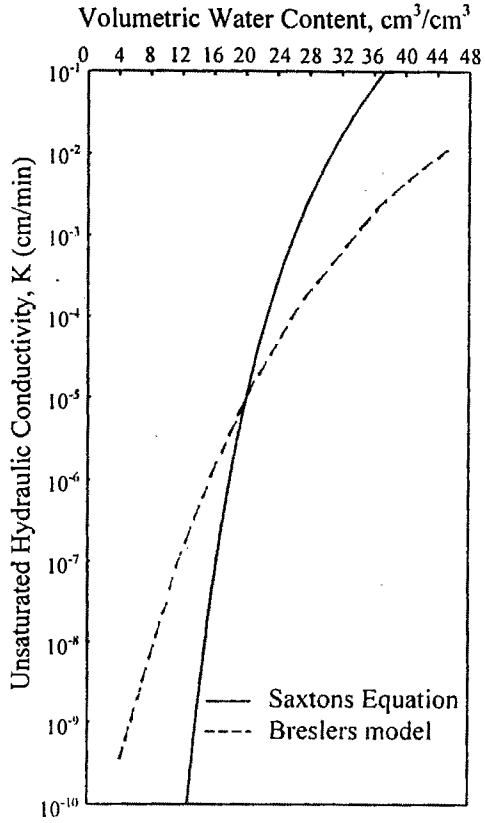

Fig. 5.2 Comparison of K - θ relationship obtained from Saxtons equation with Bresler et al. (1971) for Gilat loam soil.

h curve near saturation is zero. Hence, equation (3.14f) of **Angelaski *et al.* (1993)** was used (replacing equation 3.13c) near the saturation zone and the value of specific water capacity (C) was taken as 0.00122 (for $0 \geq h \geq h_e$).

The model is validated with the experimental and theoretical results of **Bresler *et al.* (1971)** and **Bresler (1978)** through the following numerical examples to compare the positions of wetting fronts obtained from strip as well as disc sources.

The results of the proposed model was obtained for Gilat loam soil (sand = 48% and clay = 20%). The discharge rate of the disc source (q_e) considered was 4000 cm^3/hr. The initial water content (θ_n) of the soil was taken as 0.04. The contour of θ = 0.20 was considered as the wetting front. A grid interval (h) of 4 cm and the initial time increment of 0.1 s, was used for the numerical solution. The time increment was allowed to increase by a multiplying factor of 1.5. An error (ε) of 0.0001 was allowed in the computations.

The position of wetting fronts obtained after 60, 120, 180 and 240 min. of application from the proposed model and **Bresler (1978)** model are shown in Fig. 5.3. Reasonably good agreement is seen in both, horizontal as well as vertical directions. The deviation in the positions of wetting fronts predicted by the proposed model, from the Breslers model was less than 10 per cent in both the directions. The proposed model predicted relatively higher values in the horizontal direction and lower values in the vertical direction.

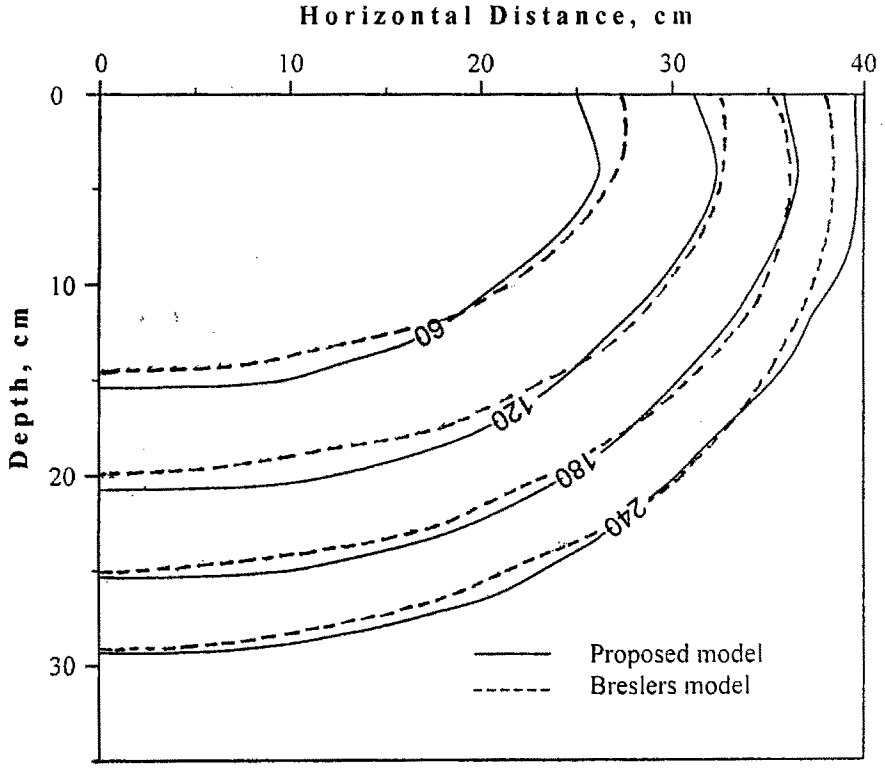

Fig. 5.3 Comparison of wetting front positions for disc source of strength 4 litre/h with the numerical results of Bresler (1978). The numbers labeling the lines indicate the duration of irrigation in minutes.

For strip source, the experimental and the predicted results of **Bresler *et al.* (1971)** were used for comparison. The wetting fronts for the air dry (θ_n = 0.04) Gilat loam soil (sand = 48% and clay = 20%) were obtained from the proposed model and were compared with the experimental and predicted results of Breslers model, as shown in Fig. 5.4. The wetting front was defined as the contour of θ = 0.20. Two application rates (q_e) of 0.495 and 0.983 $cm^3/cm/min$ were considered and the location of wetting front was obtained for different volumes of infiltrated water.

For the application rate of 0.495 $cm^3/cm/min$, the wetting fronts were predicted (Fig. 5.4a) for total infiltrated volumes of 0.3 and 1.0 litre. The position of the wetting fronts obtained, are comparable with the experimental and predicted wetting fronts of Breslers model. For both the infiltrated volumes the positions of wetting fronts obtained are under estimated in comparison to the Breslers model. In horizontal direction, the maximum deviation from the experimental results was approximately as 15 per cent and 10 per cent for 0.3 and 1.0 litre of infiltrated water, respectively.

Considering the application rate (q_e) of 0.983 $cm^3/cm/min$, position of wetting fronts were predicted from the proposed model for the total infiltrated volumes of 0.3, 1.0, 3.0 and 5.6 litre. The results of the proposed model are in good agreement with both, the experimental and the numerical results of **Bresler *et al.* (1971)** in vertical direction. However, in horizontal direction the positions of the wetting fronts have

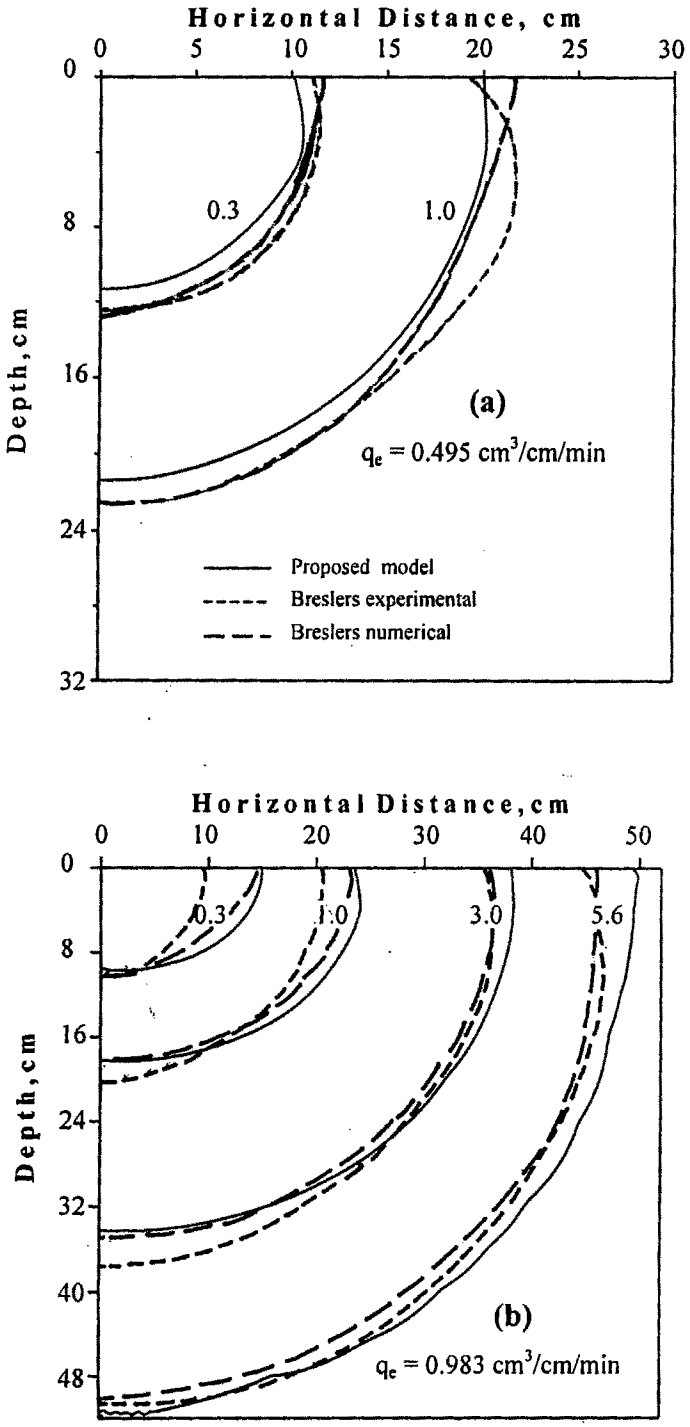

Fig. 5.4 Comparison of wetting front positions obtained for two strengths (q_e) of strip sources with the experimental and predicted results of Bresler (1971) for Gilat loam soil (numbers labeling the lines are the total volume infiltrated in litres).

been over estimated in comparison to both, experimental and predicted results of Breslers model. The maximum deviations in the position of the wetting front from the experimental results were 48, 22, 8, and 10 per cent, respectively for 0.3, 1.0, 3.0 and 5.6 litre of total volume of water infiltrated. The maximum deviations from Breslers predicted results were 29, 17, 8 and 9 per cent, respectively for 0.3, 1.0, 3.0 and 5.6 litre of total volume of water infiltrated.

The variation in the results of the proposed model may be due to the error in estimation of saturation moisture content (θ_s = 0.463) from Saxtons equation as against the discrete value (θ_s = 0.44) used by **Bresler *et al.* (1971)**. The other source of error may be in the estimation of soil-water characteristic properties.

5.1.2 Determination of emitter discharge

The procedure explained in section 4.1.2 was used for determination of emitter discharge for the given soil texture and the desired water distribution pattern. The results obtained for emitter discharge are explained with the help of examples in the following text.

Example 1

In a clay loam soil (sand = 48% and clay = 20%) with initial moisture content (θ_n) of 0.20, water is applied with a trickle source. Show the effect of change of emitter discharge on the moisture content of points having coordinates (radial distance and depth from the source in cm) of 22, 24; 22, 16; 14, 24; and 14, 16 when total volume of water

applied is 12, 14, 16, 18 and 20 litres. The trickle source may be considered to be a disc source.

Solution

The moisture content at the desired points below the source was determined using the procedure explained in section 4.1, for different flow rates. The variation of moisture content with the flow rate at different volume of infiltration is shown in Fig. 5.5. It is evident that the moisture content of all the four points decreases with increase in flow rate, irrespective of the total volume applied. This may be due to large area coming under ponding at the surface and hence infiltration is taking place from a larger disc as the discharge is increased. As a result the waterfront has advanced more in horizontal direction and less in downward direction due to smaller infiltration opportunity time. It can also be seen, in all cases, that the moisture content is approaching a constant value i.e. 0.20 for very high flow rates.

Example 2

For the a crop planted in the soil of example 1, a moisture content of 0.30 is required at a point, P, located at a horizontal distance of 22 cm and depth 24 cm from the centre of a disc source. Assuming that the moisture content in the root zone prior to irrigation (θ_n) depletes to a uniform level of 0.20, determine the discharge of the emitter if 20 litre of water is to be applied in each application.

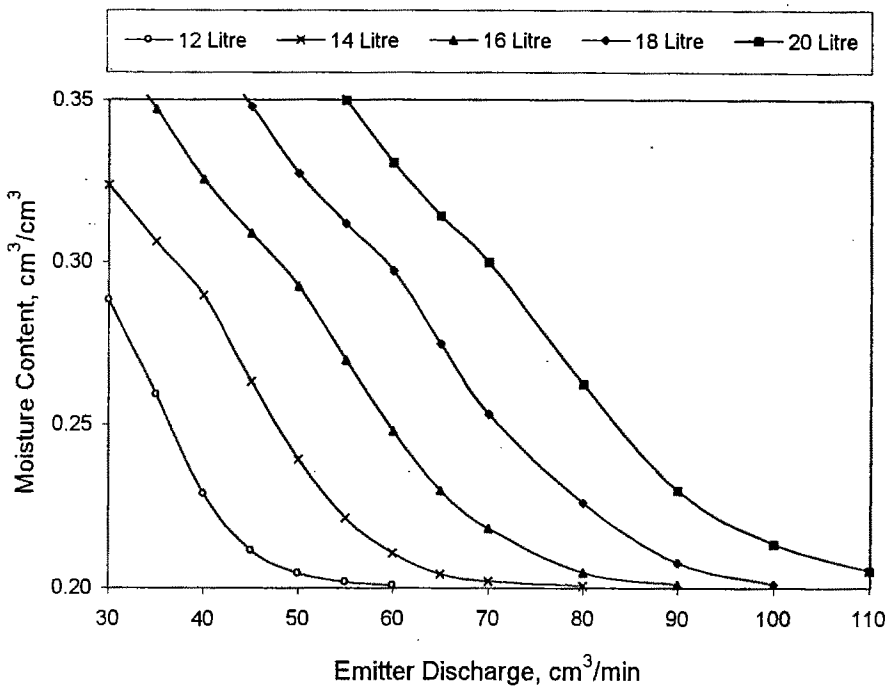

(i) r = 22 cm, z = 24 cm

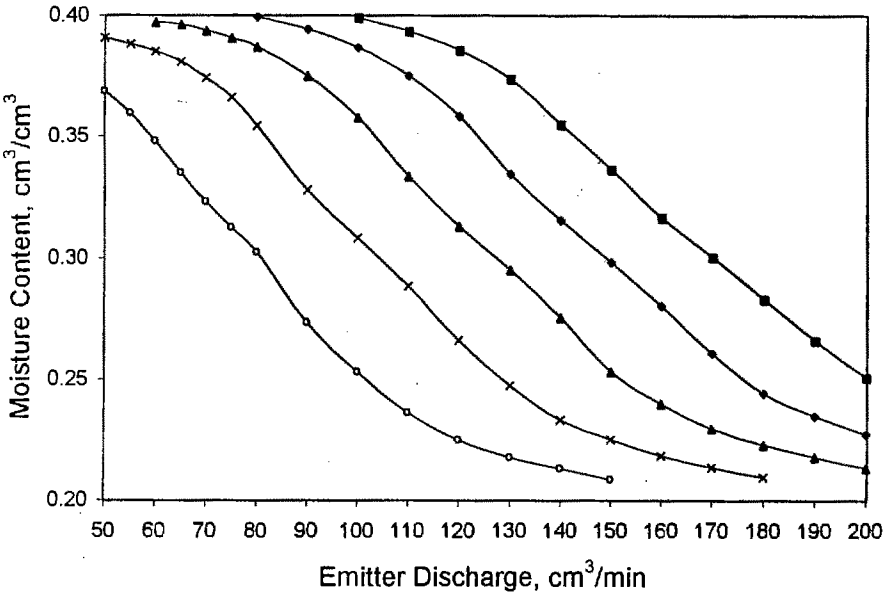

(ii) r = 22 cm, z = 16 cm

Fig. 5.5a Variation in moisture content at a point P(r, z) in the plant root zone with emitter discharge for different infiltrated volumes.

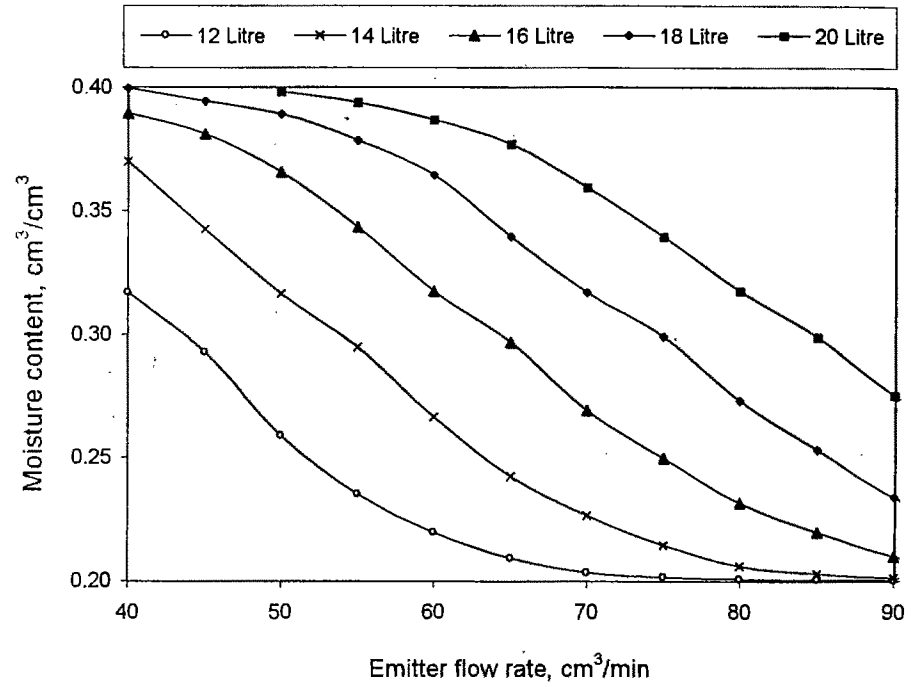

(iii) r = 14 cm, z = 24 cm

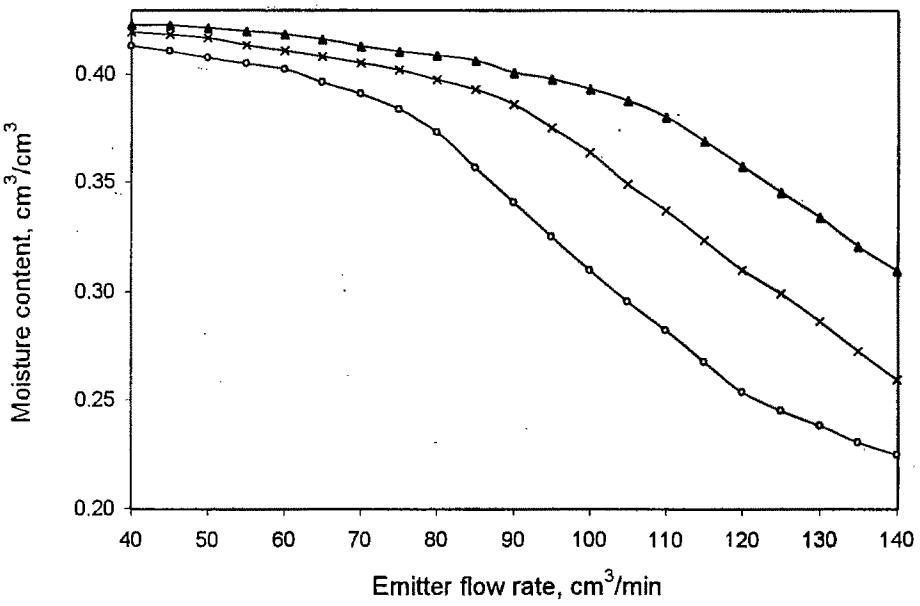

(iv) r = 14 cm, z = 16 cm

Fig. 5.5b Variation in moisture content at a point P(r, z) in the plant root zone with emitter discharge for different infiltrated volumes.

Solution

Using the procedure presented in section 4.1.2 the discharge of the emitter obtained from the proposed model is 70 cm^3/min (4.2 litre per hour), which can also be seen from Fig. (5.5a(i)). The distribution of soil moisture (Fig. 5.6) at this emitter discharge clearly shows that the region between point P and the top and left boundaries which is the root zone of the plant, has moisture content higher than the required moisture content (i.e. 0.30) at this point.

5.2 Lateral Design

The problem of design of a microirrigation system has become simpler with the introduction of lateral discharge equation approach. This approach is not only simple but is accurate as well, because of consideration of actual flow from the emitters and use of basic equations of steady pipe flow. The superiority of the power equation form (equation 3.38 or 3.39) of lateral discharge equation over the polynomial form (equation 3.37) may be explained through the following example.

When data given in Table 5.1 are used for designing the length of a single lateral a similar error is encountered while estimating the head required at the inlet of the lateral. The pressure head range selected for the downstream end of lateral was 6.5 – 12 m. The coefficients of equation (3.37), the inlet flow rates for the minimum and the maximum pressure heads (i.e. 6.5 m and 12 m) assumed at downstream end of

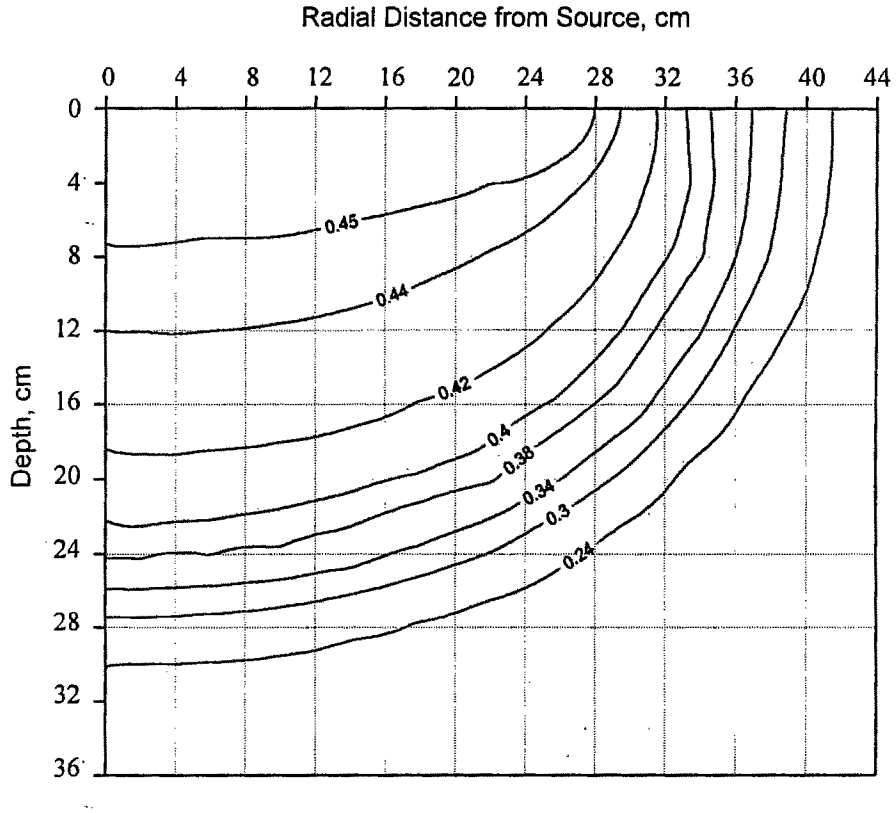

Fig. 5.6 Soil-moisture contours obtained after application of 20 litre of water with the emitter discharge of 4.2 litre per hour (example 2).

the lateral and the required inlet flow rate for the corresponding length of lateral, determined are given in Table 5.2. It is evident from Table 5.2 that the required inlet discharge for lateral length greater than 186 m, is not falling in the range of discharges for which the lateral discharge equation is simulated. Therefore, for the lengths of lateral greater than 186 m, equation (3.37) has to be extrapolated beyond its range. Fig. 5.7 shows the trend of equations (3.37 and 3.38), simulated for the lateral length of 187 m. It is clear that on extrapolation, equation (3.37) gives an absurd trend and will result in a severe error while, equation (3.38) maintains its trend and leaves no scope for such errors.

The methodology used for the design of single and paired laterals is based on the simple power equation form (equation 3.38 or 3.39) of the lateral discharge equation and their results are explained with the help of examples in the following sections.

5.2.1 Single lateral

The results of methodology developed for the design of single lateral are presented through examples separately, for both types of design problem i.e. design of diameter and design of length of the single laterals.

5.2.1.1 Diameter of single lateral

When the length of the lateral is fixed, the diameter of the lateral may be designed using the procedure given in section 4.2.1.1.

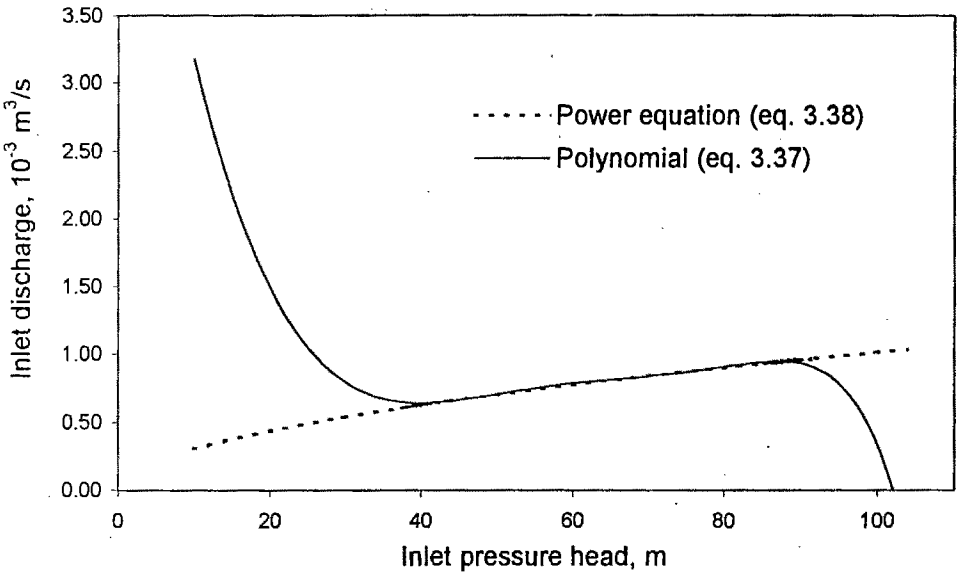

Fig. 5.7 Trend of lateral discharge equation when extrapolated beyond range for 187 m long lateral for data and field condition given in Table 5.1.

Table 5.1 Lateral parameters and field conditions for examples.

Parameter	**Value**
Lateral diameter (D)	16 mm
Emitter spacing (S_e)	1 m
Lateral length from the lateral inlet to the first emitter (S_{e1})	1 m
Field slope along lateral (down slope from the inlet)	-0.03
Required average emitter discharge (q_{req}),	3.33×10^{-6} m^3/s
Required Christiansens uniformity coefficient (UCC)	0.95
Minor loss factor due to emitter connections (k_{fit})	0.3
Emitter riser height (h_r)	1 m
Emitter riser length (L_r)	1.2 m
Emitter riser diameter (D_r)	5 mm
Emission equation	$q = 1.053 \times 10^{-6} H^{0.5}$ m^3/s

Table 5.2 Inlet discharge range, required inlet discharge and coefficients of equation (3.37) for lateral parameters and field conditions of Table 5.1.

Parameter	**Length of lateral (m)**		
	186	**187**	**188**
Inlet discharge range (m^3/s)	6.19×10^{-4} – 9.41×10^{-4}	6.26×10^{-4} – 9.51×10^{-4}	6.32×10^{-4} – 9.60×10^{-4}
Required inlet discharge (m^3/s)	6.194×10^{-4}	6.227×10^{-4}	6.26×10^{-4}
C_0	2.6419×10^{-4}	6.3698×10^{-3}	-2.5711×10^{-3}
C_1	9.3065×10^{-6}	-4.2594×10^{-6}	1.7174×10^{-4}
C_2	1.3390×10^{-8}	1.1121×10^{-6}	-2.4046×10^{-6}
C_3	-5.1389×10^{-10}	-1.4961×10^{-7}	-1.6453×10^{-8}
C_4	-2.9722×10^{-12}	1.8364×10^{-9}	5.2250×10^{-10}
C_5	8.3889×10^{-14}	-3.0556×10^{-11}	1.2583×10^{-12}
C_6	-2.4944×10^{-16}	3.0833×10^{-13}	-7.7778×10^{-14}
C_7	-1.0167×10^{-18}	-1.1972×10^{-15}	4.0000×10^{-16}

Example 3

Design the diameter of a tapered lateral 80 m long using the other lateral parameters and field conditions given in Table 5.1. The sizes (inside diameters) available for lateral are 12 mm, 16 mm and 20 mm.

Solution

Initially, the lateral was considered to be uniform in size and its diameter was determined to be 16 mm with pressure head required at inlet of the lateral (H_{rin}) of 13.55 m and UCC of 0.97. It is evident that the uniformity of emission obtained is quite higher than the desired uniformity (0.95). Therefore, the lateral was tapered with the next lower diameter available (i.e. 12 mm) to minimize its cost. The length of lateral for which 12 mm diameter can be used, was determined to be 41 m and the corresponding H_{rin} as 14.3 m. The effect of change in H_{rin} and UCC with the length of tapered section is shown in Fig. 5.8.

5.2.1.2 Length of single lateral

Design of length of microirrigation systems is the most common problem encountered in field. The reason being the limited options available for diameter of the lateral and hence, 12 mm and 16 mm are the common sizes used in most microirrigation installations. For comparison of results the example of **Kang and Nishiyama (1996a)** has been used.

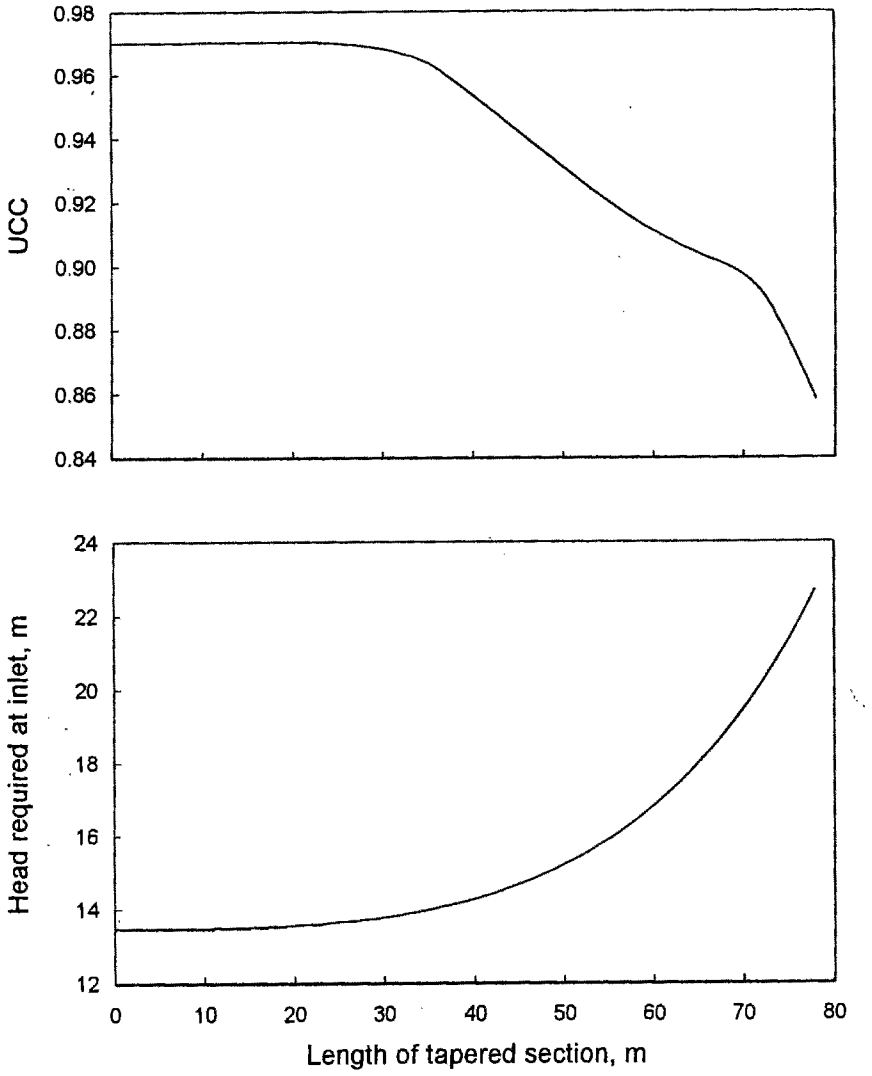

Fig. 5.8 Relationship of length of tapered section with UCC and Head required at inlet of the lateral for example 3.

Example 4

Design the length of a single lateral using lateral parameters and field conditions given in Table 5.1.

Solution

The maximum possible length of lateral was taken as 151 m. The final solution for the lateral length obtained was 91 m and pressure head required at the inlet of the lateral (H_{rin}) was 14.8 m. These results are the same as obtained by **Kang and Nishiyama (1996a, c)**. Fig. 5.9 shows the relationship of length of lateral with UCC and H_{rin}. It is clear from Fig. 5.9 that the relationships obtained are almost identical with **Kang and Nishiyama (1996a, c)**. The peaks appearing in the **Kang and Nishiyama (1996c)** model may be due to the extrapolation error of polynomial.

It is also evident from Fig. 5.9 that a lateral may have as many as three solutions of length, for the required uniformity of flow. Therefore, the largest of the three lengths is considered as designed length of the lateral for the required uniformity of flow (UCC).

5.2.2 Paired lateral

The paired laterals which are of uniform diameter also face two types of design problems i.e. design of diameter when length is fixed and design of length when diameter is fixed. The design methodology, developed in section 4.2.2 has been used for solving the design examples presented in the following sections. The example of **Kang and Nishiyama (1996a)** has been selected for comparison of results.

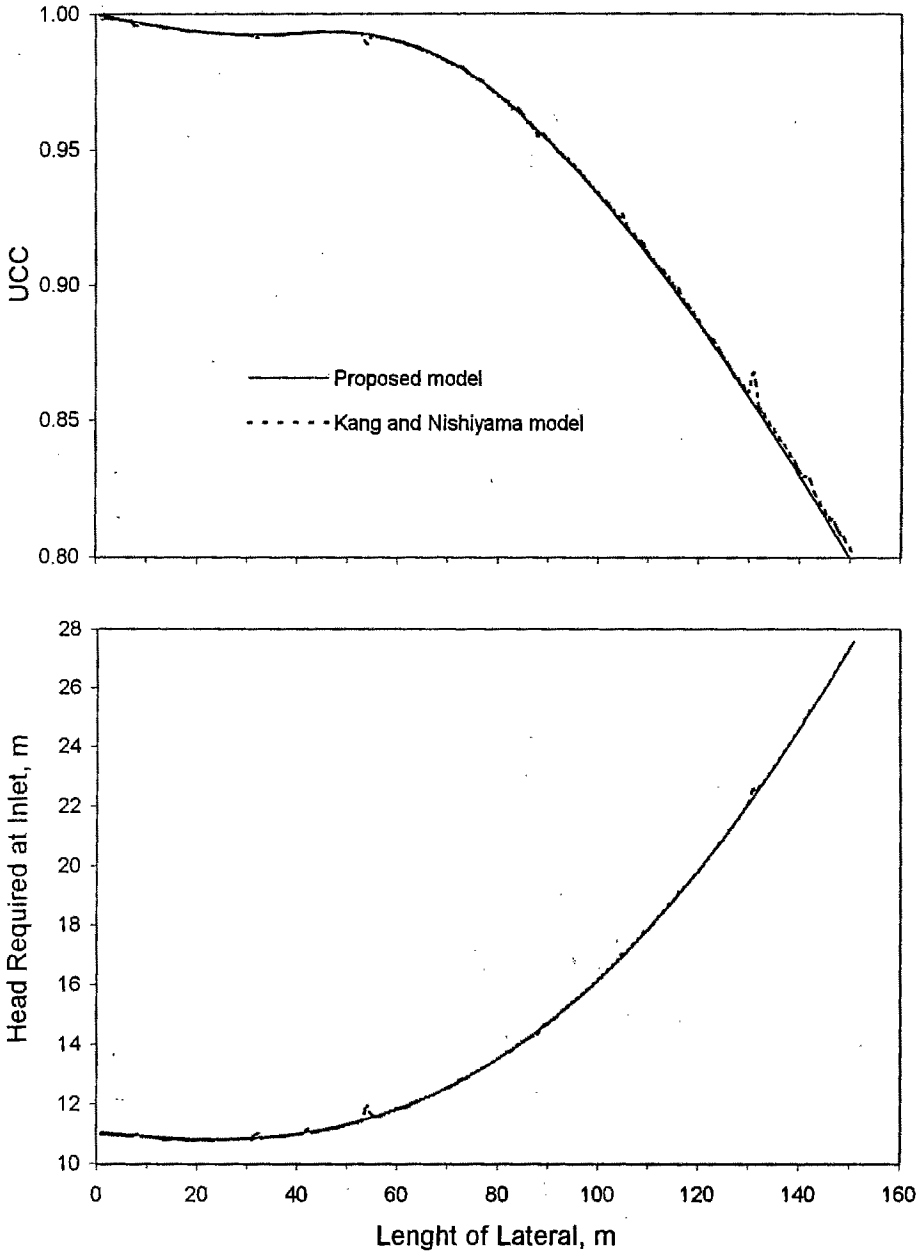

Fig. 5.9 Comparision of results of the proposed model with Kang and Nishiyama (1996c) model for a single microirrigation lateral.

5.2.2.1 Diameter of paired lateral

For designing diameter of a paired lateral, the procedure presented in section 4.2.2.1 has been used.

Example 5

Design the diameter of a paired lateral using lateral parameters and field conditions given in Table 5.3. Head loss due to emitter connections may be neglected and there are no risers to the emitters. Also show the effect of change of diameter on uniformity of flow, best submain position and the head required at the inlet. Use diameter in the range of 15 - 21 mm.

Table 5.3 Lateral parameters and field conditions for example 5.

Parameter	Value
Lateral length	208 m
Emitter spacing (S_e)	2 m
Field slope along lateral	0.03
Required average emitter discharge (q_{req})	3.33×10^{-6} m^3/s
Required Christiansen's uniformity coefficient (UCC)	0.95
Emission equation	$q=3.33\times10^{-7} H$ m^3/s

Solution

The relationship of diameter of lateral with the uniformity of flow, best submain position and the head required at the inlet, obtained is shown in Fig. 5.10. As can be seen from Fig. 5.10 that there are two solutions for the lateral diameter i.e. 16.6 mm and 20.6 mm with best submain position (P_{best}) of 68 m and 21 m and H_{rin}, 11.4 m and 10.25 m, respectively. These results are almost the same as obtained by **Kang and Nishiyama (1996a, c)**. Fig. 5.10 also shows that there may be two solutions for the diameter of a lateral with the same uniformity (UCC). Therefore, the smaller of the two diameters (i. e. 16.6 mm) must be chosen as the design diameter of the lateral with the corresponding H_{rin} (= 11.4 m) and P_{best} (= 68 m).

5.2.2.2 Length of paired lateral

The procedure presented in section 4.2.2.2 was used for designing length of the paired lateral.

Example 6

Design the length of a paired lateral using lateral parameters and field conditions given in Table 5.4. No risers are used with the emitters and head loss due to emitter connections may be neglected.

Solution

The maximum length for the lateral is taken as 220 m. The solution for the lateral length obtained is 158 m, best submain position (P_{best}) 53 m and head required at inlet of lateral (H_{rin}) 11.2 m. The length of submain was determined to be 156 m by **Kang and**

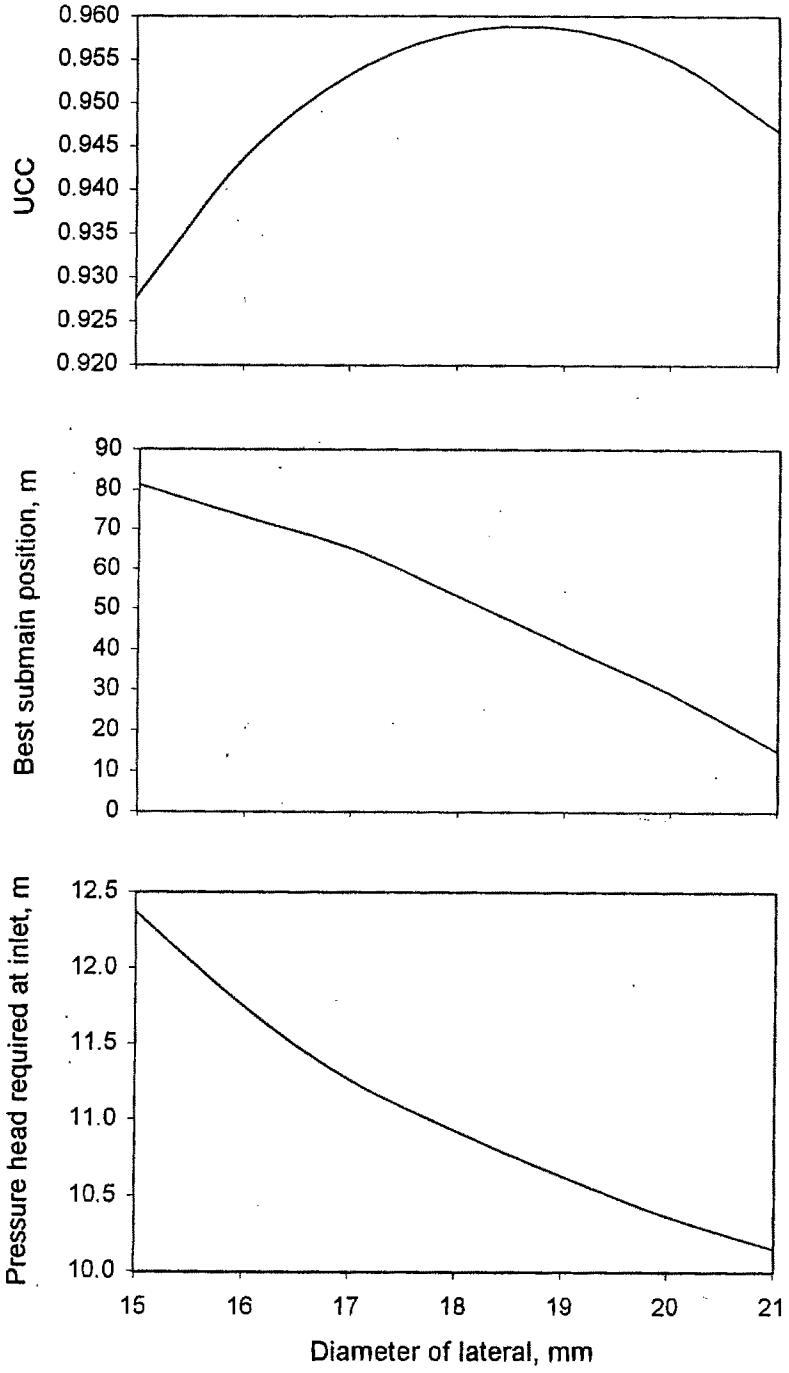

Fig. 5.10. Relationship of diameter of paired lateral with UCC, best submain position and pressure he at inlet of the lateral for example 5.

Nishiyama (1996a, c) and P_{best} as 51 m and 53 m by **Kang and Nishiyama (1996a)** and **Kang and Nishiyama (1996c)**, respectively. However, the pressure head required at the inlet of the lateral was same. The relationship of length of lateral with UCC, P_{best} and H_{rin} is shown in Fig. 5.11.

In this example (Fig. 5.11) the multiple solutions (three) for the lateral length are more prominent than as seen in example 4 (Fig. 5.8).

Table 5.4 Lateral parameters and field conditions for example 6.

Parameter	Value
Lateral diameter (D)	0.015 m
Emitter spacing (S_e)	2 m
Field slope along lateral	0.03
Required average emitter discharge (q_{req})	3.33×10^{-6} m^3/s
Required Christiansen's uniformity coefficient (UCC)	0.98
Emission equation	$q = 1.053\times10^{-6} H^{0.5}$ m^3/s

5.3 Submain Design

The design procedures presented in section 4.3 are used for designing the submain. The designed lateral parameters along with the lateral discharge equation of the laterals being operated by the submain are the input to the design of the submain.

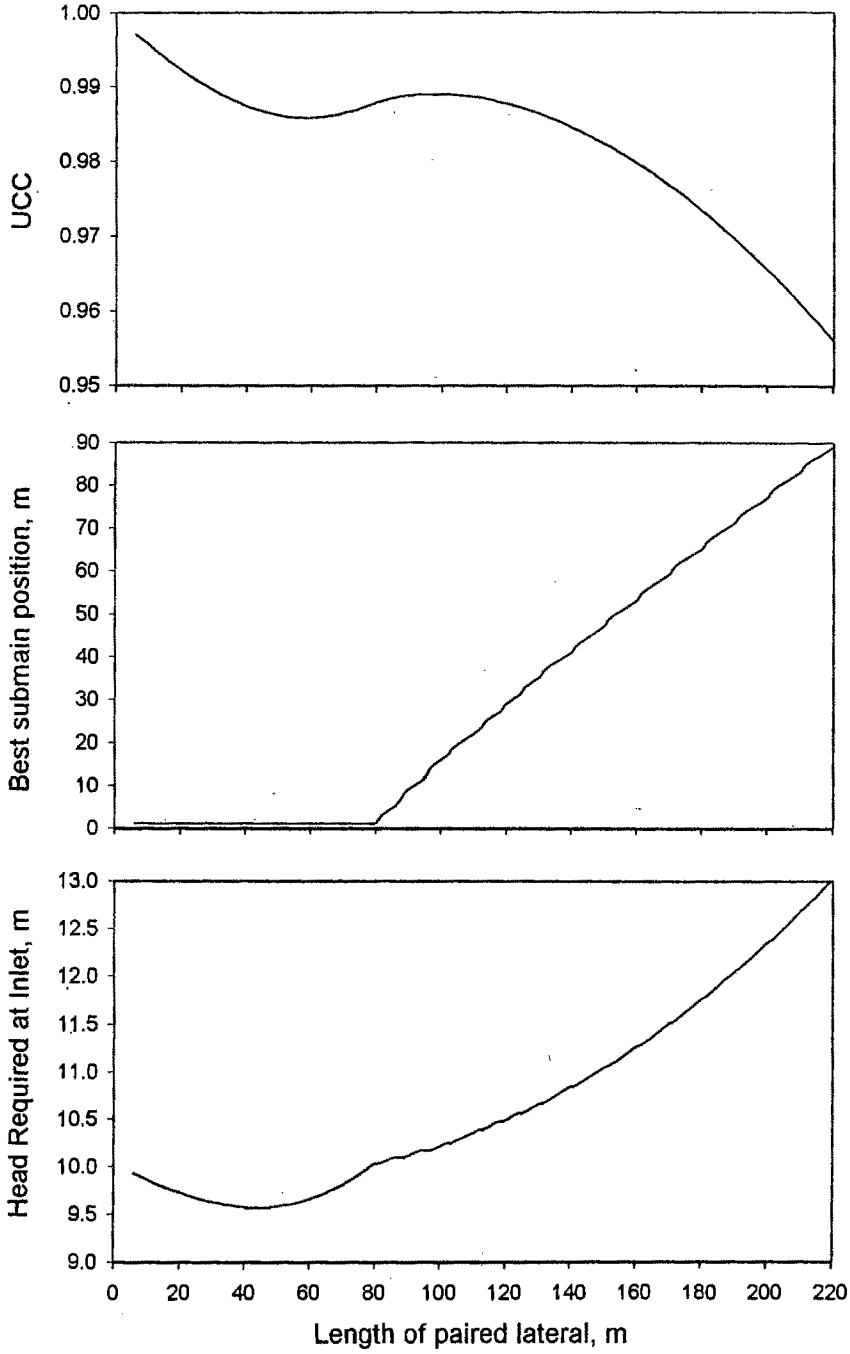

Fig. 5.11 Relationship of length of paired lateral with UCC, best submain position and Head required at inlet of the lateral for example 6.

Example 7

Design the diameter of the paired laterals and submain using the subunit parameters and field conditions given in Table 5.5.

Table 5.5 Subunit parameters and field conditions for example 7.

Parameter	Value
Lateral length, m	150
Emitter spacing (Se), m	2
Field slope along lateral	0.03
Sizes (ID) available for lateral	12, 16, 20
Lateral spacing, mm	2
Number of laterals along submain	20
Field slope along submain	0
Sizes (ID) available for submain, mm	36.8, 46.2, 59.6, 71, 85.3, 104.5
Required average emitter discharge (q_{req}), lph	12
Required Christiansen's uniformity coefficient (UCC)	0.98
Emission equation $q = 3.7908H^{0.5}$ lph	

Solution

After designing the diameter of the paired lateral the diameter of submain was designed considering the submain to be of uniform size. The next smaller diameter of the submain was used for tapering of the submain and the length of the tapered section was designed.

The designed subunit will have laterals of diameter 16 mm with the submain located at 39 m from the up slope end of the lateral. The head required at the inlet of the lateral was found to be 10.64 m to achieve the uniformity of 0.98. The diameter of the submain having 20 such laterals was determined to be 59.6 mm and the head required at the inlet of the submain was 11.24 m, when submain was of uniform size. In this case the uniformity of application obtained from the subunit was higher (0.9833) than the required uniformity (0.98). Therefore, the submain was considered for tapering with the next smaller diameter of 46.2 mm, to utilize the margin available in uniformity of application. The length of tapered section determined was 24 m and the head required at the inlet of the tapered submain was obtained as 11.44 m. For the submain of uniform size (59.6 mm) the pressure profiles of the paired laterals are shown in Fig. 5.12. When submain is tapered (with 46.2 mm) the pressure profiles of the paired laterals are shown in Fig. 5.13. The pressure profiles of the uniform and tapered submain are shown in Fig. 5.14. The variation in UCC and H_{rin} with the change in diameter of the submain is shown in Fig. 5.15.

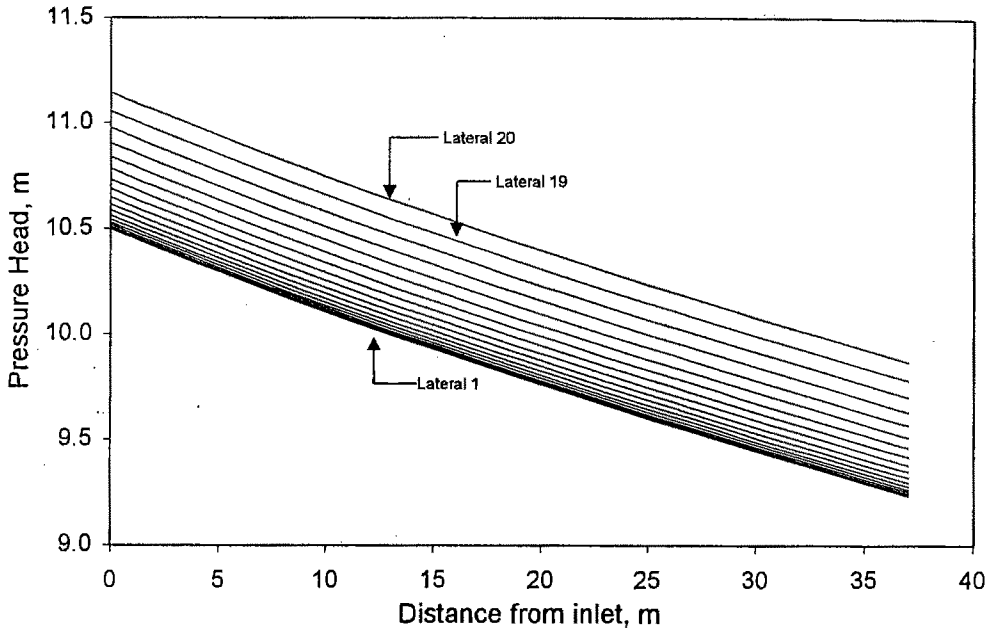

Fig. 5.12a Pressure profile of laterals at left side (up slope) of uniform submain of example 7.

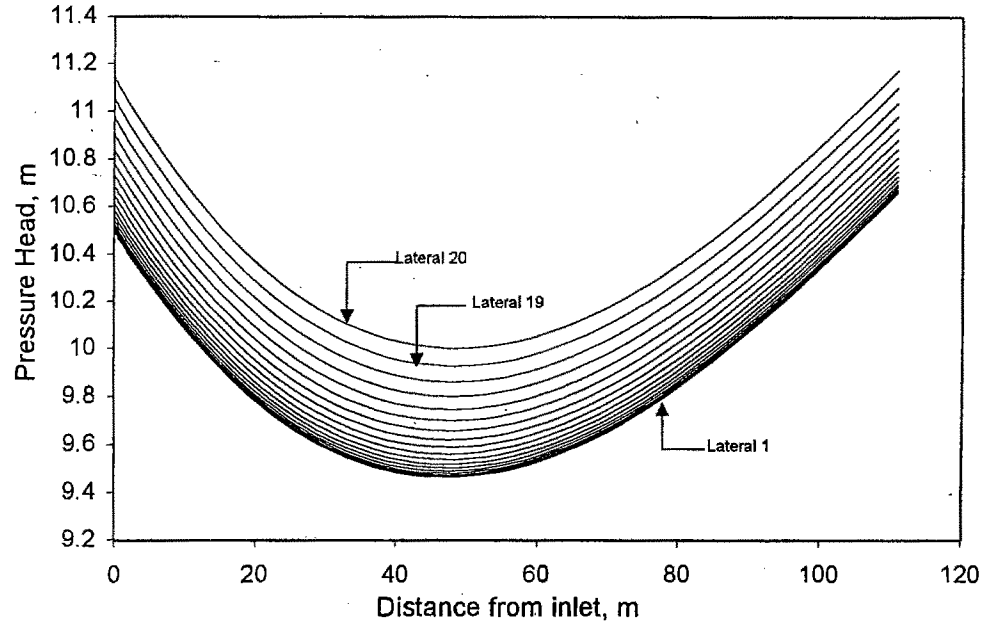

Fig. 5.12b Pressure profile of laterals at right side (down slope) of uniform submain of example 7.

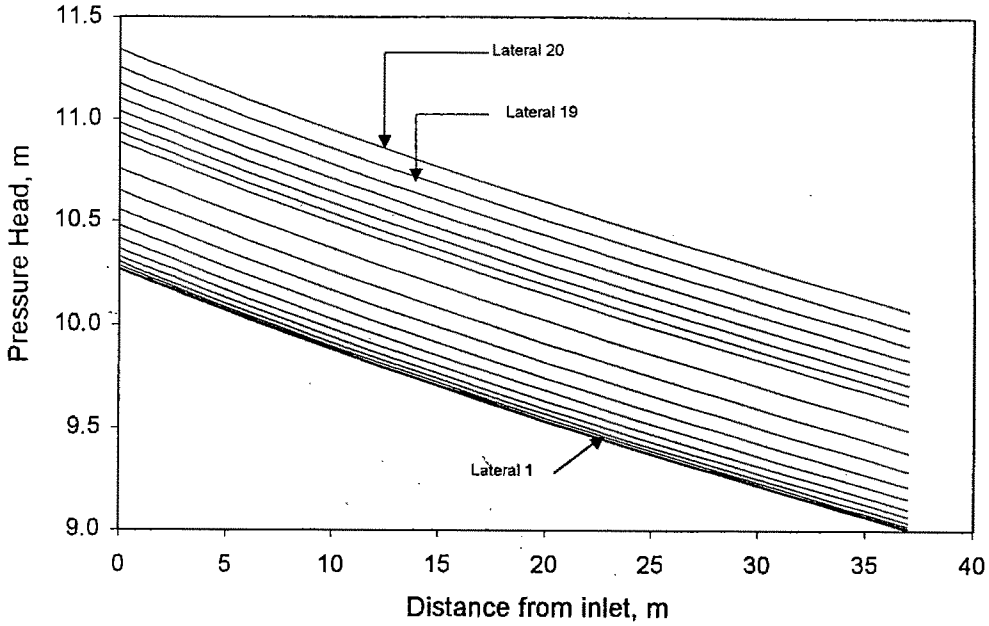

Fig. 5.13a Pressure profile of laterals at left side (up slope) of tapered submain of example 7.

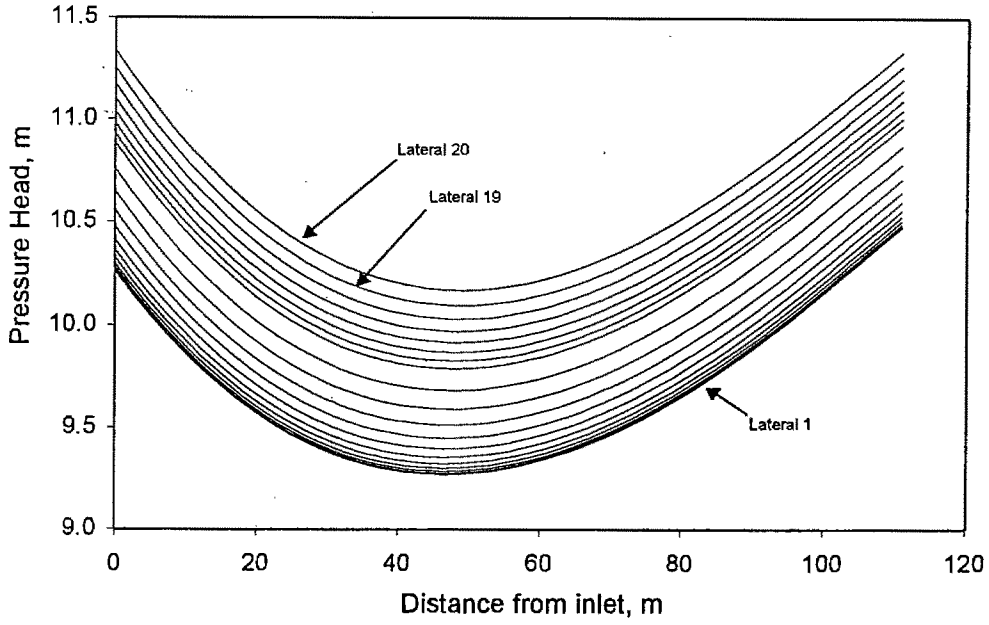

Fig. 5.13b Pressure profile of laterals at right side (down slope) of submain of example 7.

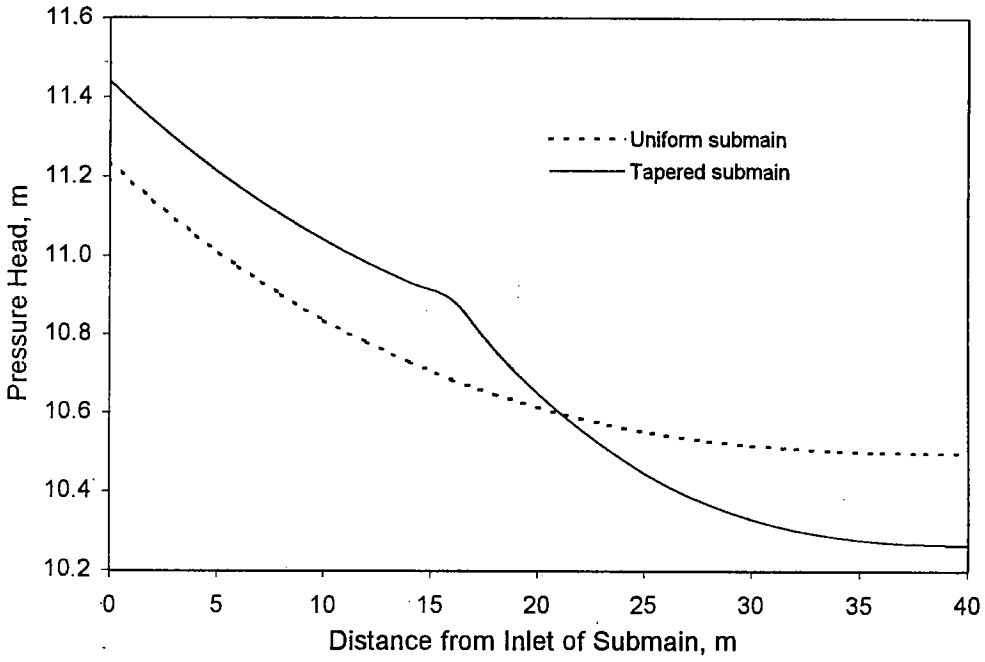

Fig. 5.14. Pressure profile along the designed uniform and tapered submain of example 7.

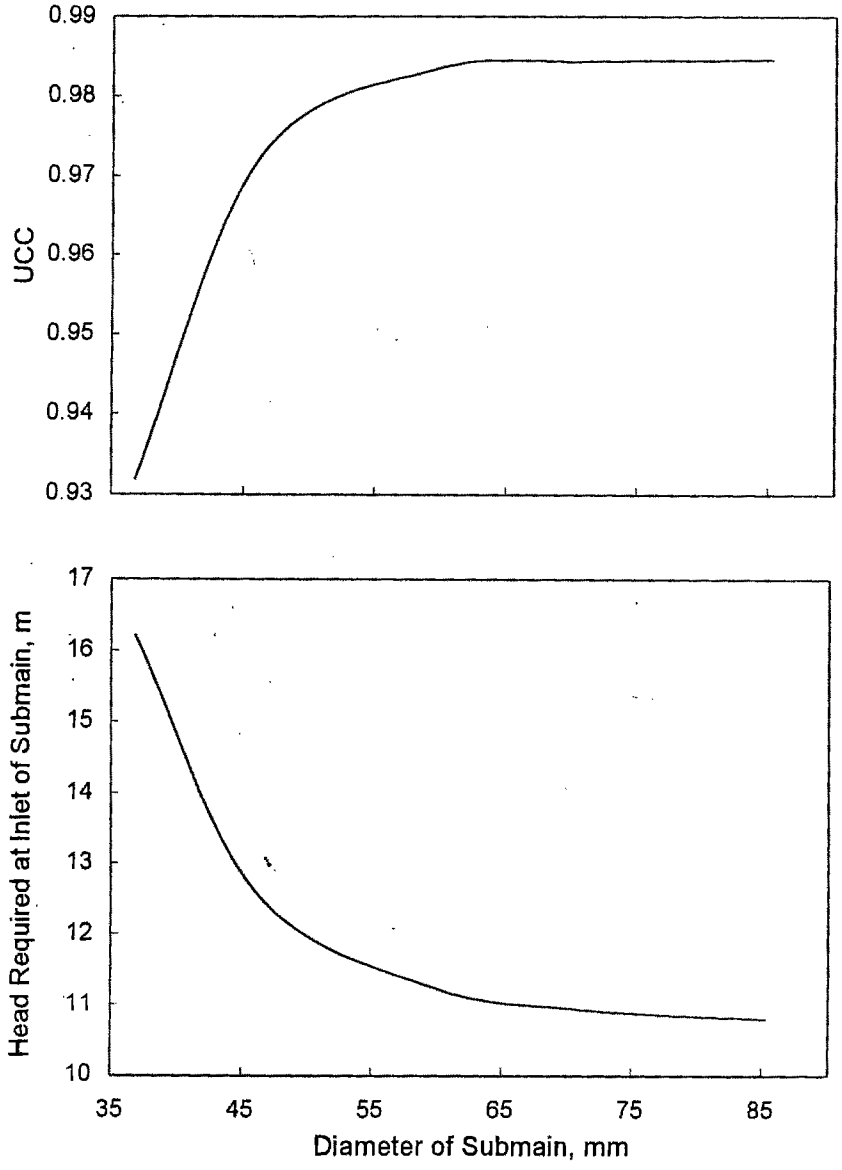

Fig. 5.15 Relationship of diameter of submain with H_{rin} and UCC for example 7.

Chapter 6

Summary and Conclusions

6. SUMMARY AND CONCLUSIONS

In spite of the popularity of microirrigation systems due to increase in production and improved quality of horticultural and vegetable crops besides saving in irrigation water, the development of appropriate design criterion still continues to be an important issue of researchers. In microirrigation systems (particularly in trickle irrigation systems), due to slow application of water at frequent intervals, water delivery is restricted to the plant root zone leaving surrounding soil dry. Efficient design of a microirrigation system needs to take care of the distribution of applied water in the root zone of the plants. For the design of a microirrigation system, the basic information required is the discharge from emitter and the daily water requirement of the crop. Appropriate values of these parameters are important not only to ensure the optimum plant growth and its yield but also for proper hydraulic design of the system for getting the best results.

Numerous mathematical models have been developed which facilitate the study of distribution of infiltrated water below point and line sources. But, most of them need a lot of information about the soil-water characteristics of the soil where the microirrigation system is to be installed. Collection of these informations is not an easy task for any design engineer. The design of a microirrigation lateral and submain

requires an accurate estimate of the emitter discharge (which is also referred as the required average emitter discharge).

On the other hand, most of the procedures available for design of microirrigation laterals and submains are based on the assumption of uniform emitter discharge, which causes error in estimation of the pressure profile of the pipeline. These methods are suitable for design of single laterals only. The step by step methods though has been modified for the design of paired laterals but, can not be used for tapered lateral design.

In the present investigation, the shape of the wetted profile below the trickle source has been considered as the criteria for determination of the emitter discharge. The position of wetting front and distribution of soil moisture in the root zone for a known emitter discharge is evaluated using a mathematical (finite difference) model. The soil-water characteristic relationships described by the texture of the soil have been input to the model. The discharge, which will distribute the water in the root zone in the desired manner, is considered as the design discharge of the emitter.

The model, which is combined with statistical equations (given by **Saxton *et al.*, 1986**) describing relationship of soil moisture with matric potential and unsaturated hydraulic conductivity in terms of the texture, has been validated through the published experimental and numerical results.

Lateral discharge equation approach has been used for design of microirrigation lateral and submain lines. In addition to simplicity and high degree of accuracy, this approach has the merit of its applicability for design of single and paired laterals on uniform and non-uniform field slopes. Instead of polynomial (as used by other researchers) a simple power equation has been used to describe the relationship of inlet flow rate and inlet pressure head of a lateral.

While designing the diameter of the lateral only standard diameters can be considered, which are available in discrete sizes only. Therefore, if the actual requirement is a nonstandard size the next higher size is considered as the design diameter of the lateral, which costs more. To reduce the cost of the lateral to some extent a procedure has been developed to taper the lateral with next smaller size. Golden section search method has been used to make the computations faster.

The lateral discharge equation approach permits to consider the submains as laterals and laterals as the emitters. With this approach, the design of microirrigation submains has been much simplified. A procedure has been developed for design of uniform as well as tapered submains of a microirrigation subunit.

User friendly computer programmes have been developed in C++ language using Borland® Version 4.5 compiler for determination of design emitter discharge and for design of lateral and submain (subunit).

The conclusions drawn from this investigation are:

1) Use of texture based soil-water characteristic relationships simplified the application of complex soil-water distribution models in design of microirrigation systems.

2) The proposed combination of models produced almost similar results obtained from the finite difference model of **Brandt et al. (1971)** for strip source and **Bresler (1978)** for disc source. The small deviations of the order of 5 – 15% may be attributed to the approximations inherited in different functional relationships i.e. equation (3.15) for $K(\theta)$ and equation (3.13) for $h(\theta)$ and in estimation of saturation water content (equation 3.14e) from soil texture.

3) The wetted profile approach, used for determination of emitter discharge facilitates to control the distribution of irrigation water in the plant root zone.

4) The power equation (equations 3.38 and 3.39) used as lateral discharge equation is simple and gives similar results as obtained by **Kang and Nishiyama (1995),** which are claimed to be the most accurate. Moreover, the chances of extrapolation error as may be encountered in Kang and Nishiyama model have been eliminated.

5) The combination of golden section search method with lateral discharge equation approach for design of tapered laterals and submains is simple.

6) The design of submain of microirrigation systems is simplified by using the lateral discharge equation approach. Use of golden section search method for obtaining required average emitter discharge from the subunit makes the computation faster without compromising with the accuracy.

References

REFERENCES

Ababou, R. 1981. Modelisation des transfers hydrques dans le sol en irrigation locallisee. Ph. D. Thesis. University of Science and Medicine and National Polutechnic Institute. Grenoble. France. (Reffered from Lafolie *et al.*, 1989)

Amoozegar-Fard, A.; Warrick, A.W. and Lomen, D.O. 1984. Design nomographs for trickle irrigation systems. *J. Irrig. & Drain. Engrg. Div. ASCE.* **110:** 107-120.

Angelakis, A. N.; Rolston, D. E.; Kadir, T. N. and Scott, V. H. 1993. Soil water distribution under trickle irrigation source. *J. Irrig. & Drain. Engrg. Div. ASCE* **119:** 484-500.

Anwar, A.A. 1999. Factor G for pipelines with equally spaced multiple outlets and outflow. *J. Irrig. & Drain. Engrg. Div. ASCE.* **125:** 34-38.

Anyoji, H. and Wu, I.P. 1987. Statistical approach for drip lateral design. *Trans ASAE.* **30:** 187-192.

Arya, L.M. and Paris, J.F. 1981. A physioemperical model to predict the soil moisture chjaracteristics from particle-size distribution and bulk density data. *Soil Sci. Soc. Am. J.* **45:** 1023-1030.

Bar-Yosef, B. and Sheikolslami, M.R. 1976. Distribution of water and ions in soils irrigated and fertilized from a trickle source. *Soil Sci. Soc. Am. J.* **40:** 575-582.

Ben-Asher, J. 1979. Trickle irrigation timing and its effect on soil water content. *Acta Hortic.* **89:** 125-131.

Ben-Asher, J., Charach, Ch and Zemel, A. 1986. Infiltration and water extraction from trickle irrigation source: The effective hemisphere model. *Soil Sci. Soc. Am. J.* **50:** 882-887.

Bhatnagar, P.R.; Chauhan, H. S. and Srivastava, V.K. 1997. Unsteady unsaturated flow from a surface disc source. *J. Hydrology.* **203:** 155-160.

Braester, C. 1973. Moisture variation at the soil surface and the advance of the wetting front during infiltration at constant flux. *Water Resour. Res.* **9:** 687-694.

Bralts, V.F. and Segerlind, L.J. 1985. Finite element analysis of drip irrigation submain units. *Trans ASAE* **28:** 809-814.

Bralts, V.F.; Kelly, S.F.; Shayya, W.F. and Segerlind L.J. 1993. Finite element analysis of microirrigation hydraulics using a virtual emitter system. *Trans. ASAE* **36:** 717-725.

Brandt, A.; Bresler, E.; Diner, N.; Hiller, J. and Goldberg, D. 1971. Infiltration from a trickle source: I. Mathematical models. *Soil Sci. Soc. Am. J.* **35**: 675-682.

Bresler, E. 1977. Trickle-drip irrigation: Principles and application to soil-water management. *Adv. Agron.* **29:** 343-393.

Bresler, E. 1978. Analysis of trickle irrigation with application to design problems. *Irrig. Sci.* **1:** 3-17.

Bresler, E.; Hiller, J.; Diner, N.; Ben-Asher, I.; Brandt, A. and Goldberg, D. 1971. Infiltration from a trickle source: II. Experimental data and theoretical predictions. *Soil Sci. Soc. Am. J.* **35:** 683-689.

Brutsaert, W. 1967. Some methods of calculating unsaturated permeability. *Trans. ASAE.* **10:** 400-404.

Bucks, D.A. and Myers, L.E. 1972. Trickle irrigation–application uniformity from simple emitters. *Trans. ASAE* **15:** 1108-1111.

Burdine, N.T. 1953. Relative permeability calculations from pore-size distribution data. *Petr. Trans. Am. Inst., Mining Metall. Engrg.* **198:** 71-77. (Referred from van Genuchten, 1980).

Carslaw, H.S. and Jaeger, J.C. 1959. Conduction of heat in solids. 2nd ed. Oxford, Clavendon. 510p.

Christiansen, 1942. Irrigation by sprinkling. *California Agric. Exp. Sta. Bull. No. 670.* University of California, Davis, California.

Clothier, B.E. and Scotter, D.R. 1982. Constant flux infiltration from a hemispherical cavity. *Soil Sci. Soc. Am. J.* **46:** 696-700.

Clothier, B.E.; Scotter, D.R. and Harper, E. 1985. Three-dimensional infiltration and trickle irrigation. *Trans. ASAE.* **28:** 497-501.

Cosby, B.J.; Hornberger, G.M.; Clapp, R.B. and Ginn, T.R. 1984. A statistical exploration of the relationships of soil moisture characteristics to the physical properties of soils. *Water Resour. Res.* **20:** 682-690.

Dandy, G.C. and Hassanli, A.M. 1996. Optimum design and operation of multiple subunit drip irrigation systems. *J. Irrig. & Drain. Div. ASCE.* **122:** 265-275.

Gardner, W.R. 1958. Some steady state solutions of the unsaturated moisture flow equation with application to evaporation from a water table. *Soil Sci.* **85:** 226-232.

Gupta, S.C. and Larsen, W.E. 1979. Estimating soil water retention characteristics from particle size distribution, organic matter content, and bulk density. *Water Resour. Res.* **15:** 1633-1635.

Haghighi, K.; Bralts, V.F. and Segerlind, L.J. 1988. Finite element formulation of Tee and Bend components in hydraulic pipe network analysis. *Trans ASAE.* **31:** 1750-1758.

Hathoot, H.M.; Al-Amoud, A.I. and Mohammad, F.S. 1993. Analysis and design of trickle irrigation laterals. *J. Irrig. & Drain. Engrg. Div. ASCE.* **119:** 756-767.

Healy, R.W. and Warrick, A.W. 1988. A generalized solution to infiltration from a surface point source. *Soil Sci. Soc. Am. J.* **52:** 1245-1251.

Herbert, E. 1971. Hydraulic design: The use of poly-plot. Trickle Irrigation, Australia, I.E.I. Australia. (Referred from Wu, 1985)

Howell, T.A. and Hiller, E.A. 1974. Trickle irrigation lateral design. *Trans ASAE.* **17:** 902-908.

Hozapfel, E.A.; Marino, M.A. and Valenzuela, A. 1990. Drip irrigation nonlinear optimization model. *J. Irrig. & Drain. Engrg. Div. ASCE.* **116:** 479-496.

India. Ministry of Information and Broadcasting. Publications Division. Research, Reference and Training Division. 1999. India – A reference annual. New Delhi.

Jain, B.H. 2000a. Micro Irrigation Technologies – Experiences and Issues Involved in their Promotion in Developing Countries, key note address, *International Conference on Micro and Sprinkler Irrigation Systems*, CBIP – JISL, Maharashtra, India.

Jain, R.B. 2000b. Development of microirrigation in India. *International Conference on Micro and Sprinkler Irrigation Systems*, CBIP – JISL, Maharashtra, India.

Kang, Y. and Nishiyama, S. 1994. Finite element method analysis of microirrigation system pressure distribution. *Trans. Japanese Soc. Irrig., Drain. and Reclamation Engrg.* **169:** 19-26. (Referred from Kang and Nishiyama, 1996a).

Kang, Y. and Nishiyama, S. 1995. Hydraulic analysis of microirrigation submain units. *Trans., ASAE.* **38:** 1377-1384.

Kang, Y. and Nishiyama, S. 1996a. A simplified method for design of microirrigation laterals. *Trans. ASAE.* **39:** 1681-1687.

Kang, Y. and Nishiyama, S. 1996b. Analysis and design of microirrigation laterals. *J. Irrig. & Drain. Engrg. Div. ASCE.* **122:** 75-82.

Kang, Y. and Nishiyama, S. 1996c. Analysis of microirrigation system using a lateral discharge equation. *Trans ASAE.* **39:** 921-929.

Kang, Y.; Nishiyama, S. and Kawano H. 1995. " Finite element analysis of large scale microirrigation systems." **In:** *Proc., Fifth International Microirrigation Congress.* 84-90. Joseph, Mich: ASAE.

Karmeli, D.; Peri, G. and Todes, M. (1985) Irrigation systems: Design and Operation. Oxford University Press, Cape Town. p 187.

Kay, M.G. 1990. Recent developments for improving water management in surface and overhead irrigation. *Agric. Water Management.* **17:** 7-23.

Keller, J. and Bliesner, R.D. 1990. Sprinkle and trickle irrigation. Van Nostrand Reinhold, New York. p652.

Kirkham, D. and Powers, W.L. 1072. Advanced soil physics.New York, Wiley-interscience, a division of John Wiley & Sons, Inc.

Lafolie, F., Guennelon, R. and van Genuchten, M. Th. 1989. Analysis of water flow under trickle irrigation: I. Theory and numerical solution. *Soil Sci. Soc. Am. J.* **53:** 1310-1318.

Lockington, D.; Parlange, J.Y. and Surin, A. 1984. Optimal prediction of saturation and wetting fronts during trickle irrigation. *Soil Sci. Soc. Am. J.* **48:** 488-494.

Lomen, D.O. and Warrick, A.W. 1978. Linearized moisture flow with loss at the soil surface. *Soil Sci. Soc. Am. J.* **42:** 396-400.

Lomen, D.O. and Warrick, A.W. 1974. Time-dependent linearized infiltration: II Line sources. *Soil Sci. Soc. Am. J.* **38:** 568-572.

Lomen, D.O. and Warrick, A.W. 1978. Time–dependent solutions to the one–dimensional linearized moisture flow equation with water extraction. *J. Hydrology.* **39**: 59-67.

Lopez, J.R. 1985. Design of manifolds for non-rectangular drip irrigation subunits. Drip/Trickle irrigation in action. **In:** *Proc. of the Third International Microirrigation Congress,* Frensco, California. **2:** 878-886.

Merill, S.D.; Raats, P.A.C. and Dirksen, C. 1978. Laterally confined flow from a point source at the surface of an inhomogeneous soil column. *Soil Sci. Soc. Am. J.* **42:** 851-857.

Mohtar, R.H.; Bralts, V.F. and Shayya, W.H. 1991. A finite element model for the analysis and optimization of pipe networks. *Trans. ASAE.* **34:** 393-401.

Maulem, Y. 1976. A new model for predicting the hydraulic conductivity of unsaturated porous media. *Water. Resour. Res.* **12:** 513-522.

Myers, L.E. and Bucks, D.A. 1972. Uniform irrigation with low pressure trickle systems. *J. Irrig. and Drain. Engng. Div. ASCE* **98:** 341-346.

Nakayama, F.S. and Bucks, D.A. 1986. Trickle irrigation for crop production. Elsevier Science, Amesterdam. p 383.

Paco, J.L. De 1985. Friction head loss in drip irrigation manifolds for trapezoidal shaped subunits. Microirrigation for a changing world: Conserving resources – changing the world. **In:** *Proc. of the Fourth International Microirrigation Congress,* Orlando, Florida, U.S.A. 74-79.

Parlange, J.Y. 1972. Theory of water movement in soils: 5. Unsteady infiltration from spherical cavities. *Soil Sci.* **113:** 96-101.

Parlange, J.Y. 1973. Theory of water movement in soils: 10. Cavities with constant flux. *Soil Sci.* **116:** 1-7.

Philip, J.R. 1968. Steady infiltration from buried point sources and spherical cavities. *Water Resour. Res.* **4:** 1039-1047.

Philip, J.R. 1969. Theory of infiltration. *Adv. Hydrosci.* **5:** 215-296.

Philip, J.R. 1971. General theorem on steady infiltration from surface sources, with application to point and line sources. *Soil Sci. Soc. Am. J.* **35:** 867-871.

Philip, J.R. 1984. Steady infiltration from circular cylindrical cavities. *Soil Sci. Soc. Am. J.* **48:** 270-277.

Philip, J.R. 1986. Steady infiltration from buried discs and other sources. *Water Resour. Res.* **22:** 1058-1066.

Philip, J.R. and Knight, J.H. 1974. On solving the unsaturated flow equation: 3. New quasi-analytical technique. *Soil Sci.* **117:** 1-13.

Pitts, D.J.; Ferguson, J.A. and Wright, R.E. 1986. Trickle irrigation lateral line design by computer analysis. *Trans. ASAE.* **29:** 1320-1324.

Pullan, A.J. 1990. The quasilinear approximation for unsaturated porous media flow. *Water Resour. Res.* **26:** 1219-1134.

Raats, P.A.C. 1970. Steady infiltration from line and furrows. Soil Sci. Soc. Am. J. **34:** 739-714.

Raats, P.A.C. 1971. Steady infiltration from point sources, cavities and basins. *Soil Sci. Soc. Am. J.* **35:** 689-694.

Raats, P.A.C. 1972. Steady infiltration from sources at arbitrary depths. *Soil Sci. Soc. Am. J.* **36:** 399-401.

Raats, P.A.C. 1976. Analytical solution to a simplified flow equation. *Trans. ASAE.* **19:** 683-689.

Raats, P.A.C. 1977. Laterally confined steady flows of water from sources and to sinks in unsaturated soils. *Soil Sci. Soc. Am. J.* **41:** 294-301.

Raats, P.A.C. and Gardener, W.R. 1971. Comparison of empirical relationships between pressure head and hydraulic conductivity and some observations in radially symmetric flow. *Water Resour. Res.* **7:** 921-928.

Rawls, W.J.; Brakensiek, D.L. and Saxton, K.E. 1982. Estimation of soil water properties. *Trans. ASAE.* **25:** 1316-1320.

Rosenberg, D.O.V. 1969. Methods for the numerical solution of partial differential equation. New York, Amer. Elsevier Publi. Company, Inc. 128p.

Roth, R.L. 1974. Soil moisture distribution and wetting pattern from a point source. **In:** *Proc. International. Drip Irrig. Congress,* 2nd San Diego, C.A. 7-14 July. Univ. of California, Riverside. Pp. 246-251. (Referred from Ben-Asher *et al.,* 1986).

Russo, D. 1983. A geostatistical approach to the trickle irrigation design in heterogenous soil. 1. Theory. *Wat. Resour. Res.* **19:** 632 - 642.

Saldivia, L.A.; Bralts, V.F.; Shayya, W.H. and Segerlind, L.J. 1990. Hydraulic analysis of sprinkler irrigation system components using the finite element method. *Trans. ASAE.* **33:** 1195-1202.

Saxton, K.E., Rawls, W.J., Romberger, J.S., and Papendick, R.I. 1986. Estimating generalized soil-water characteristics from texture. *Soil Sci. Soc. Am. J.* **50:** 1031-1036.

Scaloppi, 1986. Adjusted F factor for multiple outlet pipes. *J. Irrig. & Drain. Engng. ASCE.* **114:** 169-174.

Sharma, B.R. and Sarkar, T.K., 1994. Efficient water management – A key to sustainable food production. *Indian Farming,* **44(7):** 7-12.

Singh, A.; Singh, R.P.; Mahar, P.S. and Singh, K.K. (2000). Optimal design of tapered microirrigation submain manifolds. *J. Irrig. & Drain. Div. ASCE.* **126:** 371-374.

Smetten, K.R.J.; Parlange, J.Y.; Ross, P.J. and Haverkamp, R. 1994. Three-dimensional analysis of infiltration from the disc infiltration. 1. A capillary based theory. *Water Resour. Res.* **30:** 2925-2929.

Taghavi, S.A.; Marino, M.A. and Rolston, D.E. 1984. Infiltration from trickle irrigation source. *J. Irrig. & Drain. Div. ASCE.* **110:** 331-341.

Taghavi, S.A.; Marino, M.A. and Rolston, D.E. 1985. Infiltration from a trickle irrigation source in a heterogeneous soil medium. *J. Hydrology.* **78:** 107-121.

Van Genuchten, M. Th. 1980. A closed-form equation for predicting the hydraulic conductivity of unsaturated soils. *Soil Sci. Soc. Am. J.* **44:** 892-898.

Warrick, A.W. 1974a. Solution to the one-dimensional linear moisture flow equation with water extraction. *Soil Sci. Soc. Am. J.* **38:** 573-576.

Warrick, A.W. 1974b. Time-dependent linearized infiltration: I. Point sources. *Soil Sci. Soc. Am. J.* **38:** 383-386.

Warrick, A.W. 1992. Models for disc infiltrometers. *Wat. Resour. Res.* **28:** 1319-1327.

Warrick, A.W.; Amoozegar-Fard, A. and Lomen, D.O. 1979. Linearized moisture flow from line sources with water extraction. *Trans. ASAE* **22**: 549-553.

Warrick, A.W.; Broadbridge, P. and Lomen, D.O. 1992. Approximation for diffusion from a Disc source. Appl. Math. Modell. (Referred from Warrick, 1992).

Warrick, A.W. and Lomen, D.O. 1976. Time dependent linearised infiltration: III. Strip and disc sources. *Soil Sci. Soc. Am. J.* **40:** 639-643.

Warrick, A.W.; Lomen, D.O. and Amoozegar-Fard, A. 1980. Linearised moisture flow with root extraction for three-dimensional, steady condition. *Soil Sci. Soc. Am. J.* **44:** 911-914.

Watters, G.J. and Keller, J. 1978. Trickle irrigation tubing hydraulics. ASAE Paper No. 78-2015, ASAE, St. Joseph, Mich. pp 1-18.

Weir, G.J. 1987. Steady infiltration from small shallow circular ponds. *Water Resour. Res.* **23:** 733-736.

Wooding, R.A. 1968. Steady infiltration from a shallow circular pond. *Water Resour. Res.* **4:** 1259-1273.

Wu, I.P. 1985. A Uni-plot for drip irrigation lateral and submain design. *Trans. ASAE.* **28:** 522-528.

Wu, I.P. and Gitlin, H.M. 1973. Hydraulics and uniformity for drip irrigation. *J. Irrig. & Drain. Engrg. Div. ASCE.* **99:** 157-168.

Wu, I.P. and Gitlin, H.M. 1974. Drip irrigation design based on uniformity. *Trans. ASAE* **17:** 429-432.

Wu, I.P. and Gitlin, H.M. 1975. Energy gradient line for drip irrigation laterals. *J. Irrig. & Drain. Engrg. Div. ASCE.* **101:** 323-326.

Wu, I.P. and Gitlin, H.M. 1977. Design of drip irrigation lines with varying pipe sizes. *J. Irrig. & Drain. Engrg. Div. ASCE.* **103:** 499-503.

Wu, I.P. and Yue, R. 1993. Drip lateral design using energy gradient line approach. *Trans. ASAE.* **36:** 389-394.

Yitayew, M. and Warrick, A.W. 1988. Trickle lateral hydraulics. II. Design and examples. *J. Irrig. & Drain. Engrg. Div. ASCE.* **114:** 289-300.

Zazueta, F.S., Clark, G.A., Smajstrla, A.G. and Carillo, M. 1995. A sample equation to estimate soil-water movement from a drip irrigation source. **In:** *Proc. of the Fifth International Microirrigation Congress*, 851 – 856. Joseph, Mich. ASAE.

Appendices

Appendix-A

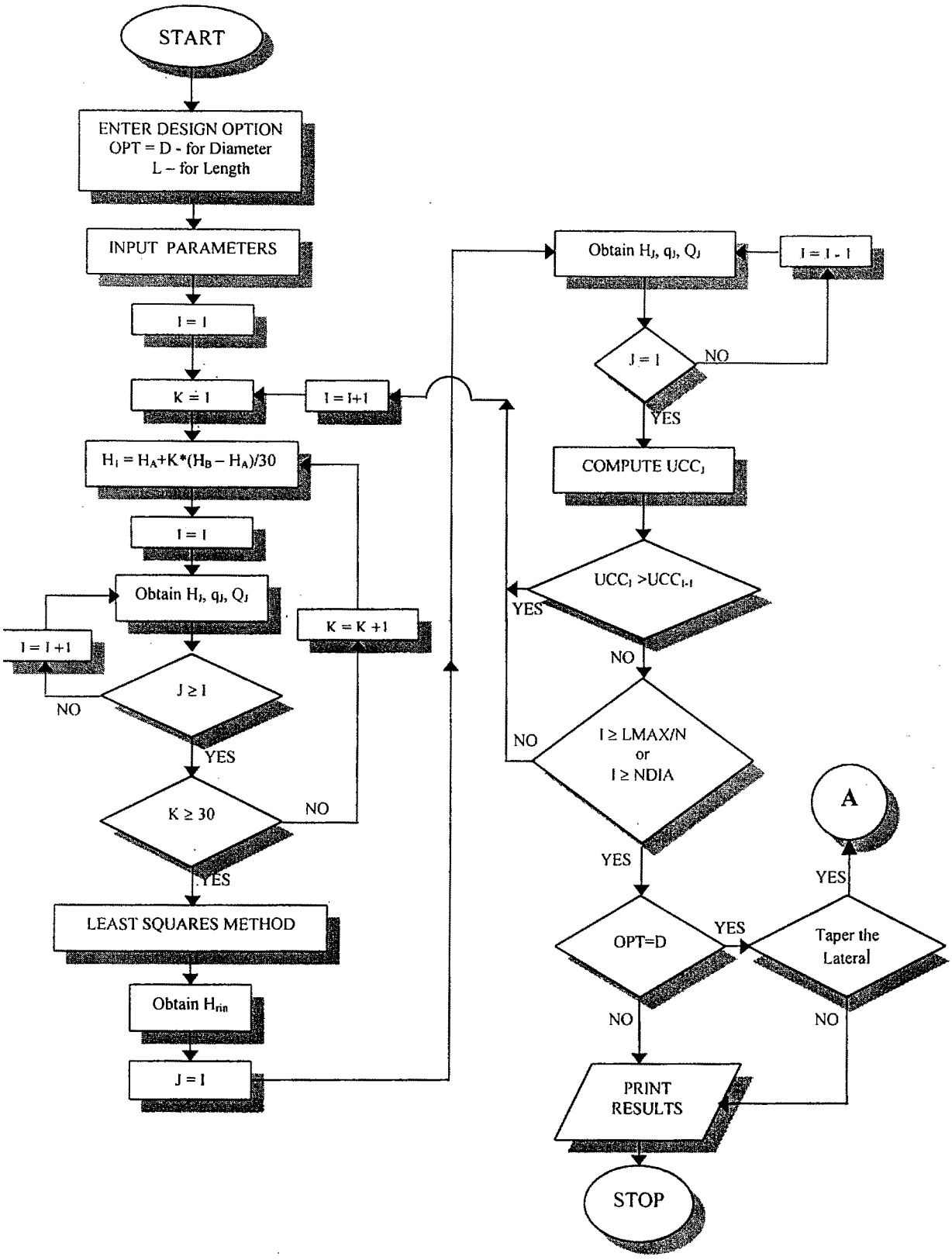

Fig. A-1 Flow chart for design of length/diameter of single laterals.

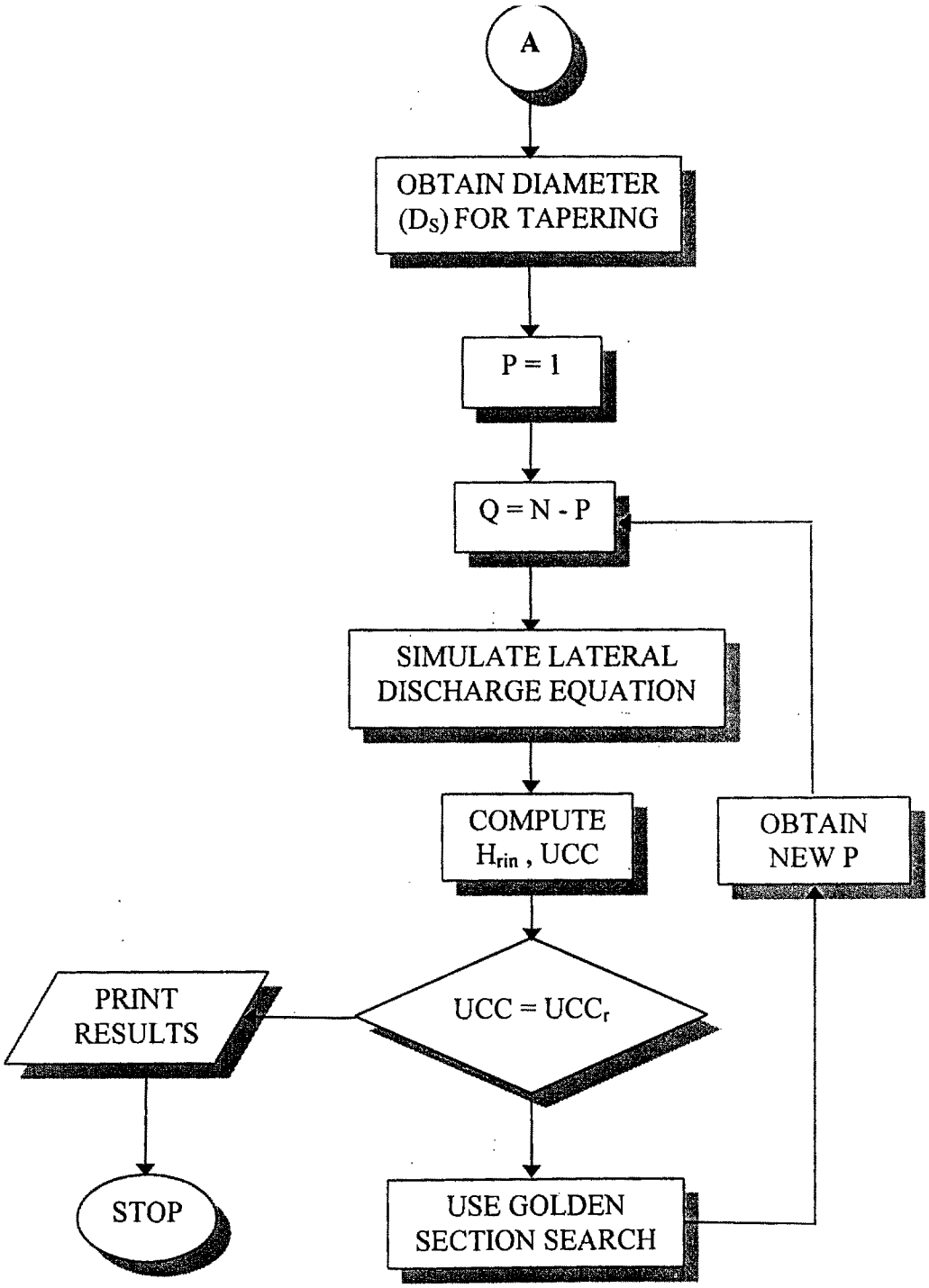

Fig. A-2 Flow chart for design of tapered diameter of single laterals.

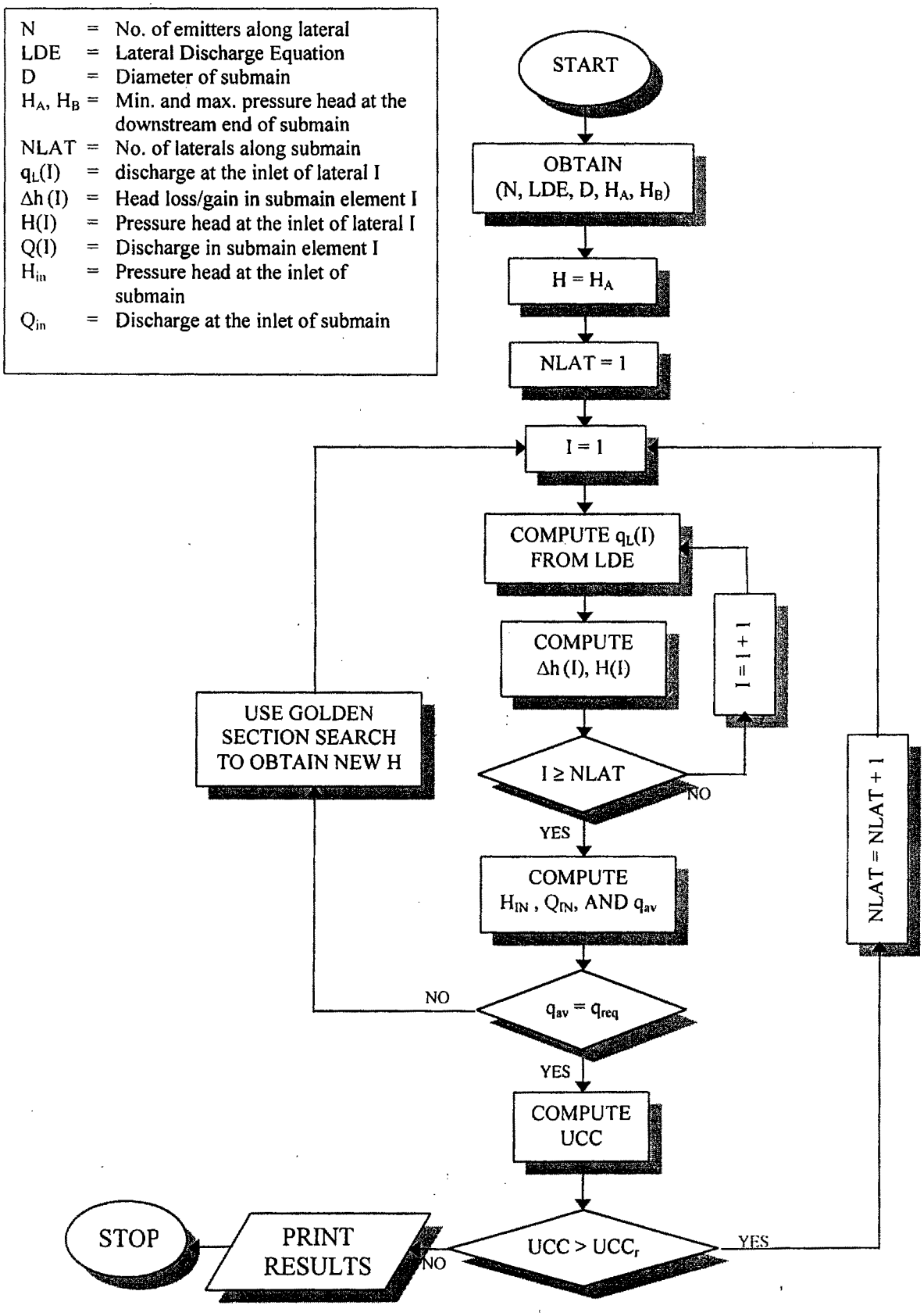

Fig. A-3. Flow chart for design of length of submain.

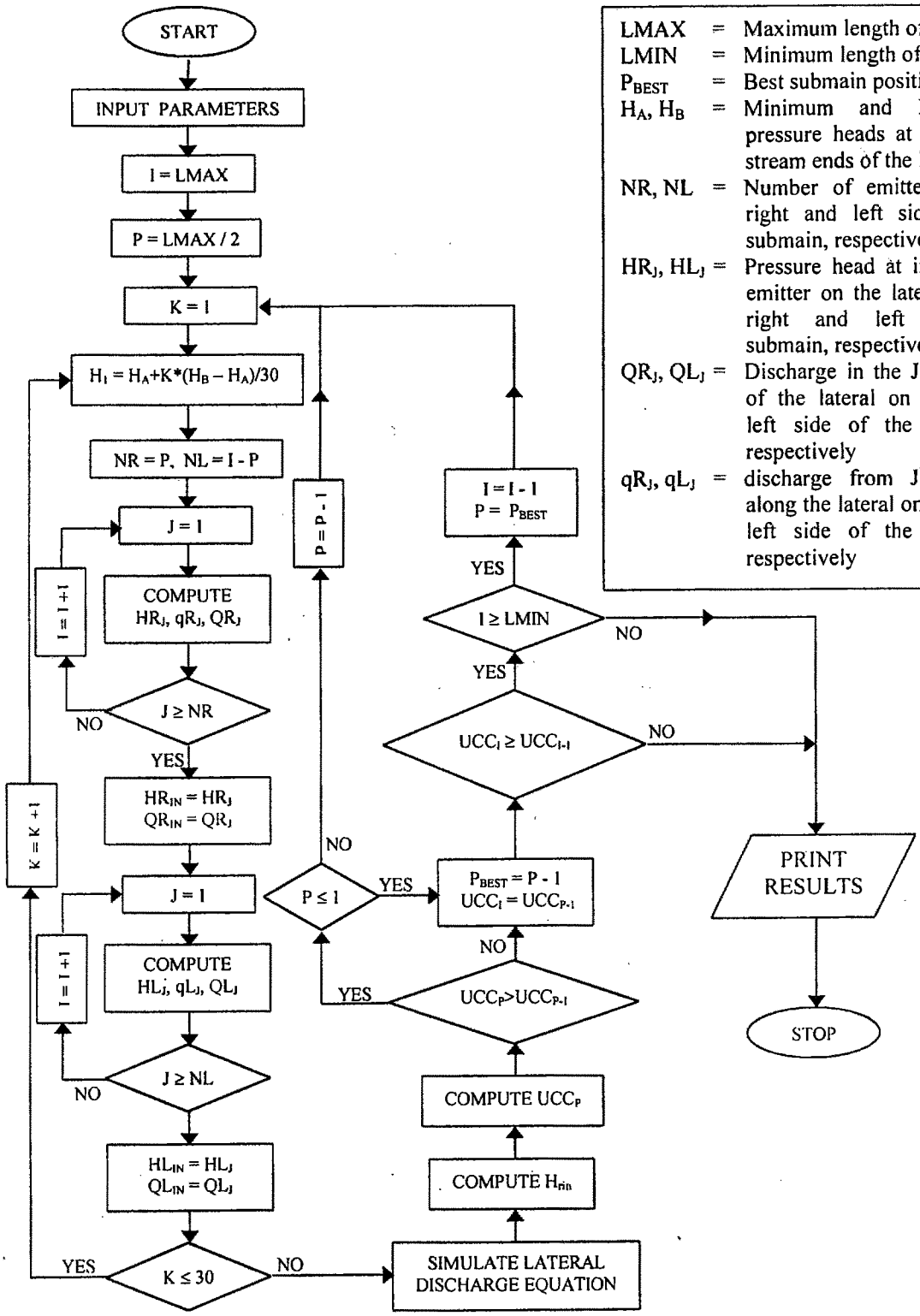

Fig. A-4 Flow chart for design of length of paired laterals.

VITA

The author, **Sudhir Kumar Jain**, *was born on 25th June, 1961 at village Bandakpur, District - Damoh of Madhya Pradesh. He passed his Higher Secondary School Examination from Board of Secondary Education, Bhopal (M.P.). He completed B. Tech. in Agricultural Engineering from J. N. Krishi Vishwa Vidyalaya, Jabalpur in June, 1984. He obtained degree in M. Tech. (Soil and water Conservation Engineering) from Indian Institute of Technology, Kharagpur in December, 1985. He joined as Assistant Professor (Irrigation and Drainage Engineering) at College of Agricultural Engineering, Rajendra Agricultural University, Bihar, Pusa, on 23rd January, 1989. From this institute he was sponsored for Ph. D. degree programme at G. B. Pant University of Agriculture and Technology, Pantnagar in the Department of Irrigation and Drainage Engineering. He joined the Ph. D. degree programme on 3rd August, 1998.*

Mailing address:

S. K. Jain
Assistant Professor,
Department of Irrigation and Drainage Engineering,
College of Agricultural Engineering,
Rajendra Agricultural University, Bihar
Pusa (Samastipur) 848 125
Phone 06274-74270, FAX 06274-74266, email rau@bih.nic.in

ABSTRACT

Name : SUDHIR KUMAR JAIN **Id. No.** 25689

Semester & year of admission : I[st], 1998 **Degree :** Ph. D.

Major : Irrigation and Drainage Engineering **Department :** Irrigation and Drainage Engineering

Thesis Title : DEVELOPMENT OF DESIGN METHODOLOGY AND SOFTWARE FOR MICROIRRIGATION SUBUNITS

Advisor : Dr. K. K. Singh

In spite of the popularity of microirrigation systems, the development of appropriate design criterion still continues to be an important issue of researchers. Efficient design of a microirrigation system needs to take care of the distribution of applied water in the root zone of the plants.

In the present investigation, methodologies have been developed for the design of three major components (viz. emitter discharge, lateral line and submain line) of microirrigation subunits.

The shape of the wetted profile below the trickle source has been considered as the criteria for determination of the emitter discharge. The position of wetting front and distribution of soil moisture in the root zone for a known emitter discharge is evaluated using a finite difference model. The soil-water characteristic relationships described by the texture of the soil have been input to the model. The proposed model has been validated through the published experimental and numerical results.

Lateral discharge equation approach has been used for design of microirrigation lateral and submain lines. A simple power equation has been used as lateral discharge equation. This lateral discharge equation can be extrapolated to obtain the head required at the inlet of the lateral. Golden section search method has been used along with this method for design of tapered (two pipe size) laterals and submains.

The model developed for determination of emitter discharge is simple to use and provides a realistic solution. The approach used for design of laterals and submains is accurate and applicable for almost all the situations of microirrigation installations.

(K. K. Singh)
Advisor

(Sudhir Kumar Jain)
Id. No. 25689